

**Biochemical, Structural and Cellular Studies on HGP1, a  
Member of the  
p47 Family of GTPases**

Inaugural-Dissertation  
zur  
Erlangung des Doktorgrades  
der Mathematisch-Naturwissenschaftlichen Fakultät  
der Universität zu Köln

vorgelegt von  
Revathy C Uthaiah  
aus Bangalore

Köln 2002

The thesis work was supported by the Graduate programme "Genetics of cellular systems " funded by the Deutsche Forschungsgemeinschaft, and also by the Land Nordrhein-Westfalen. This work was done in the Institute for Genetics, University of Köln under the supervision of Prof. Jonathan C. Howard. A part of the work was done in collaboration with the Max Planck Institute for Molecular Physiology, Dortmund, under the guidance of Dr. Christian Herrmann in the group of Prof. Alfred Wittinghofer. I am grateful to all these institutions.

Berichterstatter :

Gutachter Prof. Jonathan C. Howard

Gutachter Prof. Thomas Langer

Tag der mündlichen Prüfung :

14.02.03

To my family



**Mirth and mockery,  
Entwined in a flowing stream.  
The meadow of knowledge,  
Of progress and destruction,  
Back and forth, a move  
For poise....**

*Anonymous*



## CONTENTS

I. INTRODUCTION...	1
I.1. Infection and Immunity.....	1
I.2. Cytokines as Mediators of Innate and Adaptive Immunity .....	2
I.3. Interferon Dependent Cell Autonomous Resistance.....	4
I.3.1. Interferon Inducible GTPases Contributing to Cell Autonomous Resistance .....	5
I.3.1.1. Mx GTPases.....	6
I.3.1.2. p65 GTPase Family.....	6
I.3.1.3. p47 GTPase Family.....	7
I.4. GTPases, Functions and Features .....	9
I.4.1. Characteristic Features of the G Domain.....	10
I.4.2. Deviation from the Switch GTPases.....	11
I.5. Objective of this Work.....	12
II. MATERIALS AND METHODS .....	15
II.1. Chemicals and other Accessories .....	15
II.2. Materials .....	15
II.3. Enzymes/Proteins .....	15
II.4. Reagent Kits .....	16
II.5. Vectors... ..	16
II.6. Oligonucleotides .....	16
II.7. Constructs .....	17
II.7.1. pGEX Constructs .....	17
II.7.2. pGW1H Constructs.....	17
II.8. Media .....	18
II.9. Bacterial Strains.....	19
II.10. Antibiotics .....	19
II.11. Cells .	20
II.12. Radioisotopes.....	19
II.13. Antibodies.....	19
II.14. Detergents .....	19
II.15. Equipments .....	20
II.16. Protocols .....	20
II.16.1. <b>Molecular Biology .....</b>	<b>20</b>

II.16.1.1. Agarose Electrophoresis .....	20
II.16.1.2. Polymerase Chain Reaction.....	20
II.16.1.3. Restriction Enzyme Digestion .....	21
II.16.1.4. Purification of DNA Fragments.....	21
II.16.1.5. Ligation.....	21
II.16.1.6. Preparation of Competent Cells.....	21
II.16.1.7. Transformation .....	22
II.16.1.8. Plasmid DNA Isolation.....	22
II.16.1.9. Determination of the Concentration of DNA .....	23
II.16.1.10. Site Directed Mutagenesis .....	23
II.16.1.11. DNA Sequencing.....	23
<b>II.16.2. Expression and Purification of Proteins.....</b>	<b>24</b>
II.16.2.1. Growth and Harvest of Bacteria .....	24
II.16.2.2. Glutathione-Sepharose Affinity Chromatography.....	24
II.16.2.3. Concentration of Proteins by Ammonium Sulphate Precipitation .....	24
II.16.2.4. Size-exclusion Chromatography.....	25
II.16.2.5. Concentrating Proteins by Ultra-filtration.....	25
II.16.2.6. SDS Gel Electrophoresis .....	25
<b>II.16.3. Biochemical and Biophysical Methods .....</b>	<b>26</b>
II.16.3.1. Determination of Protein Concentration by Absorption Spectroscopy .....	26
II.16.3.2. Fluorescence Spectroscopy.....	26
II.16.3.3. Stopped Flow Apparatus.....	26
II.16.3.4. Isothermal Titration Calorimetry.....	27
II.16.3.5. Reverse-Phase HPLC .....	27
<b>II.16.4. Light Scattering .....</b>	<b>27</b>
<b>II.16.5. Crystallisation .....</b>	<b>28</b>
<b>II.16.6. Cell Biology .....</b>	<b>28</b>
II.16.6.1. IIGP1 Specific Polyclonal Rabbit Antiserum.....	28
II.16.6.2. Western Blot.....	30
II.16.6.3. Growth and Culture of Eukaryotic Cells .....	30
II.16.6.4. Immunofluorescence.....	31
II.16.6.5. Cellular Fractionation .....	31
II.16.6.6. Immunoprecipitation .....	32
II.16.6.7. Analytical Gel Filtration.....	33



III. RESULTS I .....	34
<b>III.A. Biochemical and Cellular Studies on IIGP1 .....</b>	<b>34</b>
III.A.1. Recombinant IIGP1 Expression and Purification.....	34
III.A.2. Biochemical Characterisation of IIGP1.....	35
III.A.2.1. Nucleotide Binding Features .....	35
III.A.2.1.1. Equilibrium Titrations .....	35
III.A.2.1.2. Isothermal Titration Calorimetry.....	37
III.A.2.1.3. Dynamics of Nucleotide Binding.....	37
III.A.2.2. GTP Hydrolysis.....	40
III.A.2.3. Oligomerisation .....	42
III.A.2.3.1. Time and GppNHp Dependent Oligomerisation.....	42
III.A.2.3.2. C-terminal end is Essential for the Formation of Higher Molecular Species.....	43
III.A.2.3.3. Fluorescence Scattering Experiments.....	43
<b>III.B. Cellular studies on IIGP1.....</b>	<b>45</b>
III.B.1. Localisation Studies on IIGP1 .....	45
III.B.2. Distribution of IIGP1 in the Cell .....	47
III.B.3. Interaction Molecules .....	48
III.B.3.1. Size Exclusion Chromatography .....	48
III.B.3.2. Immunoprecipitation .....	50
III.B.3.2.1. Immunoprecipitation of IIGP1 in MEFs with $\alpha$ 165.....	50
III.B.3.2.2. Co-precipitation of IIGP1 and Partners with $\alpha$ 165 in MEFs.....	50
III.B.3.2.3. $\alpha$ 165 can also Co-precipitate the Same Molecules in L929 cells.....	51
III.B.3.2.4. Immunoprecipitation with the Monoclonal Antibodies.....	54
III.B.4. Properties of Membrane Associated IIGP1 .....	55
III.B.4.1. Myristoylation is Important for Membrane Attachment .....	55
III.B.4.2. C-terminal Mutants.....	56
III.B.4.3. Myristoylation Independent Association to the Membrane.....	59
IV. RESULTS II.....	61
<b>IV.A. Structural and Mutational Analysis .....</b>	<b>61</b>
IV.A.1. Crystal Structure of IIGP1.....	61
IV.A.2. Features of IIGP1-GDP and the IIGP1-GppNHp Complex.....	62
<b>IV.B. Mutational Analysis .....</b>	<b>64</b>
IV.B.1. Biochemical Features .....	67
IV.B.1.1. Analysis of the Binding Mutants.....	67

IV.B.1.2. Analysis of the Interface Mutants.....	68
IV.B.1.2.1. Analysis of the Nucleotide Binding Parameters of the Interface Mutants .....	68
IV.B.1.2.2. Studies on GTP Hydrolysis .....	68
IV.B.1.3. <i>In vivo</i> Characterisation of the IIGP1 Mutants.....	70
IV.B.1.3.1. Cellular Localisation of the Binding and the Interface Mutants .....	70
IV.B.1.3.2. Cellular Distribution of the Binding and the Interface Mutants.....	71
V. DISCUSSION .....	73
V.1. Nucleotide Binding Parameters of IIGP1 in Comparison to Several GTPases.....	73
V.2. Significance of GTP Hydrolysis.....	75
V.3. Relationship of IIGP1 to the Family of Dynamin Like Large GTPases .....	78
V.4. Nucleotide Dependent Self Assembly.....	79
V.5. Association of IIGP1 with Membranes .....	83
V.6. Cellular Localisation .....	84
V.7. Functional Cues for IIGP1.....	85
V.8. IIGP1 in the p47 Family of GTPases .....	85
V.8. Proposed Function.....	86
VI. REFERENCES.....	87
VII.SUMMARY .....	99
VIII. ZUSAMMENFASSUNG.....	101
IX. ACKNOWLEDGEMENT .....	103
X. ERKLÄRUNG .....	105
XI. PUBLICATIONS.....	105
XII. LEBENSLAUF.....	106

## I. INTRODUCTION

### I.1. Infection & Immunity

Host-Pathogen interactions demonstrate dynamism in evolutionary processes. Pathogens try to contact, colonize, infect, evade, and damage the host through many virulence factors such as adhesins, invasins, evasins, toxins (endotoxin/exotoxin). The host on the other hand, mobilises several defence mechanisms to arrest their dissemination, to prevent damage, and expel the invaders. Consequentially, the millions of years of reciprocity and antagonism have led both the systems to have highly evolved mechanisms of evasion and survival, the host with respect to its immune system, and the pathogen to subterfuge (Casadevall and Pirofski, 2001; Levy and Garcia-Sastre, 2001; Ganusov et al., 2002; Roy and Kirchner, 2000; van Baalen, 1998). Innate immunity is an ancient defence mechanism common to both plants and animals. It serves as the first line of defense against external attack, that includes the recognition of pathogen associated molecular patterns (PAMPs) by genome encoded pattern recognition receptors (PRRs) like the Toll like receptors (TLRs) conserved from *Drosophila* to mammals. Besides, the innate system primes the adaptive immune system, which is specific to vertebrates and has the ability to adapt and remember the infectious pathogen. The adaptive system together with the innate system provide optimal host defence (Janeway, Jr. and Medzhitov, 2002; Spriggs and Sher, 1999; Ploegh, 1998).

The immune system mounts a complicated response to infection by co-ordinating several types of white blood cells. The cells that govern the innate system bear the recognition receptors, which are germ-line encoded, in the macrophages, dendritic cells (DCs), mast cells, neutrophils, eosinophils, and natural killer cells (NKs). They are activated during an inflammatory response (a localised protective reaction of tissue to infection or injury to rapidly combat microbes) without recourse to adaptive immunity. Nevertheless, the stimulation of the adaptive response becomes necessary when the innate system is unable to deal with pathogen challenge. The innate system therefore, induces the expression of co-stimulatory molecules on the surface of antigen presenting cells, induces the secretion of appropriate cytokines and chemokines directing the lymphocytes to the appropriate locations in the body. Since the recognition receptors of the antigen-specific adaptive system are encoded in gene segments (T and B lymphocytes), there is a wide range of possible variability in immune recognition. However, autoimmune disease and allergy are the main disadvantages of such a permutation, but are normally held in check by several layers of inhibitory mechanisms of the vertebrate immune system.

Therefore the two distinct immune mechanisms of innate and adaptive immunity work together to discern the pathogen, expel the pathogen, prevent self damage, and derive protection (Abbas and Janeway, Jr., 2000; Janeway, Jr. and Medzhitov, 2002).

## I.2. Cytokines as Mediators of Innate and Adaptive Immunity

The stimulation of cytokine production is crucial for the development, differentiation and regulation of the immune response. The adaptive immune response involves humoral or circulating antibody (B cells) and cell mediated immunity (T cells) which identifies antigens (foreign proteins, polysaccharides, peptides etc.) either as part of a pathogen or as a partially degraded by-product. The immune system defends the body by maintaining an elaborate and dynamic communication network of regulatory molecules, the cytokines. The multiple functions of cytokines include hematopoiesis, chemotaxis, angiogenesis, embryogenesis. They play a crucial role in regulating the extent and the duration of the immune response by stimulating or inhibiting the activation, proliferation, and /or differentiation of various cells and by regulating the secretion of antibodies or other cytokines (Hirano, 2002; Spriggs, 1999). The cytokines of immune origin mediate and regulate innate immunity through the activation of type 1 interferons, tumor necrosis factor alpha (TNF- $\alpha$ ), interleukins IL1, IL6, IL10, IL 12, IL 15 and chemokines. They also mediate specific immunity through the stimulation of IL-2, IL-4, IL-5, IL-13, IL-16, IL-17, interferon- $\gamma$  (IFN-  $\gamma$ ), transforming growth factor (TGF- $\beta$ ) and lymphotoxin. The cellular response to cytokines involves complex modulation of the immune and inflammatory responses (O'Shea et al., 2002).

Among the heterogenous family of multifunctional cytokines, interferons were first recognised for their ability to induce cellular resistance to viral infection. They function by integrating early innate responses with later events mediated by the adaptive immune system. The IFNs are categorised into two distinct groups based on their protein sequences, cellular sources and the use of distinct receptors. Type I interferons include a number of IFN- $\alpha$  sub-types (ten different) and a single species of IFN- $\beta$  (humans and mice), IFN- $\omega$  (humans) and IFN- $\tau$  (ruminants). They are produced by all cells, and predominantly by a sub-population of immature dendritic cells (DCs) during infections. Type II interferon contains a single member IFN- $\gamma$  , produced by a few specialised cells like the activated natural killer cells (NKC), Th1 subset of the T cells, activated dendritic cells and macrophages. The expression of IFN- $\gamma$  by Th1 cells is the essential bridge where the adaptive immune response reinforces macrophage based innate immunity (Hirano, 2002; Levy, 2002; Liew, 2002; Spriggs, 1996; Spriggs,1999).

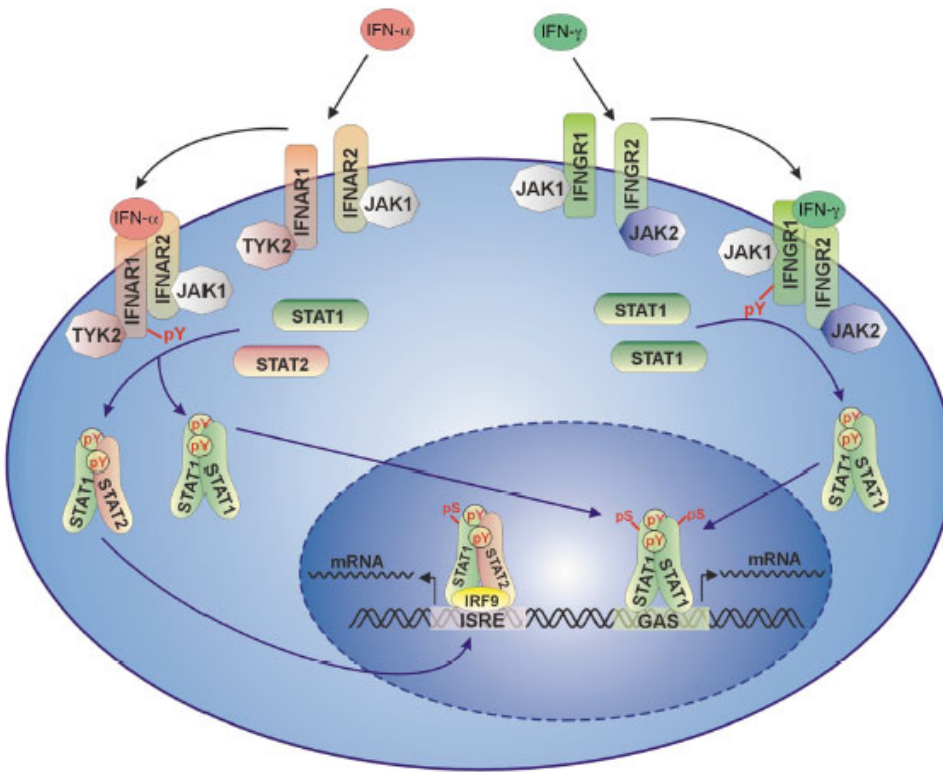


Figure 1.1 The Jak-STAT pathway of IFN- $\alpha/\beta$  and IFN- $\gamma$  (Decker et al., 2002).

The IFN- $\alpha/\beta$  and the IFN- $\gamma$  binding to their respective receptors activate the Jak-STAT pathway, followed by the translocation of the STAT homodimers, alone or with other transcription factors regulating the expression of a vast subset of genes.

Interferons bind to specific transmembrane receptors or receptor complexes on target cells, and rapidly alter the pattern of gene expression as shown in figure 1.1. They exert biological activities by binding to their specific receptors, the type 1 receptor (IFNAR), a heterodimer comprising of IFNAR1 and IFNAR2 chains, and the IFN- $\gamma$  receptor (IFNGR) forming a heterotetrameric complex with the two  $\alpha$  and  $\beta$  chains. The receptor-ligand complex formation leads to the activation of cytoplasmic proteins of the Janus kinase family, Jak1 and Tyk 2 for IFN- $\alpha/\beta$  and Jak1 and Jak2 for IFN- $\gamma$ . This allows the binding of the signal transducers and activators of transcription (STAT) to the receptor phosphotyrosine residues created by the kinases on the receptor, followed by phosphorylation, and homo- or heterodimerisation of the STATs. The STAT heterodimer is used by the IFN  $\alpha/\beta$  pathway along with another DNA binding subunit IRF-9, forming a heterotrimeric transcription factor complex (ISGF3). This complex is translocated to the nucleus and binds to specific sites in the promoter regions, the interferon stimulated response element (ISRE) leading to the expression of target genes essential for innate antiviral immunity. The STAT homodimers that are activated by the IFN- $\alpha/\beta$  or IFN- $\gamma$  pathway, termed IFN- $\gamma$  activating factor (GAF), recognise the gamma interferon associated sequence (GAS) promoter sequence, thereby regulating a vast

subset of genes involved in innate and adaptive immunity (Boehm et al., 1997; Aaronson and Horvath, 2002; Levy and Darnell, Jr., 2002; Ikeda et al., 2002; Decker et al., 2002; Ihle, 1995; Ihle, 2001). The IFN- $\alpha/\beta$  or IFN- $\gamma$  pathways activate an overlapping set of genes via the Jak-STAT pathway (Levy and Garcia-Sastre, 2001; Sato et al., 2001).

Although the cellular responses to IFN seems complex, with a regulation of several hundred genes, they can be described in terms of specific programmes conferring innate and adaptive resistance. The resistance conferred against pathogens is mediated by interactions between cells such as NK cells, T helper cells, cytotoxic T lymphocytes and macrophages with infected cells. Thus cytotoxic T lymphocytes recognise peptides derived from viral proteins when presented on the surface of infected cells in association with class I molecules of the major histocompatibility complex (MHC). This interaction leads to the lysis of the infected cell (Braciale et al., 1987, Cresswell et al., 1997). Macrophages phagocytose apoptotic cells by recognising ligands not present on normal cells (Henson et al., 2001). In contrast to the immune response based on cell-cell interactions as mentioned above, a cell-autonomous pathogen resistance mechanism has also been described. Such a resistance mechanism activated by interferons leads to intracellular pathogen inactivation, and a detailed account of the proteins modulating this function is discussed below.

### I.3. Interferon Dependent Cell Autonomous Resistance

In contrast to the indirect modulation of the immune response to pathogens by interferons, e.g the upregulation of antigen processing and display of viral epitopes at the surface of infected cells, interferons can directly protect cells by inducing intracellular resistance programmes. Such IFN induced cell autonomous resistance involves many different programmes, functioning in different ways, as for example 2'-5' Oligoadenylate synthetase (OAS), PKR, NO, Nup 96/ Nup 98, Mx proteins (see table 1.1).

The IFN inducible 2'-5' Oligoadenylate synthetase (OAS) is activated by ds RNA generated during viral infection. Activated OAS catalyses the synthesis of 2'-5' oligoadenylates, which binds to monomeric RNase L. This interaction results in the dimerisation and activation of RNase L, leading to the inhibition of protein expression by cleaving both the mRNA and rRNA in the cytoplasm, thereby arresting viral replication (Samuel, 2001). Protein kinase R is a ubiquitously expressed interferon inducible serine/threonine kinase. It is activated by dimerisation after binding to dsRNA. The eukaryotic initiation factor 2 $\alpha$  (eIF2 $\alpha$ ), one of the substrates of PKR, upon phosphorylation loses its activity resulting in the inhibition of protein synthesis. PKR has been demonstrated *in vitro* to be important in the inhibition of encephalomyocarditis virus, HIV, and VSV replication (Williams, 2001; D'Acquisto and Ghosh, 2001). The IFN inducible Nitric oxide synthetase and its

product NO are known to carry out nitrosylation of viral proteins (Bogdan, 2001). NO chemically modifies cysteine and tyrosine residues presumably disrupting protein function (by impairment of folding and/or disruption of disulphide bonds within the protein). Intracellular resistance has also been shown in the case of nup 96/nup 98 proteins which have increased levels of expression in response to IFN- $\gamma$  treatment. The vaccinia virus M protein binds to nucleoporin 96 (nup96) /nup98 and achieves mRNA export block. It has been suggested that the increased levels of these proteins saturate the inhibition caused by M protein by providing enough nup98 to mediate mRNA export (Enninga et al., 2002). Several other IFN inducible proteins which confer intracellular pathogen resistance are described in the reviews (Samuel, 2001; Guidotti and Chisari, 2001)

Table 1.1 Programmes of some of the IFN induced proteins conferring antiviral resistance (modified from Chesler and Reiss, 2002)

IFN induced proteins	Resistance activity	Susceptible organisms
RNaseL/ 2'-5' OAS	Inhibition of protein synthesis	ECMV, HIV, Vaccinia
PKR	Inhibition of protein synthesis	ECMV, HIV, VSV
NOS	Targeted nitrosylation of viral proteins	VSV, HSV-1, HIV, EBV, Coxsackie, vaccinia virus.
Nup96/ Nup98	reverts nuclear export block caused by vaccinia M protein	Vaccinia virus
Mx	i. Prevents viral primary transcription ii. Blocks viral transport into the nucleus	Wide antiviral spectrum for bunyavirus, thogotovirus, orthomyxovirus, paramyxovirus, rhabdovirus

### I.3.1. Interferon Inducible GTPases Contributing to Cell Autonomous Resistance

There has been growing evidence for intracellular resistance provided by families of interferon inducible GTPases, three of those are described below. Mx GTPases are considered a paradigm for this mechanism where resistance is conferred by destructively interfering with the life-cycle of pathogens.

### I.3.1.1 Mx GTPases

The Mx proteins are interferon inducible large GTPases localised either in the cytosol (human MxA and Murine Mx2) or in the nucleus (murine Mx1). They confer viral resistance by binding to specific viral components. The cytosolic MxA binds to the nucleocapsids of the Thogotovirus (THOV) thereby preventing viral transport to the nucleus. As a consequence, the primary transcription that takes place in the nucleus is inhibited (Kochs and Haller, 1999). The nuclear mouse Mx1 protein inhibits Influenza A virus (FLUAV) and THOV multiplication also at the level of primary transcription of the viral genome. It is suggested that the Mx1 targets and binds the PB2 subunit of the viral polymerase resulting in the inhibition of viral transcription (Pavlovic et al., 1993)

### I.3.1.2. p65 GTPase Family/ GBPs

The p65 family/ GBPs are highly conserved in vertebrates, in chicken, rat, mouse and man (Cheng et al., 1991; Strehlow et al., 1994; Asundi et al., 1994; Vestal et al., 1998, Wynn et al., 1991; Han et al., 1998; Schwemmle et al., 1996). The family comprises four members in the Mouse (mGBP1, mGBP2, mGBP3, mag-2, mGBP5) (Nguyen et al., 2002) and two in Humans (hGBP1, hGBP2) (Neun et al., 1996) with a molecular mass of 65-71 kDa. They are induced by IFN  $\alpha/\beta$  and strongly by IFN- $\gamma$  (Prochazka et al., 1985). mGBPs (1-5) are absolutely dependent on the primary transcription factor IRF-1 (Boehm et al., 1998). They possess the canonical GTP binding motifs GxxxxGKS and DxxG, but instead of the (N/T)KxD motif which is believed to confer guanine specificity in other guanine nucleotide binding proteins (Cheng et al., 1991), they have a differently structured segment in which arginine and aspartic acid interact with the base through interactions till now unique to this GTPase family (Praefcke et al., 1999). They bind GTP, GDP and GMP with similar affinity, and are able to hydrolyse GTP to GMP through a trapped GDP intermediate (Cheng et al., 1991; Praefcke et al., 1999; Staeheli et al., 1984; Schwemmle et al., 1996). With the exception of mGBP3 and mag2 (Wynn et al., 1991; Han et al., 1998), all GBPs have an isoprenylation sequence at the C-terminus, which is functional *in vivo* and *in vitro*, but the significance of this modification is unknown since they are predominantly cytosolic (Nantais et al., 1996). Moreover, it has been shown to be a mediator of inflammatory cytokines inhibiting endothelial cell growth (Guenzi et al., 2002). mGBP2 has also been claimed to have a role in IFN- $\gamma$  induced murine fibroblast proliferation (Gorbacheva et al., 2002). hGBP1 is shown to be upregulated in mammary tumors (Sun et al., 1999) and during erythroid differentiation (Han et al., 1998). The only evidence for cell autonomous resistance in the p65 family comes from experiments



with hGBP1 where it shows antiviral activity against vesicular stomatitis virus (VSV) and Encephalomyocarditis virus (ECMV) (Anderson et al., 1999).

### I.3.1.3. The p47 GTPase Family

The p47 GTPases are encoded by 22 genes in the mouse, and represent a distinct sequence and structural family. They possess all the GTP binding motifs (Bourne et al., 1990; Bourne et al., 1991), all but one of the mouse p47 genes are distributed between two clusters on chromosome 11 and chromosome 18. The exception is mCINEMA, encoded on Chromosome 7. According to the remarkable substitution of a methionine for the ubiquitously conserved lysine in the GxxxxGKS (G1 motif) which correlates with further features, three of the p47 GTPases define, the GMS subfamily (Boehm et al., 1998). The second number is given based on the order of arrangement in the chromosome for each sub family. An unrooted phylogeny based on the amino acid sequence is shown in figure 1.2.

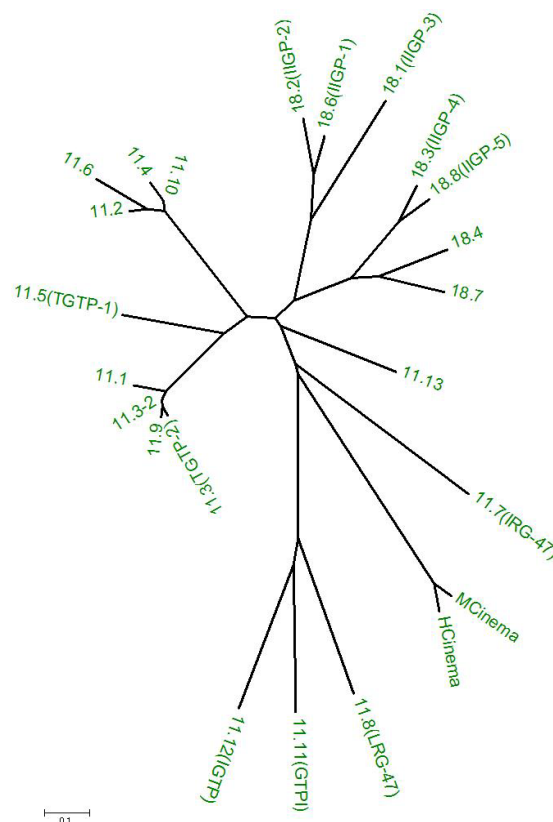


Figure 1.2. The phylogeny of the p47 GTPases (Bekpen et al unpublished data)

Neighbour joining tree based on distance method :- Amino:Poisson correction [pairwise distances]. It is tested using bootstrap test and shows high reliable branching pattern (The data not shown). Alignment of proteins was made by using default option of ClustalW 1.8 BCM (Baylor College of Medicine). Program used for construction of the trees MEGA2; Molecular 1991; Evolutionary Genetics Analysis (Kumar et al., 2001)

An extraordinary aspect of the phylogeny of the p47 GTPases is that this complex branching tree of multiple genes is (so far) present only in Murid rodents (Mouse, Rat, Hamster). In other mammalian groups (ungulates, carnivores, primates), only the single outlying p47 gene on mouse chromosome 7, mCINEMA, has a homologue, so far as is known, and this indeed a very close one (90,1% identity in humans).

The inducibility of all the p47 members has been documented to be dependent on IFN-  $\gamma$  (Boehm et al., 1998), where LRG47, IRG47, TGTP/Mg21, IGTP show similar kinetics of induction (Sorace et al., 1995; Taylor et al., 1996). Some of them are stimulated more weakly by IFN  $\alpha/\beta$  and also by bacterial lipopolysaacharide (LPS). (Taylor et al., 1996), Lafuse et al., 1995, Sorace et al., 1995, Carlow et al., 1998, Zerrahn et al., 2002). IIGP induction by LPS has been shown to be dependent on LPS-mediated induction of type I interferon (Zerrhan et al., 2002, Lapaque et al., manuscript in preparation). LRG-47, IIGP, TGTP/Mg21 are also induced by graft versus host reaction (GVHR) in mice (Wakui et al., 2001), presumably by generalised release of interferons. p47 family members have generally very low constitutive levels of transcription (Boehm 1998). They are described to be early genes as they are transcribed independent of ongoing protein synthesis (TGTP/ Mg21, IGTP, LRG47 (Lafuse et al., 1995; Taylor et al., 1996). They are shown to be inducible by several cell types either immune or non-immune; IFN $\gamma$  stimulated primary mouse embryonic fibroblasts, mouse macrophage cell line ANA-1; IIGP, GTPI, LRG47, IRG47, TGTP, IRG47 (Boehm et al., 1998), TGTP/Mg21 was also expressed in L-cells, fibroblasts, NIH3T3 cells, B cells, mouse peritoneal macrophages, macrophage cell lines (J774, P388DI, RAW 264.5 macrophages), in purified CD4+ CD8+ T cells, and P815 mastocytoma (Carlow et al., 1998); and IGTP in immune cells such as macrophages, T cells, B cells and non immune cells such as fibroblasts and hepatocytes (Taylor et al., 1996), Lafuse et al., 1995), IRG 47 in Pre-B and B lymphocytic cell lines (Gilly and Wall, 1992), LRG47 in RAW 264.5 macrophages (Sorace et al., 1995). Infection seems to upregulate IIGP as observed in *Listeria monocytogenes* infected bone marrow macrophages, endothelial cells, activated T cells (Zerrahn et al., 2002), in *L.monocytogenes* infected mouse liver and also in Scrapie infected brain tissue (Riemer et al., 2000). However, all the members are independent of the TNF pathway as shown by normal induction following infection of TNFRp55<sup>-/-</sup> mice with *L.monocytogenes* ( Boehm et al., 1998). Expression of IGTP mRNA in several mouse tissues revealed significant expression in the thymus and lower expression in the spleen, lung and small intestine; and the expression in the brain, heart, kidney, liver, skeletal muscle, and testes was very low or undetectable, suggesting their expression in immune cell populations (Taylor et al., 1996).

However, recent data from the lab show (Jia Zeng., unpublished results) IIGPI and IGTP expression predominantly in the liver, and also in other tissues of wild type and IFN receptor deficient mice.

There is irresistible evidence for the antimicrobial activity of the p47 GTPase proteins, as shown by infection studies in mice with targeted gene disruptions. Mice deficient in LRG47, IGTP, and IRG47 are highly susceptible to *Toxoplasma gondii*; LRG-47 deficient mice are additionally susceptible to *L. monocytogenes* (Collazo et al., 2001; Taylor et al., 2000). That at least a component of p47-mediated resistance is cell autonomous has been demonstrated for *T. gondii* in astrocytes. Astrocytes lacking IGTP cannot mount gamma-interferon-dependent resistance to infection with *T.gondii in vitro* (Halonen et al., 2001). Furthermore, cells transfected with TGTP showed relative resistance to plaque formation by vesicular stomatitis virus (VSV) but not herpes simplex virus (HSV) (Carlow et al., 1998).

The strong interferon inducibility of the p47 GTPases suggests a defined adaptive function associated with disease resistance. How this relates to the biochemical nature of these proteins as GTPases is an unsolved puzzle. Generally, GTPases are proteins involved in regulating complex cellular processes through conformational changes associated with their nucleotide bound states, either GTP or GDP, defining affinities for several molecular interactions respectively, thereby modulating their function.

#### I.4. GTPases, Functions and Features

Many fundamental cellular processes are regulated by GTPases with a common principle of GTP binding and hydrolysis (Bourne, 1991). The principal action of GTPases has been studied in depth for p21 Ras in the control of cell growth and differentiation (Reuther, 2000), EF-Tu, EF-Ts for initiation, elongation and termination factors in protein synthesis (Rodnina., 2001), for G protein  $\alpha$  chains in transmembrane signalling (Bourne, 1993 Hamm, 1997), for ARF GTPases in membrane trafficking (Donaldson, 1999) and for Ypt/Rab GTPases in vesicular targeting (Segev, 2000). Most of the GTPases have a conserved mechanism with a cycle of GTP and GDP bound forms, where the exchange of GDP to GTP turns on the switch and GTP hydrolysis turns it off, although there are a few exceptions.

The binding of GTP induces a change in the affinities for other macromolecules mediating key cellular functions. The GTPases are therefore regulated both at the level of GTP hydrolysis and at

the level of exchange of GDP for GTP by several other proteins. For example, GTPase activating proteins (GAPs) accelerate the hydrolysis of GTP and thereby turning off the GTPase switch, while the guanine nucleotide exchange factors (GEFs) turn on the switch by increasing the rate of GDP dissociation (Bourne, 1991).

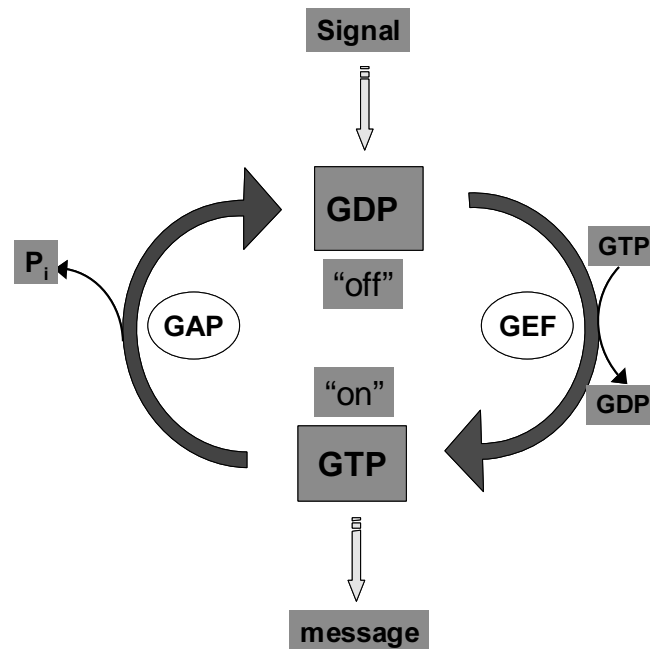


Figure 1.4. Simplified depiction of the GTPase cycle ( Bourne et al., 1991).

The switch GTPases cycling between OFF and ON states. Activation requires dissociation of protein bound GDP, is intrinsically a slow process that is accelerated by guanine nucleotide exchange factors (GEFs). The hydrolysis of GTP to GDP is intrinsically very slow and thus has to be accelerated by the GTPase activating proteins (GAPs).

The GTPase cycle in some small GTPases like Rho, and Rabs is also regulated by guanine nucleotide dissociation inhibitors (GDIs). GDI is specifically a protein inhibitor of the Rab and Rho GTPases which prevents GDP dissociation, and escorts the GTPase in the cytosol, until it reaches the membrane where it is activated (Wu et al., 1996). In addition, another regulatory molecule called the GDI displacement factor (GDF) is active on a subset of Rab proteins and is devoid of exchange activity (Olofsson, Novick).

#### I.4.1. Characteristic Features of the GTPase domain (G domain)

The G domain is highly conserved in all guanine nucleotide binding proteins. The conserved G domain has a typical fold consisting of a mixed six-stranded  $\beta$  sheet and five helices. The GTPases have canonical GTP binding sequence elements which constitute the nucleotide binding

site. The most important contributions to nucleotide binding is made by the G1 motif, designated as the phosphate binding loop (p-loop) which interacts with the  $\beta$  and  $\gamma$  phosphates, the N/TKxD sequence (G3 motif) contacts the nucleotide base. The specificity to guanine is derived by the Asp side chain from the G4 motif, DxxG, which forms a hydrogen bond with the base, and also a main chain interaction with the invariant Ala from the G5 motif (SAK). The nucleotide bound form stabilises two flexible regions termed the switch regions. switch I (forming the G2 motif) comprising the invariant threonine and the switch II (comprising the G4 motif) with the invariant glycine interacting with the  $\gamma$  phosphate.

All the members of the heterotrimeric G proteins, several Ras related proteins like Ras, Rab, Ral, Rac, rho, Cdc42, Arf, Arl, Rab, Ran have the canonical GTP binding motifs as well as the conserved fold for the G domain. The G domains of the signal recognition particle SRP and its receptor SR show a divergent topology of the  $\beta$  sheet, in addition to extensions and insertions. Tubulin and the bacterial homologue FtsZ deviate structurally from these proteins with respect to their G domain.

The switch regions are not only conserved in GTPases, but also within the family of ATP-binding motor proteins. Kinesin and myosin have switch regions which sense the presence of a  $\gamma$  phosphate, the release of which is coupled to production of mechanical energy. The switch I region here contains a conserved serine and the switch II region comprises the same DxxG motif with an invariant glycine forming a main chain contact to the  $\gamma$  phosphate.

#### I.4.2. Deviation from the Switch GTPases

The GTP bound form is critical for transducing downstream cellular functions among many GTP binding proteins. The large GTPase dynamin participates in clathrin mediated endocytic processes and endocytosis via caveolae. The fact that the large GTPase dynamin could sever clathrin coated vesicles from plasma membrane upon GTP hydrolysis started a debate on the functioning of dynamin. Whether dynamin is a mechanochemical enzyme using the energy of hydrolysis for its effector function or a switch GTPase using the time from GTP binding to GTP hydrolysis for signal transduction? The switch GTPases have a very high affinity for GTP, a very slow rate of GTP hydrolysis and do not release GDP easily. In contrast mechanoenzymes such as dynein, kinesin and myosin have a low affinity for ATP, a high rate of ATP hydrolysis and readily release ADP. Dynamin like most motor proteins is a large protein, around 100 kDa, has low affinity for nucleotides, high rate of GTP hydrolysis and readily releases the hydrolyzed nucleotide. In addition, like muscle myosins and flagellar dyneins, dynamins assemble into complex polymers. Consistently, it has been shown that GTP binding alone is insufficient to support endocytosis, but

GTP hydrolysis which allows for a conformational change in the protein is necessary. The carboxy terminus of dynamin contains a proline rich domain (PRD) that extends to interact with SH3 domain containing proteins which implicates dynamin in signalling (Schmid et al., 1998). Up to now, dynamins have been shown to participate in both cell signalling and vesicle formation (sweitzer et al., 1998; zhang et al ., 2001) through “effector binding” and “constriction of the membrane” respectively.

The prime objective of the work is to understand the GTPase functions of the IFN inducible p47 GTPases, and how they exercise their resistance function.

### I.5. Objective of this Work

IFNs promote protection of the host by activating the Jak-STAT pathway to mediate rapid transcriptional induction of several hundred genes. Deletion of any of the components of this system highlights their importance for the proper functioning of the immune system. Since, many genes are induced or repressed by IFNs, and the functional roles of only a few have been described, it seems plausible that there are many more mechanisms to be unravelled in order to understand the complex cellular response in full. For example although mice deficient for the three-major IFN mediated antiviral pathways, PKR, RNase L and Mx were indeed sensitive to viral infection, were nevertheless able to mount a measurable antiviral response after IFN treatment and show greater resistance to infection than mice lacking IFN  $\alpha/\beta$  receptors or Stat1 (Zhou et al., 1999). This provides clear evidence for the existence of other uncharacterized interferon-dependent pathways. Therefore it seems important to look at the functions of other IFN induced genes, to understand the complex cellular response of this cytokine.

The p47 family and the p65 family of GTPases are abundantly induced by IFNs, and since their presence is necessary for the survival of the individual (not shown for p65), they probably have a defined role in the IFN response against specific pathogens. Localisation studies reveal the association of the p47 GTPases with the intracellular membranes (Sascha Martens unpublished data, Zerrahn et al., 2002, Taylor et al., 1997) suggesting their role in the processing of proteins or lipids, or in the vesicular trafficking pathway. It is a hypothesis that IIGP1 might be protecting the cell by interfering with the life cycle of specific pathogens. By doing so, it probably prevents the exploitation of the ER/Golgi membrane by the pathogens.

The objective of this study is to contribute to an understanding of the function of the p47 family of GTPases, specifically of IIGP1, by analysis of the biochemical properties and structure. This will provide essential information to understand the function and mechanism of action of IIGP-1 and

other p47 GTPases in cells. The p47 GTPases are apparently present only in the Muridae, yet understanding the mechanism of action of these GTPases could, firstly, help us in understanding the whole spectrum of the IFN response. Secondly, they may help us to identify the systems that compensate for the absence of the p47 family in humans. Thirdly, they will help us to describe the uniqueness of the immune system in different organisms. Finally, we will gain insight into an aspect of pathogen vulnerability that is not apparent from human systems.

The work presented here attempts to understand the functioning of IIGP1. The first part of the work emphasizes the GTPase properties of IIGP1 by *in vitro* biochemical characterization. A detailed analysis of the nucleotide binding affinities of IIGP1, the kinetics of the binding reaction, and the kinetics of GTP hydrolysis have been investigated using various biochemical and biophysical methods. This part also describes cellular studies of IIGP1, concerning its location and distribution in the cell, and preliminary studies to identify interacting molecules. The second part describes the structure of IIGP1 and a programme of site-directed mutagenesis directed at the nucleotide binding site and residues involved in putative homotypic molecular interactions, and their *in vivo* and *in vitro* characterisation.





## II. MATERIALS AND METHODS

### II.1. Chemicals and Other Accessories

All chemicals were purchased from Aldrich (Steinheim), Amersham-Pharmacia (Freiburg), Applichem (Darmstadt), Baker (Deventer, Netherlands), Boehringer Mannheim (Mannheim), Fluka (Neu-Ulm), GERBU (Gaiberg), Merck (Darmstadt), Pharma-Waldhof (Düsseldorf), Qiagen (Hilden), Riedel-de-Haen (Seelze), Roth (Karlsruhe), Serva (Heidelberg), Sigma-Aldrich (Deisenhofen), ICN biochemicals, Oxoid, Hampshire UK, DNA standard markers from Gibco-BRL (Eggenstein), Agarose for gel electrophoresis from FMC, Bioproducts, Rockland, Maine USA, developing and fixing solution for western blot detection from G158, AGFA, Luminol (Sigma), P-coumaric acid from Fluka. Deionised and sterile water (seral™) was used for all the buffers and solutions, Ultra pure water derived from Beta 75/delta UV/UF from USF Seral reinstwassersysteme GmbH, Ransbach, Baumbach equipped with UV (185/254nm) and ultrafiltration (5000 kd cut off). pH values are adjusted for room temperature unless specified.

### II.2. Materials

Sterilefilter FP 030/3 0,2  $\mu\text{m}$  and ME 24 0,2  $\mu\text{m}$  (Schleicher and Schüll, Dassel)

Ultrafiltration device VIVASPIN 10, 30 (Vivascience (Lincoln, USA)

Nitrocellulose transfer membrane PROTRAN (Schleicher and schüll, Dassel)

3MM Whatmann paper (Sigma)

100 Sterican 0,50 x 16mm hypodermic needles(B/Braun, Melsungen AG)

0.2 $\mu\text{M}$  and 0.45 $\mu\text{M}$  sterile filters (schleicher and schuell)

Superdex 200 (Amersham Pharmacia, Freiburg)

GSH-Sepharose superflow (Amersham Pharmacia, Freiburg)

Protein A Sepharose CL4B (Amersham Phamacia, Freiburg)

Film, X-OMAT LS and AR, Kodak, Sigma

All plastic ware for cell culture was from Sarstedt, Nümbrecht and Greiner, Solingen

### II.3. Enzymes/Proteins

Restriction Enzymes from New England Biolabs (Bad Schwalbach) or Clonetech (Heidelberg)

Protease Inhibitor cocktail, Complete mini (Böhringer), Pefabloc (Roth)

Pyrococcus furiosus (Pfu) DNA Polymerase (Promega, Mannheim)

T4 DNA polymerase (New England Biolabs )

RNase A (Sigma)

Shrimp Alkaline Phosphatase (SAP),USB, Amersham)

Thrombin (Serva, Heidelberg)

1Kb ladder for Agarose gels (Gibco)

Rainbow –Molecular weight marker-Precision protein standards™ ( Biorad)

SDS-7 Protein Standard Marker 14.2; 20; 24; 29; 36; 45 and 66 kDa (Sigma, Diesenhofen)

SDS-6 protein standard marker 29; 45; 66; 97.4; 116 and 205 kDa (Sigma, Diesenhofen)

#### II.4. Reagent Kits

Plasmid Mini and Midi kit (Qiagen ,Hilden)

*Qia quick gel extraction kit* (Qiagen, Hilden)

*Terminator-cycle Sequencing kit* (ABI PRISM)

QuikChange™ *Site directed mutagenesis kit*

#### II.5. Vectors

PGW1H ( British Biotech, Oxford, England)

pGEX-4T-2 (Amersham Pharmacia, Freiburg)

#### II.6. Oligonucleotides

All oligonucleotides from Sigma ARK. They are supplied as powder and are resuspended to a final concentration of 10 nMoles. 1 µl used for each PCR reaction.

GTPI-3' CCCCCCCC GAATTCCATGGAAGAGGCAGTTGAGTCA

GTPI-5' CCCCCCCC GAATTCCTAATGATGATGATGATGATGAGGA  
TGAGGAATGGAGAGTC

L44R-s CTCAATTTGATTGAAAGAAGGATGAGAAAAGGG

L44R-As CCCTTTTCTCATCCTTCTTTCAATCAAATTGAG

K48E-s GAATTAAGGATGAGAGAAGGGAATATTC AGTTG

K48E-As CAACTGAATATTCCTTCTCTCATCCTTAATTC

K48A-s GAATTAAGGATGAGAGCAGGGAATATTCAGTTG

K48A-As CAACTGAATA TTCCCTGCTCTCATCCTTAATTC

S172R-s ATTGCCAAAGCAATCAGAATGATG AAGAAGGAA

S172R-As TTCCTTCTTCATCATTCTGATTGCTTTGGCAAT

M173A-s ATTGCCAAAGCAATCAGCGCTATGAAGAAGGAATTCTAC

M173A-As GTAGAATTCCTTCTTCATAGCGCTGATTGCTTTGGCAAT

K82A-s GAGACGGGATCAGGGGCTTCCAGCTTCATCAAT

K82A.-As ATTGATGAAGCTGGAAGCCCCTGATCCCGTCTC

D186N-s GTGAGAACCAAGGTGAATTCTGACATAACAAAT

D186N-As ATTTGTTATGTCAGAGTTCACCTTGGTTCTCAC

## II.7. Constructs

### II. 7.1. pGEX Constructs

#### II.7.1.1. pGEX p47 Constructs

Constructs	N-terminus	C-terminus
IIGP1-wt	GSPGIPGSTT-MGQ--	-
IIGP-2	GSPGIPGSTT-MGQ--	-
GTPI	GSPGIPGSTT-MPT--	-
GTPI-his	GSPGIPGSTT-MPT--	-IPHP-HHHHHH
IGTP	GSPGIPGSTT-MDL--	-
LRG-47	GSPGIPGSTT-MKP--	-

#### II.7.1.2. pGEX IIGP1 Constructs

Constructs	N-terminus	C-terminus
IIGP1-m	GSPGIPGSTT-MGQ-- -	-CL-KLGRLERPHRD
IIGP1-his	GSPGIPGSTT-MGQ-- -	-CLRN-HHHHHH
IIGP1-mutants (Interface mutants as well as binding mutants)	GSPGIPGSTT-MGQ-- -	-CLRN

- a) Interface I mutants:- L44R, K48A, K48E; b) Interface II mutants :- S172R, M173A;  
c) Double mutant :- L44R/S172R [L/S]; d) Binding mutants :- G2V, K82A, D186N.

#### II.7.2. pGWIH Constructs

Constructs	N-terminus	C-terminus
IIGP1-wt	MGQ----	-CLRN
IIGP1-m	MGQ---	-CL-
IIGP1-Nm	MAQ---	-CLRN
IIGP1-his	MGQ---	-CLRN-
IIGP1-	MGQ---	-CLRN

- a) Interface I mutants:- L44R, K48A, K48E; b) Interface II mutants :- S172R, M173A  
c) Double mutant :- L44R/S172R [L/S]; d) Binding mutants :- G2V, K82A

## II.8. Media

### Luria Bertini (LB)- Medium

10 g Bacto Tryptone

5 g Yeast Extract

10 g NaCl

Distilled water 1Litre

### LB Plate Medium

10 g Bacto Tryptone

5 g Yeast Extract

10 g NaCl

15 g Bacto Agar

Distilled water 1Litre

### Terrific Broth (TB) Medium

12 g Bacto Tryptone

24 g Yeast Extract

4 ml Glycerol

0.17 mM  $\text{KH}_2\text{PO}_4$

0.072 mM  $\text{K}_2\text{HPO}_4$

Distilled water 1 Litre

### IMDM (Iscove's Modified Dulbecco's Medium) Gibco BRL, Eggenstein.

10% FCS, 2 mM 1-Glutamine, 1 mM Sodium pyruvate, 100 U/ml Penicillin, 100 µg/ml Streptomycin, 1x non-essential amino acids. (mainly used for the growth of L929 cells).

### DMEM (Dulbecco's Modified Eagle Medium), Gibco BRL, Eggenstein.

10% FCS, 2 mM 1-Glutamine, 1 mM Sodium pyruvate, 100 U/ml Penicillin, 100 µg/ml Streptomycin, 1x non-essential amino acids. (mainly used for the growth of MEFs).

### DMEM (Dulbecco's Modified Eagle Medium)- Starvation Medium

1x, 0.1 µ filtered, with high glucose and pyridoxine hydrochloride, without sodium pyruvate, L-cystine and L-methionine. FCS was dialysed against 1x PBS overnight at 4°C and was added to the medium, also pyruvate and L-glutamine.

## II.9. Bacterial Strains

XL1-Blue - *recA1*, *end A1*, *gyrA96*, *thi-1*, *hsdR17*, *supE44*, *relA1*, *lac*, [*F'*, *pro AB*, *lacI<sup>q</sup>ZΔM15*, *Tn10* (*Tet<sup>r</sup>*)], (Bullock *et al.*, 379)

DH5α - *80dlacZΔM15*, *recA1*, *endA1*, *gyrA96*, *thi-1*, *hsdR17* (*r<sub>B</sub><sup>-</sup>*, *m<sub>B</sub><sup>+</sup>*), *supE44*, *relA1*, *deoR*, *Δ(lacZYA-argF)U169*; Bachmann (1983,1990), Sambrook J. *et al.* (1989).

BL-21 - *E. coli* B, *F<sup>-</sup>*, *omp T*, *hsd S* (*r<sub>B</sub><sup>-</sup>* *m<sub>B</sub><sup>-</sup>*), *gal*, *dcm* (Studier *et al.*, 1986)

## II.10. Antibiotics

Ampicillin (Sigma) was prepared as a stock solution of 100 mg/ml in water.

kanamycin (Sigma) stock solution was made as 10 mg/ml in water.

Penicillin/Streptomycin (Gibco BRL, Eggenstein)

## II.11. Cells

Mouse embryonic fibroblasts (MEFs)

L929 cells (Mouse fibroblast cell line)

## II.12. Radiisotope

PRO-MIX L- [<sup>35</sup>S] *in vitro* Cell Labelling Mix (Amersham-Pharmacia, Freiburg),

## II.13. Antibodies

IgG anti-Mouse peroxidase coupled (Sigma),

IgG anti-Rabbit peroxidase coupled (Sigma)

Second stage antibodies were goat anti-mouse Alexa 546, 1:100 (Molecular Probes), Goat anti-rabbit Alexa 546, 1:1000 (Molecular Probes).

α 10D7, α 10E7 and α 5D9 monoclonal antibodies (Zerrahn *et al.*)

## II.14. Detergents

3[(3-Cholamidopropyl)dimethylammonio]-1-propanesulfonate (CHAPS), Triton-X-100 (Tx-100), Polyoxyethylensorbitanmonolaureat (Tween-20), Triton-X-114 (Tx 114), Thesit, IGEPAL-CA 600 (NP-40) all from Sigma. Digitonin (Wako), sodium dodecyl sulfate (SDS) Merck, Darmstadt.

## II.15. Equipments

Centrifuges-Biofuge 13, Heraeus, Sigma 204, Sigma 3K10, Labofuge 400R, heraeus; Sorvall RC-5B, Du pont instruments, Optima TLX Ultracentrifuge, Beckmann, BioRAD Gel dryer, Model-583, BioRad Power pack 300bzw. 3000, gel electrophoresis chamber, Cambridge electrophoresis limited, Biorad Mini Protean II, PTC-100,MJ Research,Inc; Centrifuge tubes 15ml, TPP, Switzerland; 50ml Falcon, Becton Dickenson, USA.Soft-Pac <sup>TM</sup> Module, Du <sup>R</sup> Spectrophotometer.

## II.16. Protocols

### II.16.1. Molecular Biology

All the constructs mentioned above were amplified/ cloned and propagated using the following methods. All protocols were adapted from Sambrook, J., Fritsch, E.F., and Maniatis, T., Vol. 1,2,3 (1989), or from the cited references.

#### II.16.1.1. Agarose Gel Electrophoresis

DNA was evaluated by agarose gel electrophoresis where the negatively charged DNA fragments migrate through polymerised agarose (0.9%) towards the anode, by applying electric current (less than 5 volts per centimeter of the gel) in a buffer that establishes a pH and provides ions for conductivity (1x TAE; 0.04 M Tris, 0.5 mM EDTA, pH adjusted to 7.5 with acetic acid) and the DNA was stained with Ethidium bromide (0.5 µg/ml), a fluorescent dye which intercalates between nucleotide bases, and the migration of the DNA molecules was recognised by using bromophenol blue as tracking dye (Studier, 1973)

#### II.16.1.2. Polymerase Chain Reaction (PCR)

The selective amplification of specific DNA fragments from vectors for cloning was made by PCR using pfu polymerase, a thermostable DNA polymerase and two specific primers (Mullis and Faloona, 1987). The plasmid pGW1H with the 1.2 Kb insert for GTPI was resuspended in 10 mM Tris/Hcl pH 8.0. Only 1µl (1 ng) of the template, 5U polymerase; 1x PCR buffer, 5 pmol each of the 5' and the 3'primer, 0.2 mM dNTPs was added, and made to a final volume of 50 µl. The PCR conditions were 1', 95°C; 35x (30'', 95°C; 30'' 62°C; 1', 72°C); 2', 72°C; 4°C). the annealing temperature was calculated as 2 x (AT) + 4 x (GC).

#### II.16.1.3. Restriction Enzyme Digestion

The DNA to be cloned into a vector (insert DNA) and the vector DNA to be cloned into, was independently restricted with the respective enzymes to make the compatible termini with 5' phosphate residues and 3' hydroxyl moieties. All constructs were made by cloning the SalI fragments of all the p47 GTPases mentioned above into a SalI restricted pGEX / pGW1H vector. 5-10 U of enzyme was used per  $\mu\text{g}$  of DNA, 1x adequate buffer for the enzyme, 1x BSA was used when suggested for the respective enzyme, in a final volume of 20  $\mu\text{l}$  /  $\mu\text{g}$  of DNA and incubated at 37°C for 1 hour (Luria, 1970).

#### II.16.1.4. Purification of DNA Fragments

The specific size of the restricted DNA to be cloned, was cut and purified from the agarose gels after adequate separation. The purification was done based on the high pure PCR/ gel purification kit. The gel fragment is dissolved in 3 M guanidine-thiocyanate, 10 mM Tris-HCl, 5% ethanol (v/v) pH 6.6 at 50°C for 15-20 min, and then adsorbed onto glass fibres, washed with 20 mM NaCl, 2 mM Tris-HCl, pH 7.5, 5% ethanol, to remove salts, free-nucleotides (below 100 bp) and proteins. Finally the DNA is eluted with a low salt buffer 10 mM Tris-HCl, 1 mM EDTA, pH 8.5. (The initial experiments regarding the purification of DNA is well described in (Brownlee and Sanger, 1969; Carter and Milton, 1993)

#### II.16.1.5. Ligation

1: 3 molar ratio of linearised vector prior dephosphorylation (pM) as opposed to insert DNA (purified), T4 DNA ligase (1U), 1x DNA ligase buffer in a final volume of 10  $\mu\text{l}$ , and incubated overnight at 16°C (Bercovich et al., 1992; Michelsen, 1995). De-phosphorylation was done on the linearised vector to prevent intramolecular ligation. The linearised vector was incubated at 65°C for 20 min to inactivate the restriction enzyme, shrimp alkaline phosphatase (.1U/  $\mu\text{g}$  DNA), incubated for 1h at 37°C, and inactivated at 65°C for 20 min. The dephosphorylated DNA was purified as described above.

#### II.16.1.6. Preparation of Competent Cells

A single colony from a particular strain of *E.coli* (DH5 $\alpha$  and BL-21) was grown overnight in 2 ml LB medium with 0.02 M MgSO<sub>4</sub>, 0.01 M KCl with vigorous shaking (~300 rpm). It was diluted 1:10 into fresh medium with the same constituents for an hour and a half, at 37°C to an OD<sub>600</sub> of 0.45, on ice for 10 min after which the cells were resuspended by spinning at 6000 rpm,

4°C for 5' in a centrifuge which was prior cooled to 4°C. The cells were resuspended in TFB I (30 ml/100 ml culture), 5 min on ice, cells pelleted again by centrifugation at 6000 rpm, 4°C for 5', resuspended in TFB II (4 ml /100 ml culture). 100 µl aliquots of the competent bacteria were made and were frozen in -80°C (Chung and Miller, 1988).

Composition of the buffers:- TFB I (30 mM potassium acetate, 50 mM MnCl<sub>2</sub>, 100 mM RbCl<sub>2</sub>, 10 mM CaCl<sub>2</sub>, 15% w/v glycerin, pH 5.8; TFBII (10 mM Mops, pH 7.5, 75 mM CaCl<sub>2</sub>, 100 mM RbCl<sub>2</sub>, 15% w/v glycerin. Both the solutions were sterilised and stored at 4°C. DH5α was used for the maintenance of the plasmids and BL-21 cells for protein expression)

#### II.16.1.7. Transformation

Competent bacteria (100 µl) were thawed in ice, the ligation mix was added to the competent bacteria and incubated on ice for 30 min, heat-shock was given at 42°C for 90 sec, 1 ml of LB medium added and incubated at 37°C in a Rotator for an hour. The bacteria were pelleted by centrifuging at 8000 rpm for 1 min, resuspended in 100 µl medium and plated in LB agar plates with Ampicillin (1 mg/ml) (Cohen et al., 1972).

#### II.16.1.8. Plasmid DNA Isolation

The plasmid DNA was prepared using the Qiagen midi-prep protocol. A single colony was inoculated into LB medium with Ampicillin (1 mg/ml) was grown overnight with vigorous shaking (~300 rpm) at 37°C, 1:10 diluted into fresh LB/Ampicillin medium and grown overnight (100 ml culture). The cells were pelleted, and resuspended in 50 mM Tris, pH 8.0, 10 mM EDTA, 100 µg/ml RNase A; and were lysed with 200 mM NaOH (denatures proteins, plasmid and chromosomal DNA), 1% SDS (solubilises phospholipid and protein constituents of the cell membrane (Birnboim and Doly, 1979), The RNA was cleaved by RNase A during this alkaline lysis, and the lysate was neutralised by adding 3M potassium acetate pH 5.5, which leads to salt detergent complexes as SDS precipitates and all the cellular debris, chromosomal DNA and denatured proteins settle down, leaving the plasmid DNA in the supernatant. The whole lysate mix was then passed through Qiafilter cartridges which further remove all the debris, and the supernatant was selectively bound to the Qiagen anion exchange resin where the negatively charged phosphates in DNA bind to the DEAE (Diethylaminoethanol) groups on the surface of the resin (silica beads). All the impurities are further removed upon washing the resin with a medium salt buffer like 1M NaCl, 50 mM MOPS, pH 7.0, 15% isopropanol and finally the bound plasmid was eluted with the high salt buffer 1.25M NaCl, 50 mM MOPS, pH 8.5, 15% isopropanol.



The eluted DNA was desalted and concentrated by isopropanol precipitation at RT, and the DNA pellet was further washed with 70% ethanol, as it is more volatile and to remove the remaining salt, the pellet was air-dried and resuspended in a small volume of Tris / EDTA pH 8.0. All the plasmids and constructs were prepared using this method, and were used for transfection studies, and sequencing studies.

#### II.16.1.9. Determination of the Concentration of DNA

The concentration of DNA was measured using a spectrophotometer at 260 nm. The purity of the DNA solution was estimated using the ratio of OD readings at 260 nm and 280 nm, where pure preparations of DNA have an OD<sub>260</sub>/OD<sub>280</sub> ratio of 1.8. The concentration was calculated according to the following equation (Glasel, 1995).  $c = A_{260} \times 50 \mu\text{g/ml} \times \text{dilution factor}$

#### II.16.1.10. Site Directed Mutagenesis

Site directed mutagenesis was carried out using the using the “QuikChange™ XL Site-Directed Mutagenesis” protocol from Stratagene. PCR was carried out using pGEX-IIGP1 as the template, the two respective oligonucleotide primers (sense and antisense) for each of the mutants, each primer complementary to opposite strands of the vector. Therefore new strands synthesised during temperature cycling by Pfu polymerase (Stratagene), under these conditions ; denaturing temperature of 95°C for 30s, annealing temperature of 55°C for 60s and an extension with 72°C for 13min involving 15 cycles. The PCR product was then digested with Dpn1 enzyme (10U) at 37°C for 1 hour. Since Dpn1 restricts methylated and hemi-methylated DNA, only the newly synthesized DNA with the mutations are selected, and they are transformed into BL-21 competent cells (Wilkinson et al., 1983; Winter et al., 1982).

#### II.16.1.11. DNA Sequencing

All the plasmid DNA was sequenced using the *ABI Prism<sup>R</sup> BigDye<sup>TM</sup> Terminator Cycle Sequencing Ready Reaction Kit* (PE Applied Biosystems), using fluorescently labelled dideoxynucleotides based on the dideoxy-chain termination method by Sanger et al 1977 (Lee et al., 1992). DNA sequencing was done for the analysis of all the plasmid constructs and also the mutants. DNA (0.5  $\mu\text{g}$ ), respective primer (5 pmole), 2  $\mu\text{l}$  (*Big Dye<sup>TM</sup> terminator ready reaction mix* from ABI), in a total volume of 10  $\mu\text{l}$ . Sequencing reaction was carried out (5', 96°C; 25x (30'', 96°C; 15'' 50°C; 4', 60°C); 4°C, infinity)). The annealing temperature was calculated using the equation  $2x (\text{AT}) + 4x (\text{GC})$ .

The DNA was precipitated with 1/10<sup>th</sup> volume 3M sodium acetate and 2 volumes of 100 % ethanol (Maniatis *et al.* 1989), -20°C for 30 min, centrifuged at 10,000 rpm, 4°C, 15 min, 70 % alcohol

wash, pellet dried at 65°C. the sequencing was done on an automated sequencer (ABI 373A), by Ms. Rita Lange.

## II.16.2. Expression and purification of proteins

### II.16.2.1. Growth and Harvest of Bacteria

All pGEX constructs were transformed into *E.coli* BL-21 cells. Cells were grown in a 37°C shaker at 180 rpm to an  $A_{600}$  of 0.4 and IIGP1 was expressed as a GST fusion protein upon overnight induction with 1 mM Isopropyl- $\beta$ -D-thiogalactoside at 18°C where the proteins were most soluble. (The proteins were also expressed under varying temperature conditions (ranging from 18°C to 37°C), and different IPTG concentrations (0.1 mM to 1 mM), and induction at different optical density ( $A_{600}$  0.3 to 0.9) and varying the time of induction (2h- to overnight), in order to attain maximum solubility). The induced cells were pelleted at 1500 g for 10 min, 4°C; the cells were weighed and resuspended in 1x PBS, 2 mM DTT; (3 ml/gm) and were frozen at -80°C (Studier et al., 1990).

### II.16.2.2. Glutathione-Sepharose Affinity Chromatography

The cells were thawed, 200  $\mu$ M Pefabloc (Roth) was added to prevent protein degradation, and were lysed using a microfluidizer (Microfluidics corporation, USA) at a pressure of 600 kPa. The protein was extracted from the soluble fraction after centrifugation at 50,000 g, 4°C, 30 min. The protein was purified in a glutathione-Sepharose-Superflow affinity column (Amersham-Pharmacia Biotech) which has a volume of 50 ml with a flow rate of 5 ml/min after equilibration with 1x PBS (40 mM  $\text{Na}_2\text{HPO}_4$ , 10 mM  $\text{NaH}_2\text{PO}_4$  pH 7.5, 50 mM NaCl) and 2 mM DTE (two column volumes). The column was then washed with 10 column volumes of the buffer. The GST domain was cleaved by overnight incubation of the protein with thrombin (10 U/ml from Serva) on the resin at 4°C. The cut protein was eluted with 1x PBS, 2 mM DTT, 200  $\mu$ M Pefabloc. The cut GST fragment was eluted with 20 mM Glutathione in 1x PBS buffer. The column was regenerated by washing with two column volumes of 6M Guanidinium hydrochloride in 1x PBS, and further with 1xPBS (Guan and Dixon, 1991).

### II.16.2.3. Concentrating Proteins by Ammonium Sulphate Precipitation

The eluted proteins from the glutathione affinity column was concentrated by ammonium sulphate precipitation. Ammonium sulphate was added to the eluted protein slowly to a final concentration of 3 M for an hour at 4°C, and then centrifuged at 15,000g for 30 min, 4°C.

#### II.16.2.4. Size-Exclusion Chromatography

The protein was subjected to size exclusion chromatography in order to exchange the buffer and as a further purification procedure, in a Superdex 75 column either (small or big depending on the amount of the protein) (Amersham-Pharmacia Biotech) equilibrated in buffer 2 (50 mM Tris/HCl (pH 7.4), 5 mM MgCl<sub>2</sub>, 2 mM DTE). The protein was loaded in a volume of 500 µl for the small column, or 2 ml for the large column, with a respective flow rate of 0.5 ml/ min and 0,1 ml/ min respectively. All the fractions were collected and subjected to SDS-polyacrylamide gel electrophoresis. The fraction collector used was SigmaChrom GFC-1300 (Supelco, Belfonte, USA) (Bollag, 1994).

#### II.16.2.5. Concentrating Proteins by Ultra-filtration

After analysis of the fractions by SDS/PAGE, they were concentrated by a centrifugal concentrator (Vivascience, Lincoln, USA) by centrifugation at 3000g, 4°C, to 50 mg/ml with a 10 kDa cut off filter. Aliquots were shock-frozen in liquid nitrogen and were stored at -80° C.

#### II.16.2.6. SDS-Polyacrylamide Gel Electrophoresis (Shapiro and Maizel, Jr., 1969).

For the analysis of proteins, discontinuous one-dimensional gel electrophoresis was carried out under denaturing conditions in the presence of 0.1 % SDS (Laemmli method). It comprises a separating gel (10% or 12%) overlaid by a stacking gel (5%) as documented by Coligan *et al* 1997). The protein samples were dissolved in 1x SDS sample buffer (60 mM Tris/HCl pH 6.8; 2.3% w/v SDS, 5% Glycerol; 0.1 mg/ml bromophenol blue (Sigma). B-mercaptoethanol (7%) was used as a reducing agent (added fresh), to disrupt the disulphide bonds. The samples were boiled at 100°C for 5 minutes prior loading. The gels were run at 20 mA for 2 hours (small gels) or 40 mA (large gels) in a running buffer with 25 mM Tris; 190 mM Glycine; 0.1% SDS in mini-Protean<sup>R</sup>II gel chambers (Biorad) or the big gel chambers. Ammonium persulfate (APS) Roth, Karlsruhe, Acrylamide (Roth), N,N,N',N'- Tetramethyl-ethylenediamine (TEMED), sigma (deisenhofen). After SDS-PAGE the gels were stained with Coomassie staining solution (1.25g Coomassie Brilliant Blue R-250 (Sigma), 500 ml methanol ; 100 ml acetic acid; 400 ml water) at RT, shaker for 20 min, destained with 30% methanol, 10% acetic acid, at RT, shaker, by repeatedly exchanging with fresh destain (Sedmak and Grossberg, 1977). The gels were dried under vacuum pressure at 80°C for 2 hours.

### II.16.3. Biochemical and Biophysical methods

#### II.16.3.1. Determination of Protein Concentration by Absorption Spectroscopy

The concentration of IIGP1 was determined by ultraviolet-visible spectrophotometry at 280 nm with the calculated molar absorption coefficient based on the number of tyrosines, tryptophan and cysteine residues (Gill and von Hippel, 1989). All the purified proteins were concentrated in the range of 40- 80 mg/ml.

#### II.16.3.2. Fluorescence Spectroscopy

Mant-nucleotides (mant = 2'3'-O-(N-methylanthraniloyl)) were used as fluorescent probes as they exhibit protein-binding properties similar to those of natural nucleotides. The mant fluorophore allows the detection of conformational changes upon nucleotide-binding therefore serving as a monitor for protein-protein or protein-ligand interactions. The fluorescence measurements were done in Fluoromax 2 Spectro fluorimeter (SPEX instruments S.A., Inc., Edison, USA) in 0.4 x 1 cm<sup>2</sup> cuvettes at 20°C in 50 mM Tris/HCl, pH 7.5, 5 mM MgCl<sub>2</sub>, 2 mM DTE.

In the fluorescence titrations, the mant-nucleotides (0.5 μM) were excited at 360 nm and the fluorescence was monitored at 430 nm (Fluoromax 2, Spex Industries). The increase in fluorescence upon addition of the protein was measured, and at each step the values were averaged over one minute. The equilibrium dissociation constants  $K_d$  was obtained by drawing a fit to the data as described by (Herrmann and Nassar, 1996)

#### II.16.3.3. Stopped Flow Apparatus

The binding of mant-nucleotides (mGMP, mGDP, mGTP and mGTPγS) to all three purified IIGP1 proteins was measured by stopped-flow. In the stopped-flow experiments, at least a (5:1) ratio of protein to nucleotide concentrations were mixed together providing conditions for pseudo first-order binding kinetics. The time course of the increase in mant fluorescence upon binding of the protein to the mant-nucleotides was recorded (SM-17, Applied Photophysics, UK). Mant fluorescence was excited at 360 nm and monitored through a 405 nm cut off filter. In each case a single exponential function could be fitted to the data, yielding the observed rate constant  $k_{obs}$ . A linear fit of the plot of  $k_{obs}$  versus protein concentration was obtained, the slope of the straight line denoting the association rate constant ( $k_{on}$ ) and the intercept, the dissociation rate constant ( $k_{off}$ ). The  $K_d$  values are calculated from the ratio of  $k_{off}$  and  $k_{on}$ .

#### II.16.3.4. Isothermal Titration Calorimetry

Isothermal titration calorimetry (Microcal Inc., USA) was used to measure the binding of non-labelled nucleotides to IIGP1. The heat of binding was detected upon stepwise addition of nucleotide into a cell containing the protein. The data was fitted using the manufacturer's software, yielding the enthalpy of the reaction, the dissociation constant ( $K_d$ ) and the stoichiometry factor ( $N$ ) as described in (Wiseman et al., 1989).

#### II.16.3.5. Reverse-Phase HPLC

The kinetics of hydrolysis of GTP to GDP by IIGP was monitored by Reverse-phase HPLC. Different concentrations of nucleotide and protein were mixed and incubated at 37°C in buffer 2 and at different time points, aliquots were removed and subjected to HPLC analysis. Samples were run isocratically on a reverse phase  $C_{18}$  column (0.4 x 25 cm filled with 5 $\mu$ m ODS Hypersil, Bischoff, Leonberg, Germany) with a  $C_{18}$  pre-filter (10 x 4.6 mm with 5 $\mu$ m ODS Hypersil) in 7.5% acetonitrile in buffer 3 (10 mM tetrabutylammonium bromide, 100 mM  $K_2HPO_4/KH_2PO_4$  (pH 6.5), 0.2 mM  $NaN_3$ ) at a flow rate of 2ml/min. Nucleotides were detected at 252 nm in a UV absorption detector (Beckmann system gold 166). The concentration dependent GTPase activity of IIGPwt/IIGPm/IIGPHis was measured at a GTP concentration of 700  $\mu$ M, and a range of protein concentrations.

#### II.16.4. Light scattering

Dynamic light scattering (DLS) was performed using a DynaPro molecular sizing instrument (Protein Solutions) equipped with a temperature control unit. The sample was filtered through a microsampler cuvette where 50  $\mu$ l of the sample was passed through a filtering device using a 0.02  $\mu$ m filter into a 12  $\mu$ l Quartz cuvette. The sample (either protein alone, or protein with different nucleotides) in buffer 2 was illuminated by a 25 MW, 750 nm wavelength solid state laser. The time scale of scattered light intensity fluctuation for each measurement was evaluated by autocorrelation from which the translational diffusion coefficient ( $D_T$ ) was calculated. The molecular weight (MW) was estimated from the hydrodynamic radius  $R_H$  which was derived from the  $D_T$  using the Stokes-Einstein equation and the sample temperature ( $T= 4^\circ C$ ) using the standard curve of Mw versus  $R_H$  for globular proteins.

The data was analysed by Dynamics 4.0 and Dyna LS software. For qualitative measurements, a conventional fluorescence spectrometer was used, where the sample was excited at 350 nm and monitored at the same wavelength.

#### II.16.5. Crystallisation

IIGP1 was crystallised using the vapour diffusion method at RT in hanging drops over a reservoir solution containing 10% PEG-20K (w/v), 200 mM MES pH 6.5, and 5% ethanol (v/v) with a protein concentration of 15mg/ml. The crystals grew over a time of 2-3 days to a size of 0.2-0.3 mm<sup>3</sup>. Seleno-methionine crystals were grown at 4°C, using hanging drop setups with a reservoir solution containing 7.5% PEG 20K (w/v), 170 mM MES pH 6.5, 12.5 mM DTE and 1.5% heptanetriol (w/v) and a protein concentration of 10 mg/ml.

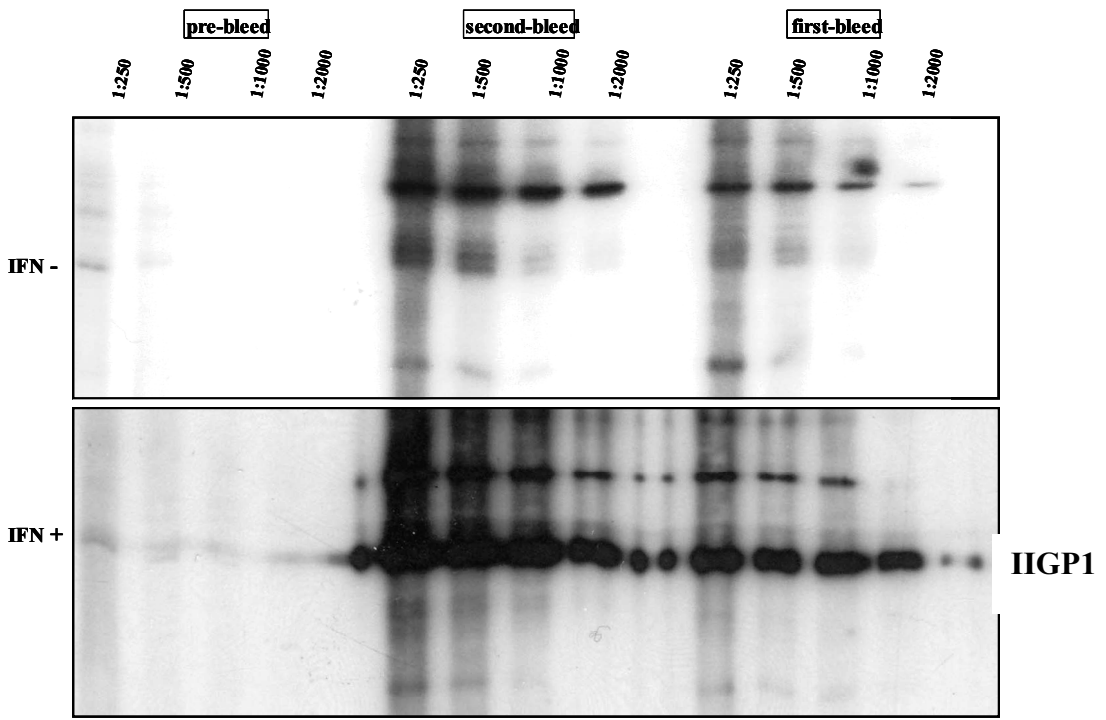
#### II.16.6. Cell Biology

##### II.16.6.1. IIGP1 Specific Polyclonal Rabbit Antiserum ( $\alpha$ 165)

A 6 month old rabbit was obtained from a local breeder. The rabbit was sensitized subcutaneously with 100  $\mu$ g purified recombinant IIGP1 in 'complete Freund's adjuvant' (Difco Lab., Detroit, MI). Booster injections were given subcutaneously after four weeks (100  $\mu$ g purified IIGP1 in 'incomplete Freund's adjuvant' (Difco Lab., Detroit, MI) and intravenously after another three weeks (50 $\mu$ g purified IIGP1 in 0.01 M phosphate-buffered saline (PBS), pH 7.2). The final bleed was taken three weeks after another intravenous injection of 50 $\mu$ g purified IIGP1 in 0.01 M PBS, pH 7.2. Antisera from all the bleeds, the pre-bleed prior immunisation, first, second, third, and the fourth bleeds were obtained by centrifugation of the clotted blood at 2000g and stored at -20°C (Gilles et al., 1980).

Western blots were done on IFN- $\gamma$  induced and uninduced L929 cell lysates using different dilutions of the pre-bleed, first bleed, second bleed and the third bleed to check the specificity for IIGP1 as shown in the figure 2.1A and 2.1B. The first, second and the third bleeds recognise induced IIGP1 as indicated in the figure, as opposed to no staining in case of the uninduced and the pre-bleed control. The first and the second bleed do show additional background staining which is not observed in the third bleed.

2.1A



2.1B

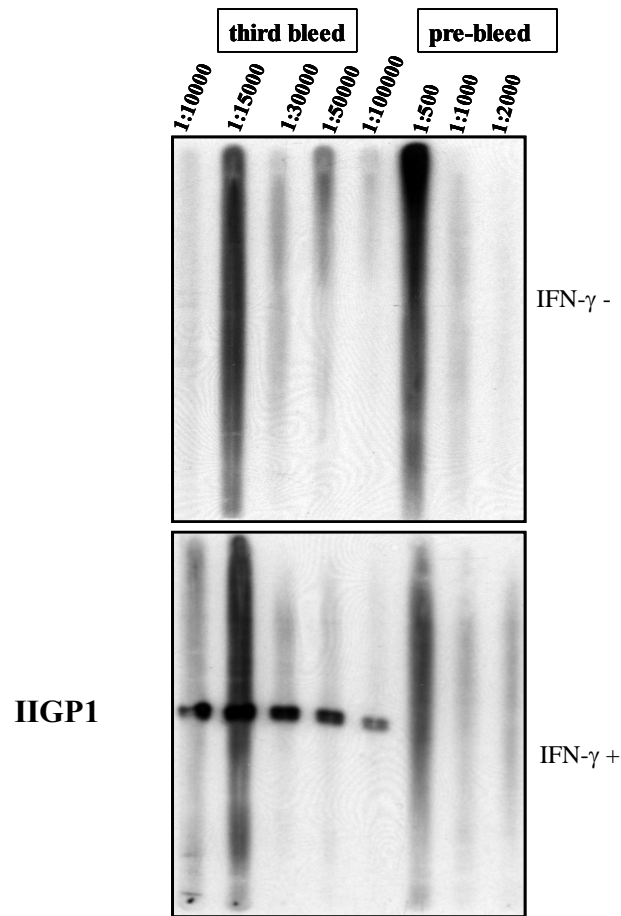


Figure 2.1 Immunoblots of IFN- $\gamma$  induced and uninduced L929 cells lysates with  $\alpha$  165 antiserum. L929 cells were either induced or uninduced with 200 U/ml IFN- $\gamma$ , 24 h post induction cells were lysed under hypotonic buffer conditions, and the post-nuclear supernatant and pellet were subjected to SDS-PAGE and western blotting. The blots were processed with several dilutions of the different bleeds of the  $\alpha$  165 antiserum, pre-bleed, first bleed and second bleed as shown in figure 2.1A and pre-bleed and the third bleed in figure 2.1B.

#### II.16.6.2. Western Blot (Burnette, 1981)

The gels after SDS-PAGE were transferred to nitrocellulose membranes by electroblotting. The gel was placed in contact to a nitrocellulose transfer membrane, and was sandwiched between four sheets of 3 MM Whatmann paper, two porous pads, and two plastic supports on either sides, soaked in a transfer buffer containing 25 mM Tris; 190 mM Glycine. The sandwich was then placed between platinum plate electrodes, with the nitrocellulose filter facing anode, and the transfer was carried out at RT for 1 hour with a current of 0.5V. Ponceau S staining was used to locate proteins (0.1% (w/v) Ponceau S (Sigma) in 5% (v/v) acetic acid) after western blotting. It is a rapid, reversible stain (washed with water) which has no deleterious effects on the proteins (Nakamura et al., 1985).

#### II.16.6.3. Growth and Culture of Eukaryotic Cells

##### Mouse Embryonic Fibroblasts (MEFs)

Primary embryonic fibroblasts were isolated from C57BL/6J and 129/sV mice at day 14 post coitum [Torres, 1997] and cultured as described in [Boehm, 1998].

B. L929 cells (ATCC CCL-1) is a fibroblast cell line from CH3/An mouse (kindly received from Ulrich Kalinke; EMBL, Monterotondo, Italy)

L929 cells and MEFs were grown in 75cm<sup>2</sup> polystyrene tissue culture flasks (Sarstedt) with 5% CO<sub>2</sub> at 37°C in a incubator. IMDM with high glucose, without sodium pyruvate (Gibco); 15% fetal calf serum (FCS, Sigma), 1 mM sodium pyruvate; Gibco BRL), 100U/ml penicillin (Gibco BRL), 100 µg/ml streptomycin (Gibco BRL), 2 mM Glutamine (Gibco BRL), 1x non essential amino acids (Gibco). The cells (~ 10<sup>6</sup> cells /ml ) were washed twice in cold 1x PBS after trypsinisation (1x Trypsin, 2 min, RT), and resuspended in FCS (sigma) and 10% di-methylsulfoxide (DMSO, Sigma), immediately frozen at -80 °C. Transient transfection was done in L929 cells (grown upto 80% confluency) in 60 mm dishes by using FuGENE™ 6 reagent (Roche applied Science), a multiple component (mixture of cationic lipids) lipid based transfection reagent that complexes with DNA and transports DNA to the nucleus. 3µl Fugene /µg plasmid DNA was used, prior to diluting the Fugene reagent with serum free media.



#### II.16.6.4. Immunofluorescence

L929 cells were induced with 200U/ml of IFN- $\gamma$  or uninduced for 24 hours on sterile 22\*22 mm cover slips, or transfected with the respective constructs (harvested 48 hours post-transfection). The coverslips with cells were washed with 1xPBS for 5 min at room temperature (RT), and fixed with 3% paraformaldehyde at RT for 20 min, and further three subsequent washes with 1x PBS was done. The cells were permeabilised with wash buffer (1x PBS, 0.1% saponin) for 10 min and incubated with blocking buffer (1x PBS, 0.1% saponin, 3% BSA) for 1 hour. The respective primary antibody diluted to the appropriate working concentration with blocking buffer was used to stain the cells, in a Humid chamber for an hour. The cells were washed extensively with 10 ml wash buffer and incubated with the secondary antibody coupled to fluorescent Alexa 546 dye in a fluorescent chamber, and washed extensively as above. The cover-slips were mounted on the slides with a drop of Mowiol (anti.fade agent). The slides were analysed using an Axioplan II fluorescence microscope, a cooled CCD camera (Quantix) and the metamorph software (version 4.5, Universal Imaging Corp.). For deconvolution the Auto Deblur software (version 6.001, AutoQuant Imaging Inc.) was used. Mowiol was prepared by mixing 6 g glycerol with 2.4 g Mowiol (Calbiochem) and 6 ml ultrapure water at RT for 2 h. Further, 12 ml 0.2 M Tris, pH 8.5 was added to the mix, and incubated in hot water (50°C), O/N with frequent stirring to dissolve the Mowiol, centrifuged at 5000 g for 15' to remove the undissolved substances. Aliquots were frozen at -20°C.

#### II.16.6.5. Cellular Fractionation

L929 cells (80% confluent) in 100 mm dishes were induced with 200U/ml of IFN- $\gamma$  or uninduced for 24 hours, or transfected with the respective mutants as described above. The cells were scraped using a cell scraper in 1x PBS after removing the medium, and resuspended in a hypotonic buffer (10 mM Tris, pH 7.5, 10 mM NaCl, 1.5 mM MgCl<sub>2</sub>, and one tablet of Protease Inhibitor cocktail/10 ml buffer), 500  $\mu$ l /10<sup>7</sup> cells, for 30' at 4°C, ultracentrifuged using the Optima TLX Ultracentrifuge at 100,000g, 4°C, for 30 min. The supernatant (cytosolic fraction) was removed, the pellet (membrane fraction) was washed two times with hypotonic buffer to remove the residual cytosolic proteins loosely attached to the membrane. The membrane fraction was further lysed with a detergent buffer (1% Tx 100 in 1x PBS), for 30', 4°C, and the lysate was homogenised by passing through a 22 <sup>1</sup>/<sub>2</sub> g needle, centrifuged at 15,000 g, 4°C, 15 min to remove the residual pellet. The pellet was washed two times with Tx-100 buffer, before processing them for SDS-PAGE. Solubilisation with different detergent buffers (NP-40, Tx-100 are non-ionic detergents; Chaps is an Zwitterionic detergent and digitonin, a neutral detergent) were done as

described above for Tx-100, using 1% w/v detergent solution in 1x PBS. Tx -114 extraction was done using 1% Tx-100 in 1x PBS, on IFN- $\gamma$  induced L929 cells. The cells were incubated in the buffer for 1 hour, centrifuged at 15,000 g, 4°C, 15 min, and the post-nuclear supernatant was incubated at room temperature for 2-3 min, and centrifuged at 15,000 g, RT, 1' to separate the aqueous and detergent phases. The detergent phase is washed twice to remove the residual soluble proteins.

#### II.16.6.6. Immunoprecipitation (Harlow and Lane 1988)

L929 cells (80% confluent) in 150 mm dishes were induced with 200 U/ml of IFN- $\gamma$  for 24 hours. The media removed, washed with 1x PBS, and starved with DMEM starvation medium for 1h. The cells were labelled with PRO-MIX L- [<sup>35</sup>S ] *in vitro* cell labelling Mix, 150  $\mu$ Ci for each plate, for 4 h. The cells were washed two times with 1x PBS, and then scraped into the lysis buffer (1x PBS, 1% of the desired detergent, and protease inhibitors), incubated for 1h at 4°C. The lysate was centrifuged at 15,000 g ,15 min, 4°C to remove the nuclear material, and the supernatant was incubated at 4°C, for 2h with protein A beads coupled to the pre-bleed of the serum/ or a normal rabbit serum (coupling was done by mixing 50 $\mu$ l protein A beads and 50  $\mu$ l serum or pre-bleed, at 4°C, rotator, 2h) in order to reduce the nonspecific binding. The lysate was then incubated with protein A beads covalently coupled to  $\alpha$  165 antiserum or 10D7, 10E7, 5D9 monoclonal antibodies at 4°C, in a rotator O/N. The beads were washed extensively after removing the supernatant, and the bound proteins were eluted with 1.5mM Tris pH 8.5, 0.5 % SDS by rotating at 4°C, 30 min. The samples were treated with 1x loading buffer, boiled for 5 min, and subjected to SDS PAGE. The gels were stained with Coomassie blue stain and de-stained as described above, and dried as a saran wrap/gel/3MM Whatmann sandwich in the BioRAD Gel dryer (Saran wrap facing up) for 2h at 60°C. The dried gel was subjected to autoradiography using a Kodak X-Omat AR film, and developed in a AGFA Curix 60 X-ray device.

Cross-linking of the  $\alpha$  165 antiserum coupled to protein A beads was done to covalently couple the complex. The protein A beads (50  $\mu$ l) and  $\alpha$ 165 antiserum (10 $\mu$ l) was coupled at 4°C for 2 h, washed 5 times with 1x PBS, and then washed with 10 volumes of 0.2 M sodium borate (pH 9.0). Dimethyl pimelidimate (DMP) was used to a final concentration of 20 mM in 0.2 M sodium borate (pH 9.0), for 30 min, 4°C, in a Rotator. The reaction was stopped by adding 0.2 M ethanolamine (pH 8.0), and the beads were incubated with 0.2 M ethanolamine (pH 8.0) for 2h, 4°C, in a rotator. The beads were then washed with 100 mM Glycine (pH 3.0) to remove the non-covalently bound complex, and washed with buffer before adding the lysates. The beads were pelleted at 10,000 g for 30 sec during all the washes.

#### II.16.6.7. Analytical Gel Filtration

L929 cells (80% confluent) in 150 mm dishes were induced with 200 U/ml of IFN- $\gamma$  for 24 hours, and the cells were lysed in a 1% thesit in 1x PBS as described above. Thesit belongs to the Triton series of non-ionic detergents which does not have an absorption at 280 nm. The thesit lysates (0.5 ml) was fractionated in a calibrated Superose 6H R size exclusion column, equilibrated with 1% thesit in 1x PBS with a flow rate of 0.2 ml/min, and collected 0.2 ml fractions. The calibration of the column was done with several Molecular size markers. For the estimation of molecular size, elution volume ( $V_e$ ) was analysed for several proteins, 29 kDa carbonic anhydrase has a elution volume ( $V_e$ ) of 18.8 ml, 66 kDa Bovine Serum Albumin has a  $V_e$  of 17.3 ml, 150 kDa Alcoholic dehydrogenase has a  $V_e$  of 16.8 ml, 200 kDa B-amylase has a  $V_e$  of 16 ml, 443 kDa Apoferritin has a  $V_e$  of 15.3 ml, 665 kDa Thyroglobulin as a  $V_e$  of 13.7 ml. The void volume  $V_o$  was calculated as 8.2 ml by running Blue dextran which is 2000 kDa (Cutler, 1996).

### III. RESULTS I

#### III.A. Biochemical and Cellular Studies on IIGP1

##### III.A.1. Recombinant IIGP1 Expression and Purification

Recombinant IIGP1 proteins (IIGP1-wt, IIGP1-m and IIGP1-his) were expressed as N-terminal GST fusion proteins in *E.coli* BL-21 cells. Table 3.1 describes the three proteins, having the extension GSPGIPGSTT – at the N-terminus. The IIGP1-m protein originated from a cloning artefact: it differs from the wild-type by a two residue C-terminal truncation followed by the addition of 11 extra C-terminal residues. IIGP1-his has 6 histidine residues originally introduced as a C-terminal epitope tag.

Table 3.1. Description of the IIGP1 constructs.

	N-terminus	C-terminus
IIGP1-wt	GSPGIPGSTT-MGQetc	-CLRN
IIGP1-m	GSPGIPGSTT-MGQetc	-CL-KLGRLERPHRD
IIGP1-his	GSPGIPGSTT-MGQetc	-CLRN-HHHHHH

The purification of IIGP1-m is shown in figure 3.1. The incubation conditions were adjusted to maximise the yield of soluble proteins by varying the concentration of IPTG, temperature, time of induction and cell density as described in Materials & Methods. A considerable amount of the protein was found to be soluble upon overnight induction with 1mM Isopropyl- $\beta$ -D-thiogalactoside at 18°C at an  $A_{600}$  of 0.4.

Lane 1 and Lane 2 show the insoluble and the soluble portions of the induced protein after fractionation of the induced cell lysates. The soluble fraction was purified by affinity chromatography as described above (the expressed proteins are bound to the resin, as we see only a tiny amount in the flow through of the column as shown in lane 3). The GST domain of the fusion protein was cleaved by incubation with thrombin on the resin (lane 4). The eluted protein was further purified by size exclusion chromatography (lane 6). The purified protein was found to be nucleotide-free by reverse-phase HPLC.

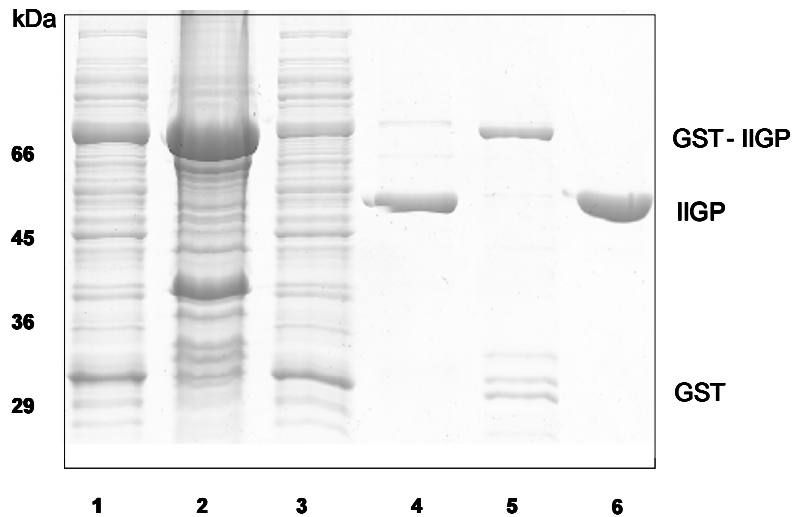


Figure 3.1. Recombinant expression and purification of IIGP1-m

Induced lysates of IIGP1-m expressing BL-21 cells fractionated to the soluble and insoluble forms (lanes 1, 2); The soluble fraction that remains unbound to the glutathione sepharose column is shown in lane 3. The eluate from the column after thrombin cleavage (lane 4). Lane 5 shows a fraction of the uncleaved protein as well as the cleaved GST domain after a wash with reduced glutathione. The pooled eluate (lane 4) after a Superdex 75 gel filtration run is shown in lane 6.

### III.A.2. Biochemical Characterisation of IIGP1

Comparative analysis of the biochemical properties of IIGP1-wt and two C-terminal modified forms, IIGP1-m and IIGP1-his is explained in this section. Firstly, nucleotide binding parameters are described for the three proteins, followed by kinetics of GTP hydrolysis.

#### III.A.2.1. Nucleotide Binding Features

##### III.A.2.1.1. Equilibrium Titrations

Nucleotide binding to IIGP1-m was monitored using mant-nucleotides. The increase in fluorescence upon mant nucleotide binding to the protein is used to determine nucleotide affinities. Figure 3.2 shows the titration curve for the increase in fluorescence upon the binding of 0.5  $\mu\text{M}$  mant-GDP (mGDP) to IIGP1-m. IIGP1-m was added from a 600  $\mu\text{M}$  stock solution and at each step the values for the increase in fluorescence were averaged over a period of one minute. Dissociation constants were calculated from curves fitted to the data as described in Materials and Methods.

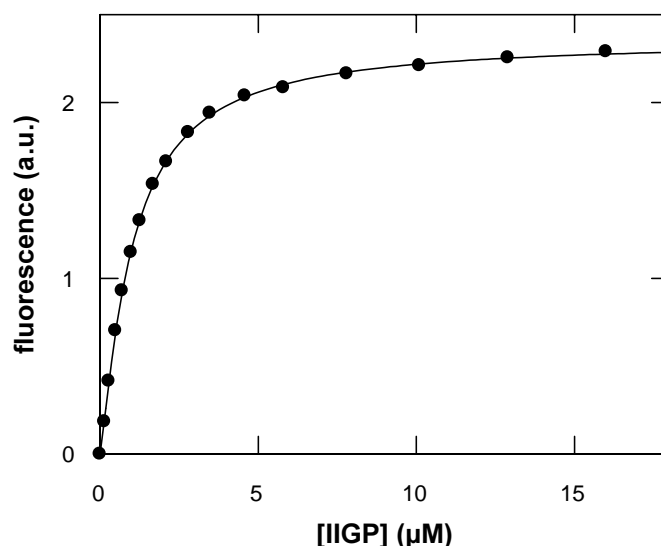


Figure 3.2. Equilibrium titrations

The increase in fluorescence upon binding of the mant-labelled GDP (0.5 μM) to IIGP1-m was measured at 430 nm, excited at 360 nm. A theoretical curve is fitted to the data yielding the  $K_d$  value.

The nucleotide binding of mGDP, mGTP $\gamma$ S, mGppNHp and mGDP.AIF $_x$  were determined by equilibrium titrations (table 3.2a). The binding affinities are in the micromolar range and mGDP shows higher affinity than mGTP $\gamma$ S. mGppNHp, another non-hydrolysable analogue of GTP, shows weak binding in comparison to the other nucleotides ( $K_d$  of ~130 μM). Interestingly, we could not detect any binding of mGDP.AIF $_x$  to IIGP1 (data not shown), probably due to the relatively strong binding of mGDP itself, suggesting that AIF $_x$  may not be required to stabilise the binding.

Table 3.2a.  $K_d$  value (μM) for the binding of fluorescent and non fluorescent nucleotides to IIGP1-m by different methods.

Nucleotides	Equilibrium Titrations	Calorimetric Titrations	Stopped-Flow
	A.2.1.1	A.2.1.2	A.2.1.3
GDP		2.45	
mGDP	0.90		0.97
mGTP			16.1
mGTP $\gamma$ S	5.20		15.7
GTP $\gamma$ S		8.0	

### III.A.2.1.2. Isothermal Titration Calorimetry

The interaction of unlabelled nucleotides with IIGP1 was measured by isothermal titration calorimetry in order to control for possible interference of the mant-group in the fluorescence-based binding assay. Figure 3.3 (upper lane) shows the raw data for binding upon step-wise addition of GDP to IIGP1-m. The exothermic process is reflected in a negative power pulse from which the heat of the reaction is calculated by integration. The enthalpy of the reaction normalised to the concentration of injected GDP was plotted against the molar ratio of GDP and IIGP1-m as shown in the lower panel. The parameters defining the theoretical curve yielded a  $K_d$  of 2.5  $\mu\text{M}$ , and an enthalpy of association of  $-15$  kcal/mol. In addition, 1:1 stoichiometry is evident from the data. The results from table 3.2a suggest that IIGP1-m has similar binding affinities to mant-labelled as well as unlabelled nucleotides.

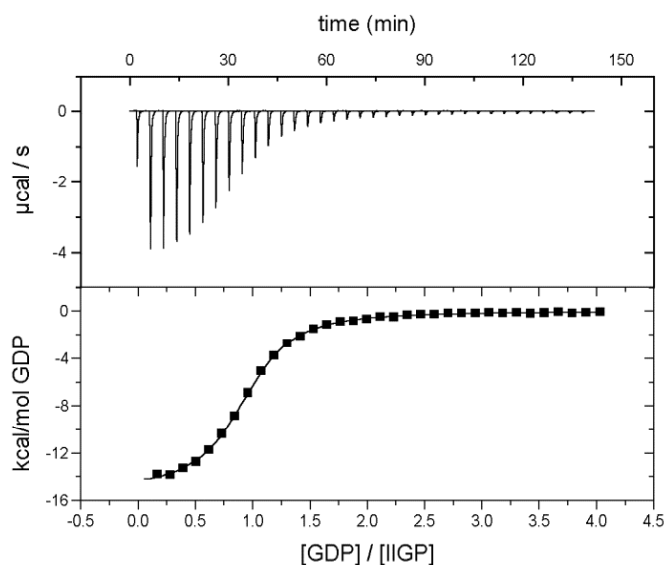


Figure 3.3. Isothermal titration calorimetry

Thermodynamics of GDP binding to IIGP1-m was analysed by ITC. The upper panel shows the change in heating power upon injection of 1.66 mM GDP into a cell containing 43.8  $\mu\text{M}$  IIGP1-m solution. The heat of the reaction is plotted against the molar ratio of GDP to IIGP1-m in the lower panel.

### III.A.2.1.3. Dynamics of Nucleotide Binding

The dynamics of nucleotide binding to IIGP1 were determined by stopped flow using mant nucleotides. The IIGP1 protein was used in a large molar excess over the nucleotide in order to obtain pseudo-first order reaction kinetics (shown for IIGP1-m in figure 3.4A).

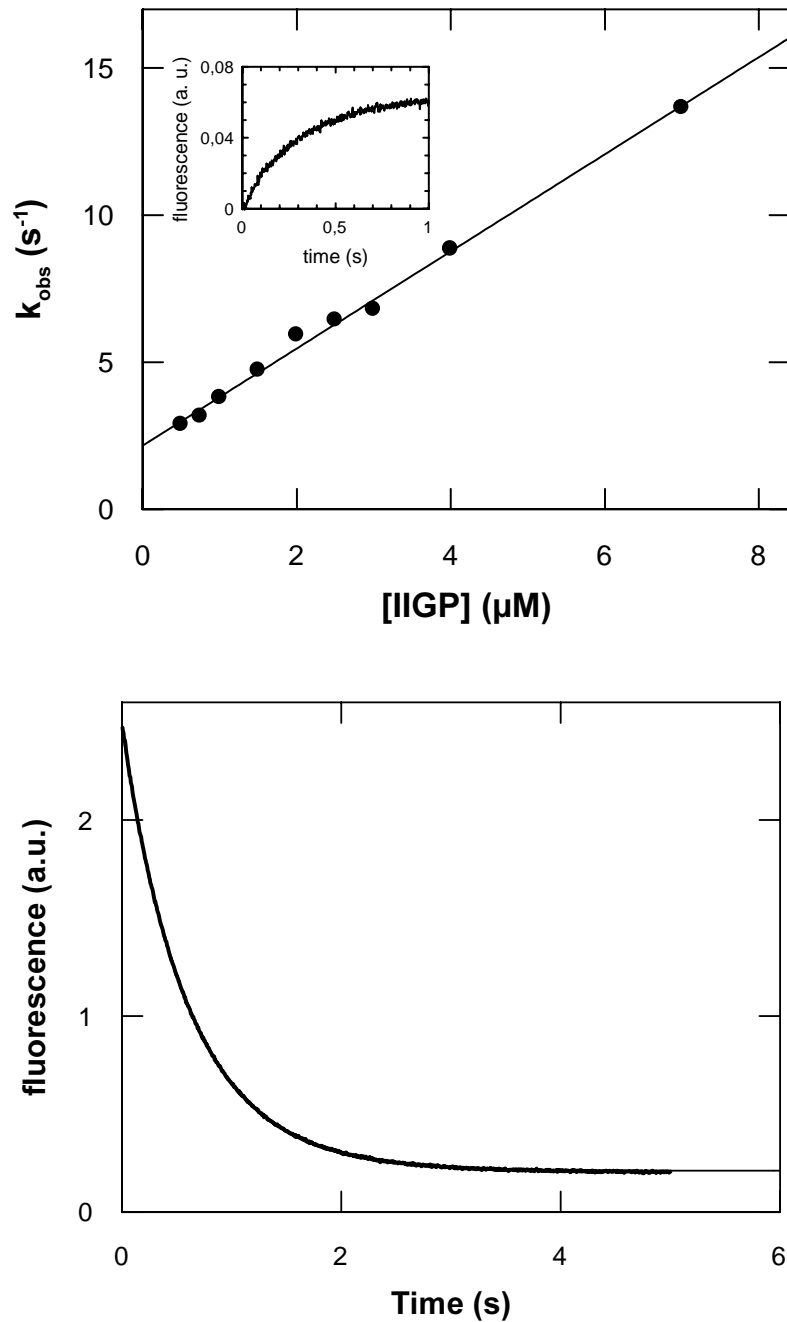


Figure 3.4. Stopped flow measurements

A. The increase in fluorescence upon mixing 0.2 μM mGDP with 4 μM IIGP1 is monitored through a 405nm cut off filter after excitation at 360nm. A single exponential curve is fitted to the data (inset above) to obtain the observed rate constant  $k_{\text{obs}}$ , and a linear fit to the plot of the observed rate constant versus protein concentration is shown in the figure, deriving the  $k_{\text{on}}$  and  $k_{\text{off}}$ . B. The exponential decrease of fluorescence upon addition of excess GDP (400 μM) to IIGP1 (4.8 μM) – mGDP (3.9 μM) pre-formed complex is shown in the inset below yielding the  $k_{\text{off}}$ .

A single exponential function is fitted to the data, where the resulting time constant corresponds to the inverse observed rate constant  $k_{\text{obs}}$  (figure 3.4A, upper inset). The observed rate constants for the binding of mGDP were plotted against IIGP1 concentration. The slope of the curve denotes the



association rate constant ( $k_{on}$ ) and the intercept, the dissociation rate constant ( $k_{off}$ ).  $k_{off}$  was also measured in a displacement experiment by the addition of excess unlabelled nucleotide to IIGP1-mGDP pre-formed complex. This leads to a quasi-irreversible dissociation of mGDP and therefore to a single exponential decrease of fluorescence as shown in Figure 3.4B. The binding of different nucleotides to IIGP1-m using equilibrium methods (above) is compared with  $K_d$  values determined by stopped flow, represented in Table 3.2a. The three employed methods show comparable results for nucleotide binding. The nucleotide binding affinities for IIGP1-wt, and the two C-terminal mutants IIGP1-m and IIGP1-his are tabulated in table 3.2b, where it is apparent that they have similar values, and the C-terminal end of IIGP1 is not important for nucleotide interactions.

Table 3.2b. Association and dissociation rate constants and  $K_d$  values for the binding of fluorescent nucleotides and non hydrolysable analogues to IIGP1- wt / IIGP1- m / IIGP1- his.

Nucleotides	$k_{ov} \mu M^{-1}s^{-1}$	$k_{off}$ (displacement) $s^{-1}$	$K_d$ ( $\mu M$ )
<b><u>mGDP</u></b>			
IIGP1-wt	1.55	0.99	0.64
IIGP1-m	1.65	1.6	0.97
IIGP1-his	1.31	0.70	0.53
<b><u>mGTP</u></b>			
IIGP1-wt	0.98	21.6	22
IIGP1-m	1.30	21	16.1
IIGP1-his	1.11	14.28	12.9
<b><u>mGTP<math>\gamma</math>S</u></b>			
IIGP1-m	4.20	66	15.7

In detail, the association rate constants are similar for the different nucleotides, but the dissociation rate constants vary. The smaller  $k_{off}$  for mGDP accounts for stronger binding compared to mGTP and its non-hydrolysable analogue, as observed in the equilibrium titrations described above (table 3.2a). In summary, results from all different methods employed show that IIGP1 has micromolar binding affinities for different nucleotides and GDP has a 15-fold higher affinity to IIGP1 than GTP.

### III.A.2.2. GTP Hydrolysis

In GTPases, the identity of the nucleotide bound to the protein and the rate of conversion of GTP to GDP by hydrolysis are crucial factors determining their functional regulation (Bourne et al., 1991). The rate of GTP hydrolysis and GDP formation was analysed by reverse-phase HPLC. The activity of the three forms of IIGP1, IIGP1-wt, IIGP1-m and IIGP1-his at 2 – 50  $\mu$ M was analysed over varying GTP concentrations (0.05 – 2 mM). Figure 3.5 documents the hydrolysis of GTP to GDP by IIGP1.

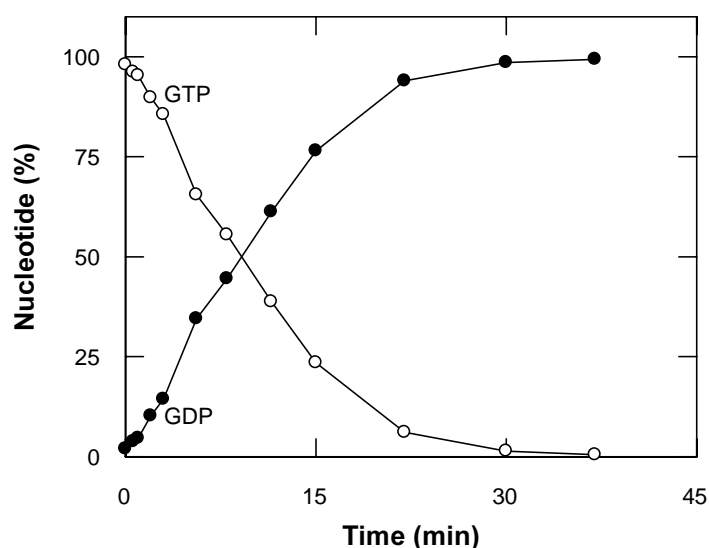


Figure 3.5. Time course of GTP hydrolysis by IIGP1 at 37°C

The rate of GTP hydrolysis and GDP formation was analysed by HPLC as described in Materials and Methods. IIGP1 hydrolyses GTP to GDP. The percentage breakdown of 700  $\mu$ M GTP (open circles) with 50  $\mu$ M IIGP1 to GDP (closed circles) with time is shown in the figure.

ATP was not hydrolysed, confirming nucleotide specificity and indicating that our preparations were free of phosphatases. IIGP1 hydrolyses GTP to GDP and not to GMP as described for hGBP1, the member of the p65 GTPase family (Praefcke et al., 1999). A representative curve for the time course of GTP hydrolysis by IIGPm at 37°C is shown in figure 3.5. The rate constant for GTP hydrolysis was obtained using initial rates as product inhibition was observed with the progression of the reaction. The catalytic activity of IIGP1 at different protein and nucleotide concentration was determined as shown in figure 3.6. Michaelis Menten equation was applied to a plot of specific activity (at a range of protein concentration) versus substrate concentration. Intriguingly, a small increase in  $K_m$  was observed, with varying protein concentrations. This suggests functional cooperativity between IIGP1 molecules.

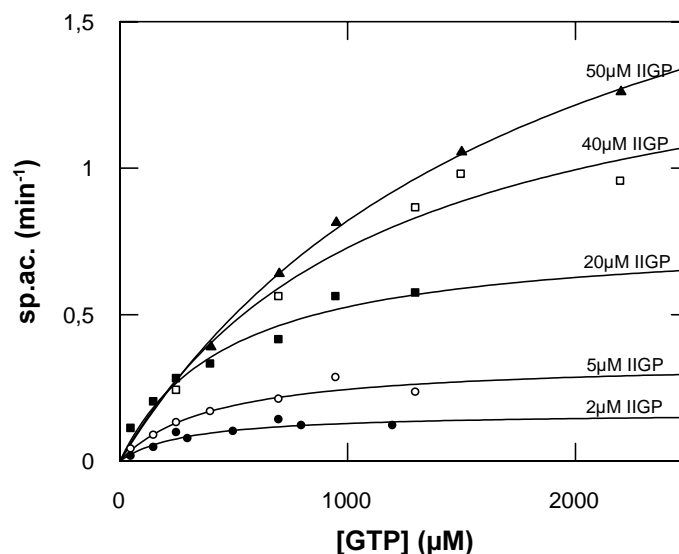


Figure 3.6. Michaelis Menten plot

The specific activity of IIGP1 at a range of protein concentrations (2 – 50  $\mu\text{M}$ ) were plotted against the substrate concentration. The Michaelis Menten equation was fit to the data to derive the parameters.  $V_{\text{max}}$  of  $2 \text{ min}^{-1}$  was obtained for the highest concentration checked (50  $\mu\text{M}$  IIGP and 2 mM GTP).

In order to investigate this effect more precisely, the dependence of the specific GTPase activity on IIGP1 concentration was measured at a fixed GTP concentration of 700  $\mu\text{M}$  as shown in Figure 3.7 (black circles- IIGP1-m, open circles- IIGP1-wt). The specific activity increased approximately 7-fold with increasing protein concentration, from the lowest measured activity at  $0,1 \text{ min}^{-1}$  to about  $0,7 \text{ min}^{-1}$ . The maximum specific rate of GTP hydrolysis by IIGP1 was close to  $2 \text{ min}^{-1}$  (see Fig. 3.6 where 50  $\mu\text{M}$  IIGP1-m and 2 mM GTP was used). The increase in activity of the protein with increase in protein concentration observed in the case of IIGP1-wt and IIGP1-m demonstrates a cooperative mechanism of GTP hydrolysis. Intriguingly, the GTP hydrolysis rate of IIGP1-his C-terminally modified protein showed marginal if any protein concentration dependence over the tested range, remaining at or close to the basal rate of  $0,1 \text{ min}^{-1}$  (figure 3.7 black triangles). There is a slight increase in the activity of IIGP1-his is observed, which was also noticed when the activity assay was repeated in the presence of BSA.

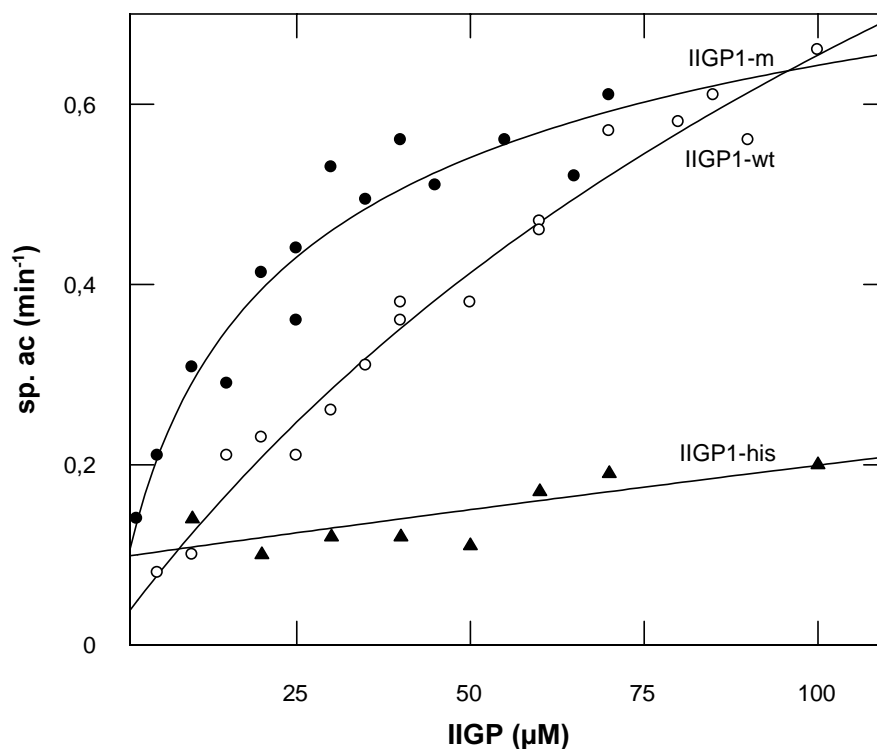


Figure 3.7. Co-operativity

IIGP1 shows a co-operative GTPase activity, with a seven fold increase in the specific activity of the protein at a concentration of 700  $\mu\text{M}$  GTP in the case of IIGP1-wt (open circles) and IIGP1-m (closed circles) is shown in the figure. The IIGP1-his protein (closed triangles) fails to show co-operativity.

### III.A.2.3. Oligomerisation

#### III.A.2.3.1. Time and GppNHp Dependent Oligomerisation

GTPases with co-operative activity are known to form enzymatically active oligomers in the presence of nucleotides (Haller and Kochs, 2002). The oligomerisation of IIGP1-m was investigated using dynamic light scattering at 20°C at protein concentrations of 50-100  $\mu\text{M}$  and nucleotide (GDP, GTP and GppNHp) concentrations of 1 mM. The change in the hydrodynamic radius ( $R_H$ ) of IIGP1 (derived from the unimodal fit analysis by Dynamics 4.0 software) versus time was plotted for each of the data sets with and without nucleotides. Figure 3.8 shows the time dependent oligomerisation of IIGP1-wt with GTP and GppNHp. A striking increase in hydrodynamic radius was detectable after the addition of GTP, and also after the addition of GppNHp, but to a lesser degree in the latter case. No detectable higher molecular forms were found with the apoprotein (nucleotide free) or in the presence of GDP as they have a hydrodynamic radius ( $R_h$ ) of 3.1 nm, corresponding to the expected molecular weight of 47 kDa. The difference in oligomer formation between GTP and GppNHp bound forms could be due to their difference in binding affinities.

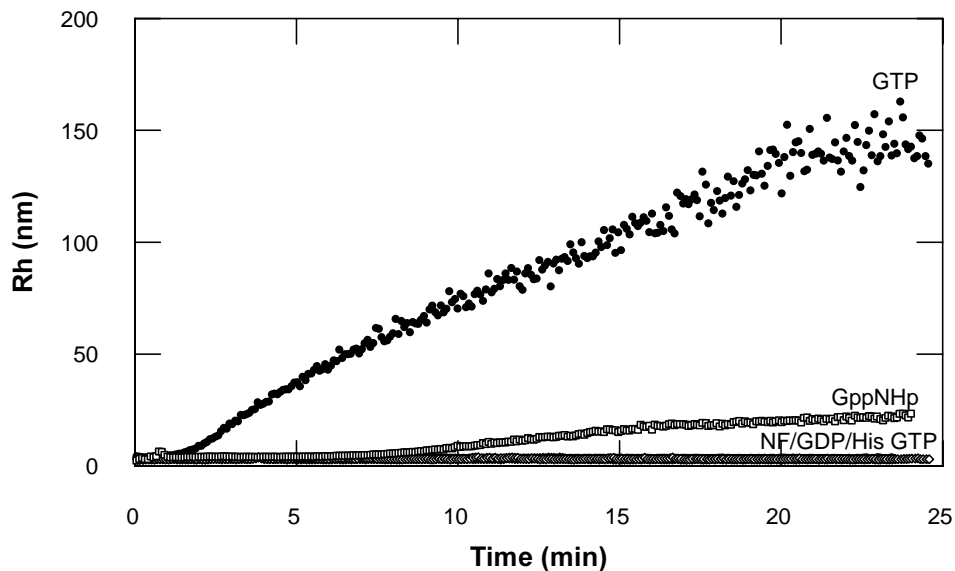


Figure 3.8. Dynamic light scattering

The time dependent increase in the hydrodynamic radius (Rh) protein oligomers in the absence and presence of nucleotides are depicted for IIGP1-wt and IIGP1-his. The difference in oligomer size of IIGP1-wt with GTP and with GppNHp is clearly visible. The values for the nucleotide free IIGP1-wt (NF), IIGP1-wt-GDP (GDP), and IIGP1-his GTP (His GTP) overlap due to their same Rh, and is visible as a single curve. 50  $\mu$ M of IIGP and 1 mM nucleotides were used. The Rh of 3 nm corresponds to 47 kDa.

### III.A.2.3.2. C-terminal end is Essential for the Formation of Higher Molecular Species

As shown in figure 3.7, modification of the C-terminus of IIGP1 by addition of a His tag prevented IIGP1-his from showing co-operative GTPase activity. It was therefore of interest to know whether the C-terminal modification also blocked the formation of nucleotide triphosphate binding oligomers. Using the dynamic light scattering assay, IIGP1-his analysis, unlike IIGP1-wt, did not build up oligomers in the presence of GTP and GppNHp. (figure 3.8, where IIGP1-his shows an overlap with IIGP1-wt, IIGP1-wt GDP). The hydrodynamic radius of IIGP1-his in the presence of GTP persists at around 3 nm, thus a monomer.

### III.A.2.3.3. Fluorescence Scattering Experiments Confirming GTP Dependent Oligomerisation

Since oligomerisation was possible only in the presence of GTP or GppNHp, and not in the presence of GDP, the reversibility of these oligomers was tested with respect to GTP hydrolysis. In order to show directly the relationship between IIGP1 catalysed GTP hydrolysis and oligomer formation, light scattering was done in a fluorescence cuvette from which aliquots for nucleotide analysis were taken simultaneously. The time course of the oligomerisation in a solution of GTP (1 mM) and IIGP1 wt (50  $\mu$ M) is shown in figure 3.9.

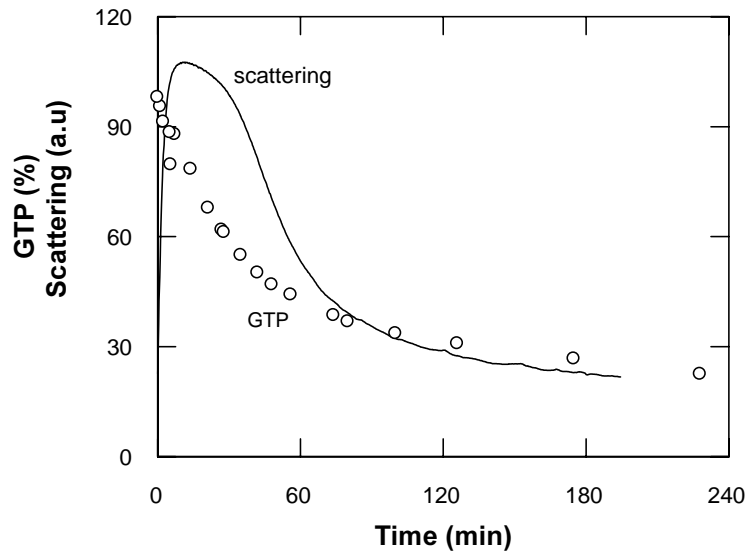


Figure 3.9. Light scattering

GTP dependent oligomerisation shows reversibility upon GDP formation. The time course of the scattered light intensity was detected at 350 nm, in a solution of 1 mM GTP and 50  $\mu$ M IIGP solution. The time dependent oligomerisation and the time course of GTP hydrolysis (open circles). is overlaid in the graph to show the association of these two processes.

The initial rise in light scattering is followed by a slow decrease due to progressive hydrolysis of GTP. This time dependent oligomerisation leads to a turbid solution, is visible, but reverts to a clear solution. The decrease in turbidity is therefore not due to flocculation (falling down of particles in the cuvette), but due to GTP hydrolysis and dissolution of the particles. The formation of GDP inhibits oligomerisation, as it has a high binding affinity, as well as competition with GTP to bind IIGP1. The light scattering trace in figure 3.9 showing the reversibility of the IIGP oligomers, and is overlaid with the time course of GTP hydrolysis (for the same nucleotide and protein concentrations) to delineate the relationship between the two processes. However, the reversibility of the oligomers was not visible in the previous experiment due to the measurements only in short time ranges.

### III.B. Cellular Studies on IIGP1

To describe the properties of IIGP1 *in vivo*, a detailed cellular characterisation of IIGP1 was carried out. For cellular studies, L929 mouse fibroblasts or mouse embryonic fibroblasts (MEFs) were grown and cultured in IMDM or DMEM respectively as described in Materials & Methods. The IIGP1 wt and mutant constructs were all cloned into the eukaryotic expression vector pGW1H, and all transfections were done using a lipid based transfection reagent as described above. The cells were stimulated with 200 U/ml of Mouse IFN- $\gamma$  for 24 hours unless specified.  $\alpha$  165 rabbit antiserum was generated against recombinant purified IIGP1 as described.

IIGP1 is stimulated preferentially by IFN type I and also by IFN type II in various cells including *L. monocytogenes* infected, or LPS stimulated macrophages, endothelial cells, activated T cells and mouse embryonic fibroblasts. The expression of IIGP1 has also been documented in *L. monocytogenes* infected spleen and liver cells. Constitutively expressed IIGP1 was not detectable in the mRNA level, as well as the protein level (Boehm et al., 1998; Zerrahn et al., 2002). Localisation of IIGP1 was done by Martens and Boehm et al (unpublished data) showing the association with the endoplasmic reticulum. However, the localisation of IIGP1 in Golgi apparatus has been documented by Zerrahn et al 2002.

To understand the cellular properties of IIGP1, and its importance, this section attempts to describe IIGP1 with respect to its localisation, cellular distribution, the associated molecules and several features of membrane attachment.

#### III.B.1. Localisation Studies on IIGP1

Immunofluorescence studies was done on L929 fibroblasts that were stimulated with 200 U/ml of Mouse IFN- $\gamma$  / or transfected with IIGP1-wt, to analyse the endogenous and the transfected IIGP1. The C-terminally tagged IIGP1-his was initially made to be used in several cell biological analysis. 24 hours post transfection or induction, the cells were stained with IIGP1 specific  $\alpha$  165 rabbit antiserum. Endogenous IIGP1 localisation is defined by a typical perinuclear, nuclear envelope / ER staining with  $\alpha$  165 as shown in the upper panel of figure 3.10, whereas transfected IIGP1 has a slightly different pattern of dots (not identified) in addition to the ER staining.

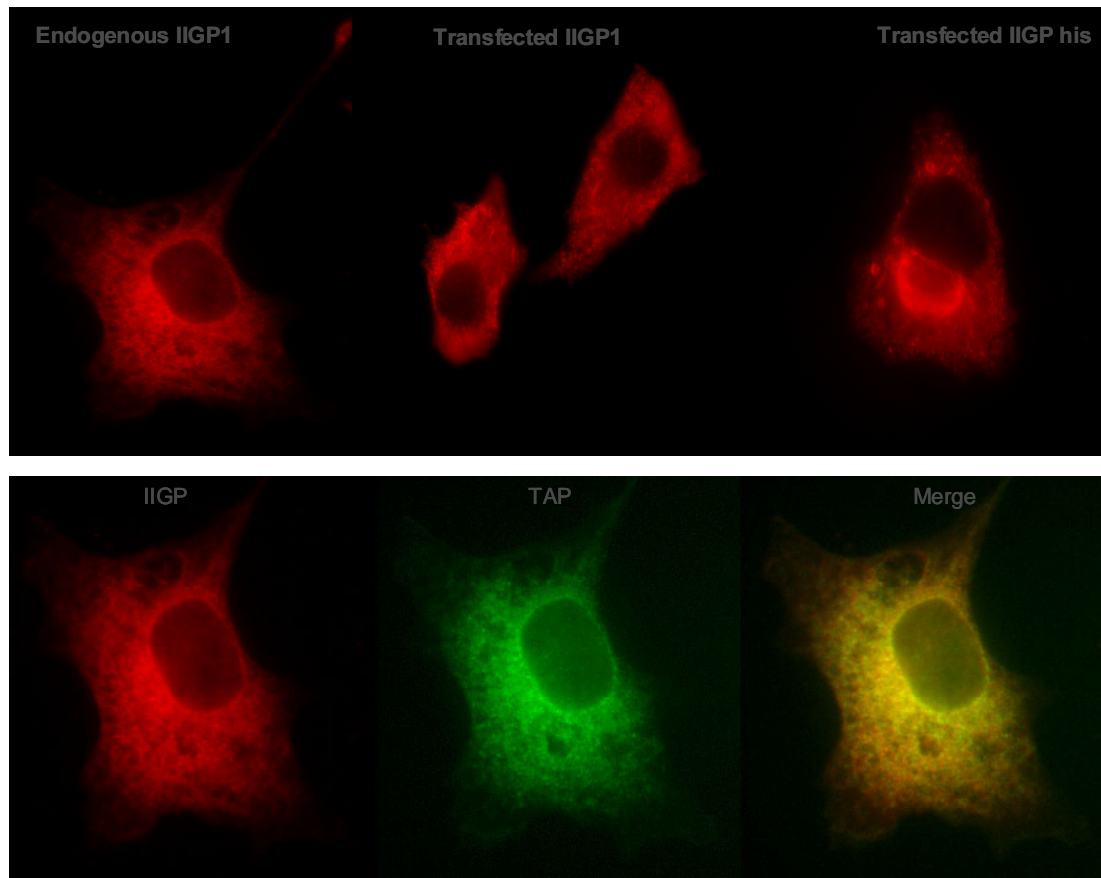


Figure 3.10. Localisation of IIGP1.

Cells grown on cover-slips were exposed to control conditions or to 200 U/ml IFN- $\gamma$  or transfected with FuGENE<sup>TM</sup> 6 reagent, a multiple component lipid based transfection reagent. The cells 24h post transfection/induction were fixed with 3% paraformaldehyde, and permeabilised with 0.1% saponin and stained with  $\alpha$ 10D7 antibody, and used Alexa 546 coupled secondary antibody. The staining was analysed using Axioplan II fluorescence microscope, a cooled CCD camera and the pictures are processed using a metamorph software. The distribution of IFN- $\gamma$  induced, transfected IIGP1 and IIGP1-his respectively is shown in the upper panel. The lower panel shows the co-localisation of endogenous (IFN- $\gamma$  induced) IIGP1 merged with transporter associated with antigen processing (TAP) .



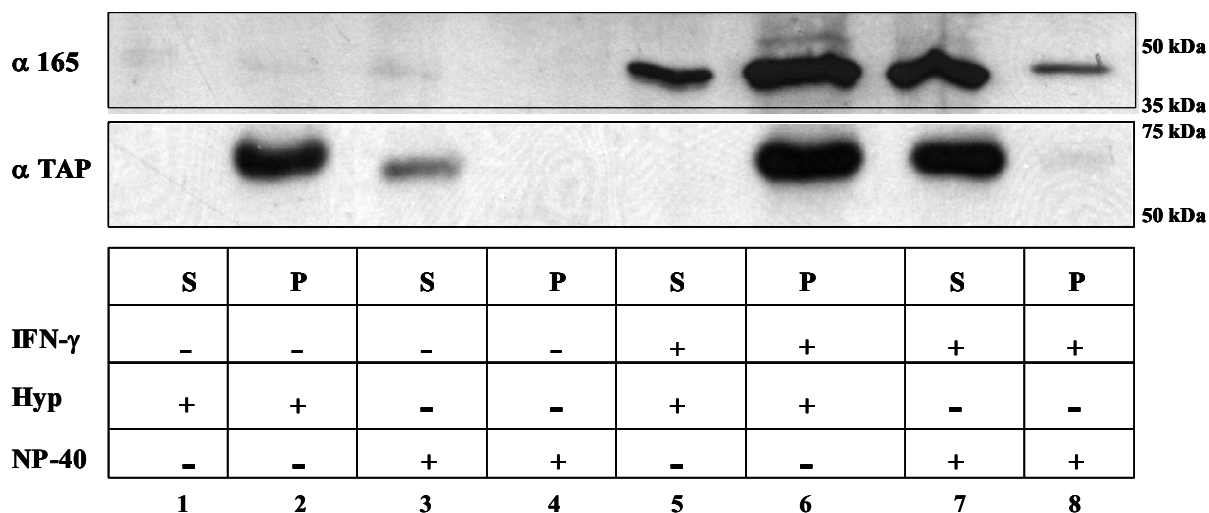
The transfected IIGP1 his forms a ring like pattern in the perinuclear region, in addition to the typical reticular ER stain and sometimes, the dotted pattern. The localisation of IIGP1 in the ER was confirmed by colocalisation with an ER transmembrane protein transporter of antigen presentation (TAP) in the lower panel of figure 3.10. The ER staining of IIGP1 is shown in red, and the TAP staining in green, and the colocalisation is clearly demonstrated by the merge, as shown. However, there is an additional dotted and the ring pattern of IIGP1, the identity of which is unknown. The co-localisation studies were done by Martens et al (unpublished results)

### III.B.2. Distribution of IIGP1 in the Cell

IIGP1 sequence contains neither any signal sequences, or ER retention or retrieval signal sequences (Nilsson and Warren, 1994; Kalies and Hartmann, 1998). Therefore we suppose that IIGP1 is not located in the lumen of the ER, and is probably associated peripherally with the ER, from the cytosolic side. To understand the location of IIGP1, IFN- $\gamma$  induced L929 mouse fibroblasts were lysed in a hypotonic buffer and separated the membrane and soluble fractions. This led to the partitioning of IIGP1 to a prominent membrane bound fraction and a smaller cytosolic fraction. This is depicted in figure 3.11A as the supernatant (S) and the Pellet (P) fractions representing the soluble and the membrane bound forms in lane 5 and 6 respectively. The levels of IIGP1 constitutive expression in the IFN- $\gamma$  uninduced control experiment seems to be undetectable (lane 1-4).

In order to study the membrane associated IIGP1, very mild detergents were used to solubilise membranes. They can isolate lipoproteins into detergent micelles, without significant denaturation of the protein, because of their weaker detergent action (Neugebauer, 1990). Lane 7 shows the detergent solubilisation of IIGP1 with NP-40 as described in Materials & methods, a very small amount of insoluble IIGP1 is seen in lane 8. TAP the ER transmembrane protein is used as a positive control for the partitioning, where all the protein is membrane bound (lane 2,6), and is completely solubilised upon detergent lysis (lane 3,7). TAP is constitutively expressed in the cell (lane 2), and is also stimulated upon IFN- $\gamma$  induction as shown in lane 6 (Seliger et al., 1997). Additionally, the solubilisation of the membrane bound IIGP1 with several mild detergents were tested, as they have distinct solubilisation properties (NP-40, Tx-100 are non-ionic detergents; Chaps is an Zwitterionic detergent; digitonin, a neutral detergent). The solubilisation of IIGP1 with different detergents is shown in figure 3.11 B

### 3.11 A



### 3.11 B

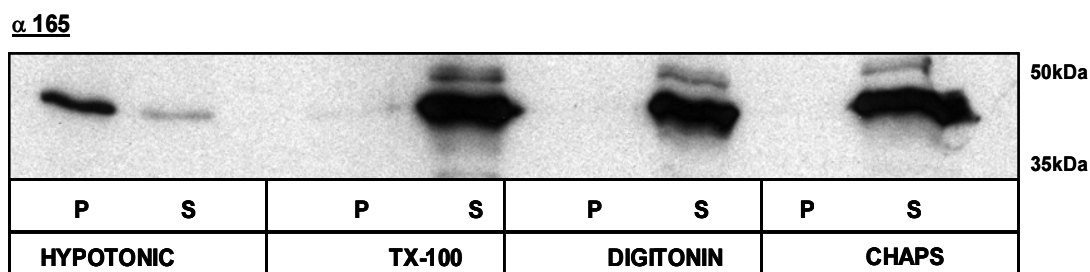


Figure 3.11. Distribution of IIGP1 in the IFN- $\gamma$  induced L929 cells.

L929 cells induced or uninduced with 200 U/ml IFN- $\gamma$ , 24h post induction, cells were lysed under different buffer conditions (hypotonic buffer/Tx-100/Digitonin/Chaps/NP-40), and the post-nuclear supernatant and pellet were subjected to SDS-PAGE and western blotting. A. Comparison of the distribution of IIGP1 in IFN- $\gamma$  induced and uninduced (NP-40/ hypotonic) lysates using TAP as control. B. Solubilisation of IIGP1 with different detergents.

## III.B.3. Interaction Molecules

### III. B.3.1. Size Exclusion Chromatography

*In vitro* characterisation of IIGP1 recombinant protein showed nucleotide dependent oligomerisation. To analyse whether endogenous IIGP1 exists in a monomeric or oligomeric state, size exclusion chromatography was carried out on IFN- $\gamma$  induced, 1% thesit treated L929 cells. The proteins in the lysate fractionated into various molecular size components depending on their size as shown in figure 3.12.

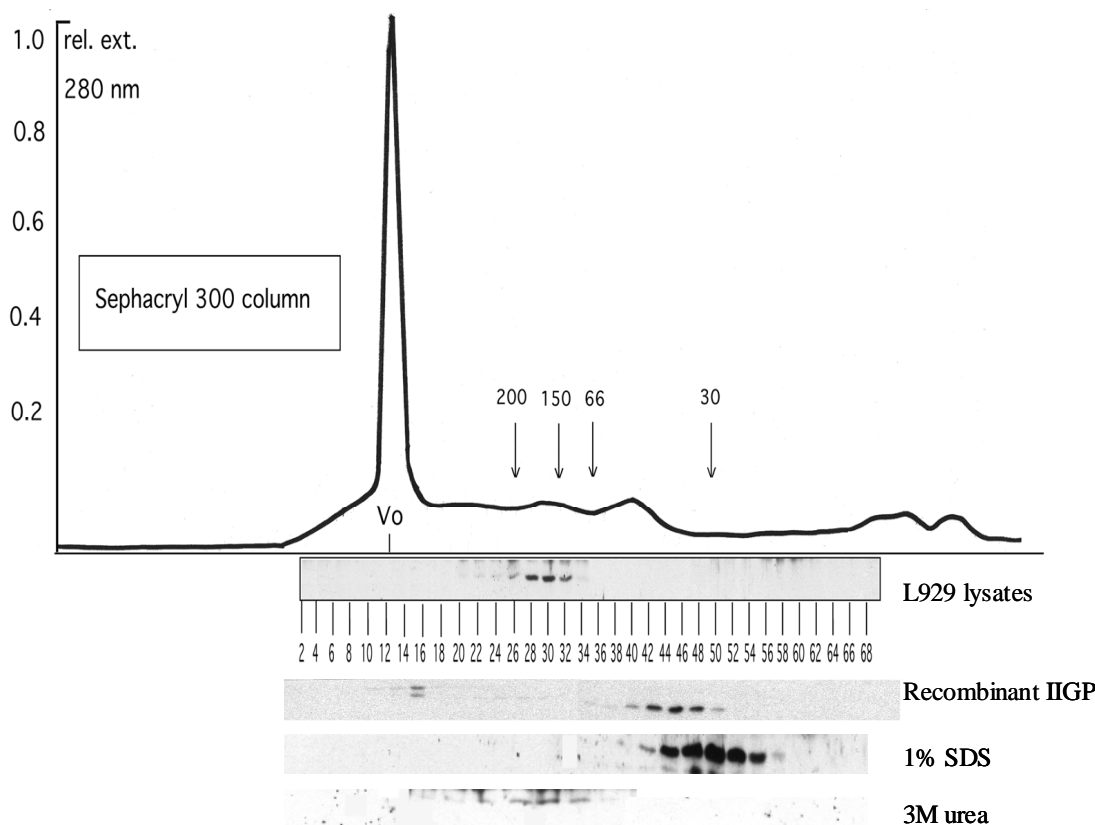


Figure 3.12. IIGP1 forms a higher molecular complex.

L929 cells induced or uninduced with 200 U/ml IFN- $\gamma$ , 24h post induction, cells were lysed with 1% thisit buffer, and the post-nuclear supernatant is loaded on a Sephacryl 300 column. All the fractions were collected and subjected to western blotting. The profile of the column run is aligned to the blots of the collected fractions. Immunoblot of the fractions of the different column runs shown are recombinant IIGP1, 1% SDS, and 3M urea and  $\alpha$ 165 antiserum was used for the analysis. [ $V_0$  = 12.5 ml;  $V_e$  for the different markers are indicated].

Immunoblot of all the collected fractions with the  $\alpha$ 165 polyclonal serum sorted IIGP1 subsisting as a higher molecular complex of ~ 150 kDa. On the contrary, recombinant IIGP1 fractionated as a monomer corresponding to the peak fractions 42-45. Interestingly, when the membrane and the soluble forms were fractionated (lane 5 and 6 in figure 3.11A) and subjected to size exclusion chromatography, different elution profiles were observed for the two fractions, molecular sizes of ~150 kDa and ~ 47 kDa respectively (figures not shown). Henceforth, association to membranes is likely to be an important feature for the maintainance of this complex.

However, the nature of the complex was checked by treatment with denaturants (1 % SDS, 3M urea), prior loading the lysates on the column. The complex can be disrupted by the addition of 1% SDS as indicated by the elution as monomers in the figure, but not with 3M urea which still retains the complex (3M urea was probably not mild to disassociate the complex). However, the disassembly of the complex with SDS asserts the credibility for lipid mediated interactions. IIGP1 has the myristoylation sequence MGQLFSS, in the N-terminal region. This modification is probably responsible for IIGP1 molecules to stick together, either forming a homotypic complex or a heterotypic complex with other proteins due to their increased hydrophobicity.

### III.B.3.2. Immunoprecipitation

#### III.B.3.2.1. Immunoprecipitation of IIGP1 in MEFs with $\alpha$ 165

Another approach was taken to analyse the molecules associated with IIGP1, whether there exists a stable IIGP1 complex, and if so, to identify components of the complex. Since  $\alpha$ 165 is a good reagent for immunofluorescence and western blotting as described before, the ability to immunoprecipitate endogenous (IFN- $\gamma$  induced) IIGP1 with this polyclonal serum was analysed. IFN- $\gamma$  induced mouse embryonic fibroblasts (MEFs) was subjected to immunoprecipitation with  $\alpha$ 165 coupled protein A sepharose beads. IIGP1 was selectively extracted from the whole cell lysate analysed by the immunoblot with  $\alpha$ 165 in figure 3.13A. The IFN- $\gamma$  induced lysate (control) shows the expression of IIGP1 indicated by the arrow ~ 47 kDa. The precipitation of IIGP1 with  $\alpha$ 165 is clearly seen in comparison to the lack of signal in the uninduced cell lysate (negative control).

#### III.B.3.2.2. Co-precipitation of IIGP1 and Partners with $\alpha$ 165 in MEFs.

As shown in figure 3.12, IIGP1 subsists as a higher molecular weight complex, either homotypic or heterotypic. Since the IIGP1 specific polyclonal serum,  $\alpha$ 165 precipitated IIGP1 from IFN- $\gamma$  induced mouse embryonic fibroblasts, the co-precipitation of other molecules along with IIGP1 was checked by metabolic labelling. IFN- $\gamma$  induced, [<sup>35</sup>S] Met labelled, MEF cell lysates were subjected to immunoprecipitation with  $\alpha$ 165 coupled protein A beads. Prior, the lysate was passed through protein A coated beads bound to a non-relevant serum to remove the unnecessary background (pre-clear).

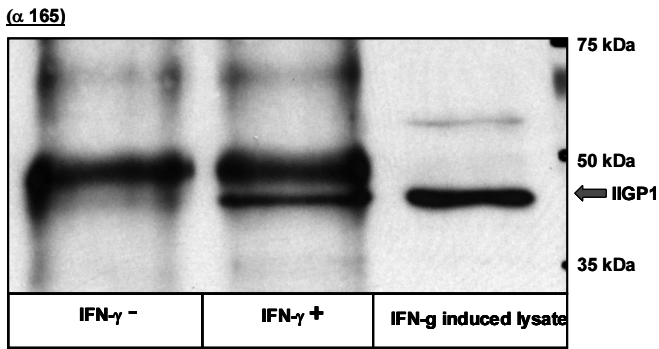


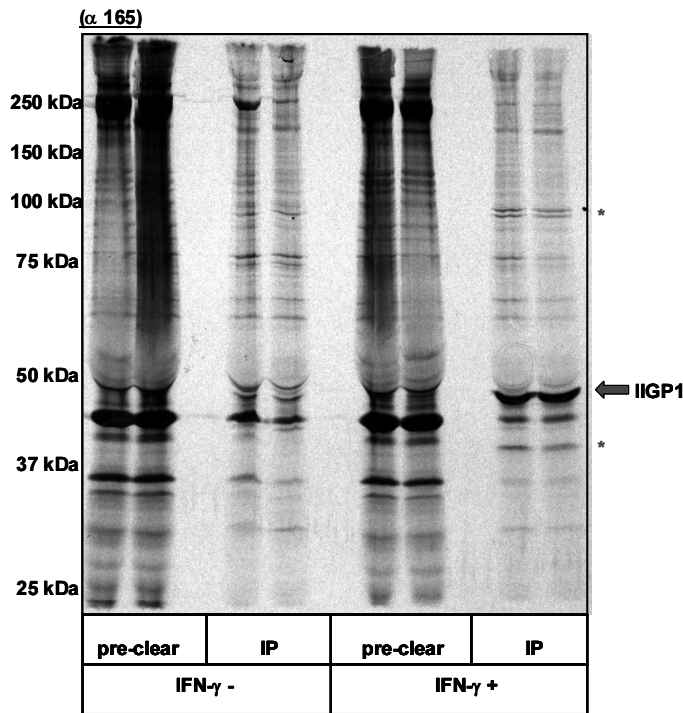
Figure 3.13.A. Immunoblot showing the precipitation of IIGP1.

MEFs induced or uninduced with 200 U/ml IFN- $\gamma$ , 24h post induction, were lysed with 1% NP-40 containing buffer, and precipitated with  $\alpha$ 165 coupled protein A sepharose beads. The IFN- $\gamma$  induced lysate showing IIGP1 expression (lane 3). The immunoprecipitated IIGP1 (~ 47 kDa indicated by blue arrow) from induced MEF lysates (2<sup>nd</sup> lane) in comparison to no IIGP1 in the uninduced lysates (1<sup>st</sup> lane).

The 35S Met incorporated immunoprecipitated proteins are separated on a 10% SDS PAGE as shown in the figure 3.13B, where the uninduced lysate (IFN- $\gamma$ ) is used as negative control, and all the samples are loaded in duplicate. IIGP1 is immunoprecipitated as indicated by the arrow ~ 47 kDa which is not present in the uninduced, and additionally, two other proteins of different sizes are co-precipitated as depicted (~ 100 kDa and ~ 40 kDa). These molecules seem not to be present in the induced pre-clear ruling out the possibility that these two molecules are interacting nonspecifically with the  $\alpha$ 165 serum.

### III.B.3.2.3. $\alpha$ 165 can also Co-precipitate the Same Molecules in L929 Cells.

In order to confirm the previous results, the co-immunoprecipitation experiment was repeated with L929 cells, additionally the lysates were prepared using different detergents for membrane solubilisation. The solubilisation of IIGP1 from the membrane with several detergents has been shown in figure 3.11A and 3.11B. IFN- $\gamma$  induced and uninduced [35S] Met/Cys labelled L929 cells were lysed with buffer containing 1% NP-40/ 1% Chaps/ 1% Tx-114. Additionally,  $\alpha$ 165 serum was covalently coupled to the protein A beads in order to reduce the background from the antibody from loose coupling to the beads.



### 3.13.B. Co-immunoprecipitation in MEFs

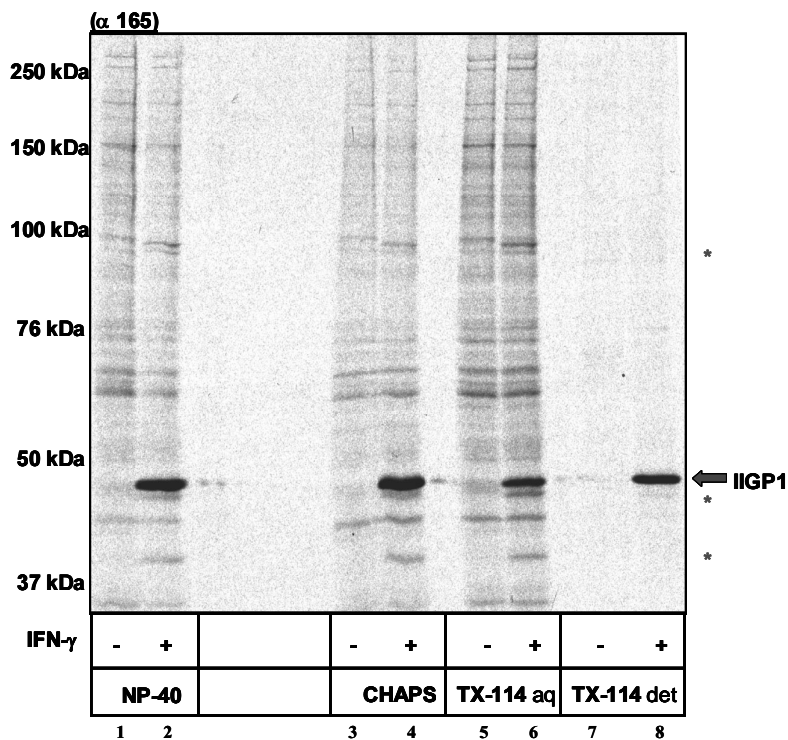
IFN- $\gamma$  induced or uninduced MEF cells, were metabolically labelled with [35S] Met, and were lysed with 1% NP-40 containing buffer and precipitated with  $\alpha$ 165 coupled protein A sepharose beads. The samples are loaded in duplicates. Prior immunoprecipitation (IP), the lysates were pre-cleared with the pre-immune serum denoted as pre-clear in the autoradiogram. In addition to the precipitation of IIGP1, there appears to be co-precipitation of two bands in IFN- $\gamma$  induced samples which is not visible in the uninduced control lanes, marked by the red asterix.

Immunoprecipitation under these conditions obtained the same two proteins of distinct size described before, and another additional protein ~ 47 kDa was visible which is not seen in the uninduced samples. This observation was consistent regardless of the detergent used, NP-40 or Chaps (figure 3.14A ; lane 1 and 3 uninduced, lane 2 and 4 induced). Besides, the differential distribution of IIGP1 in the membrane and the cytosol has been documented (figure 3.11A, lane 5 & 6), and also the different molecular forms in the respective fractions (soluble form showing ~ 47 kDa and membrane bound form ~150 kDa, data not shown). This led to the supposition for different patterns of co-precipitating molecules with the soluble and membrane bound forms. Therefore, the detergent Tx-114 was used since it has a temperature induced phase partitioning (4°C to 37°C), where the hydrophilic proteins (in this case, luminal or peripherally associated

proteins) into the aqueous phase, and the hydrophobic proteins (integral membrane proteins or amphipathic) in the detergent phase. Upon using these aqueous and detergent fractions for immunoprecipitation with the  $\alpha 165$  serum, the co-precipitation of the three proteins prevailed in the aqueous phase along with IIGP1 precisely as before, whereas only IIGP1 was precipitated in the detergent fraction, although equal distribution of IIGP1 in both the fractions was evident (figure 3.14A).

To conclude, the aqueous phase showing similar results to the whole cell lysates is not understood. Either, the co-precipitated proteins observed in the aqueous phase are not specific, or Tx-114 solubilises a portion of the complex from the membrane (two populations of 47 kDa and 150 kDa observed when the Tx-114 aqueous phase is subjected to size exclusion column as opposed to only 47 kDa with the soluble IIGP1, data not shown). On the other hand, the three co-precipitating molecules were not observed, possibly due to the temperature shift in this experiment which destroys the complex.

3.14A



3.14B

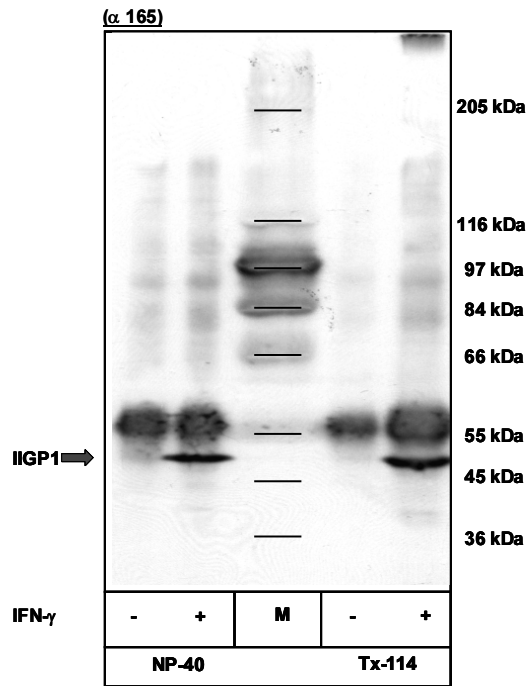


Figure 3.14. Three different proteins co-precipitate with IIGP1 in L929 cells.

A. IFN- $\gamma$  induced and uninduced L929 cells were metabolically labelled with [35S] Met/Cys and lysed in either 1% NP-40, 1% Chaps or 1% Tx-114 containing buffer, and immunoprecipitated with  $\alpha$ 165 coupled protein A sepharose beads. Autoradiography of the precipitated proteins shows three proteins along with IIGP1 in the induced lane, in comparison with the bands in the uninduced samples. B. Immunoblot of the IP samples from NP-40 and Tx-114 detergent lysis shows no staining of the co-precipitating proteins.

Immunoblotting with  $\alpha$ 165 on the immunoprecipitated material from Nonidet P-40 (NP-40) and Tx-114 derived IFN- $\gamma$  induced and uninduced L929 cell lysates. Only IIGP1 was detected by  $\alpha$ 165 and not the three putative co-precipitated proteins, as in figure 3.14 B. This strongly suggests that the co-precipitating proteins bind specifically to IIGP1. However, these molecules are yet to be analysed and identified.

#### III.B.3.2.4. Immunoprecipitation with the Monoclonal Antibodies

To determine the specificity of the co-precipitated molecules, immunoprecipitation of IIGP1 was analysed using monoclonal antibodies designated 10D7, 10E7, 5D9. IFN- $\gamma$  induced and uninduced L929 lysates were immunoprecipitated with the monoclonal antibodies as previously described. Immunoblot of the immunoprecipitated lysates with  $\alpha$ 165 serum was carried out to monitor IIGP1 precipitation by the monoclonal antibodies. The lysate control shows a distinct protein corresponding to the size of IIGP1, which is 47 kDa. All the antibodies precipitate IIGP1 with 10D7 giving a very weak signal in comparison to the other antibodies in figure 3.15, upper



panel. On the other hand, to test the interaction of the other p47 GTPases with IIGP1, the same immunoprecipitated samples were analysed by western blotting with reagents specific for three other members of the p47 family. No positive staining was visible for the three p47 GTPases analysed;  $\alpha$  IGTP,  $\alpha$  LRG47,  $\alpha$  TGTP. The expression of these proteins upon IFN- $\gamma$  induction are shown in the first lane. To conclude, the P47 GTPases that are tested in this experiment do not interact with IIGP1.

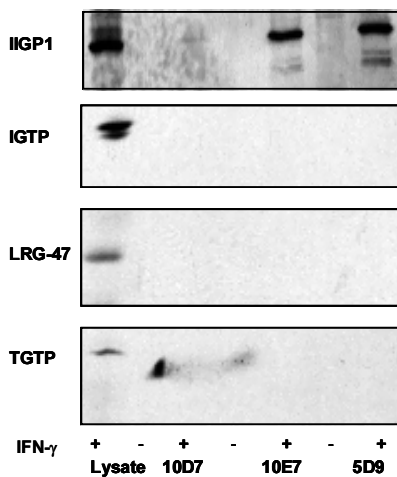


Figure 3.15. Immunoprecipitation with three distinct monoclonal antibodies.

L929 cells were induced or uninduced with 200 U/ml IFN- $\gamma$ , 24h post induction, cells were lysed with 1% NP-40 containing buffer, and precipitated with either  $\alpha$  10D7,  $\alpha$  10E7,  $\alpha$  5D9 coupled protein A sepharose beads. Immunoblot showing the precipitation of IIGP1 with the monoclonal antibodies; 10D7, 10E7 and 5D9 is shown in the upper panel. The subsequent panels stained for IGTP, LRG-47 and TGTP do not show any positive staining on the IIGP1 precipitated samples. The first two lanes indicate control lysates (the induced and the uninduced), the first lane of the last three panels show the expression of IGTP, LRG47 and TGTP respectively upon IFN- $\gamma$  induction.

### III.B.4. Properties of Membrane Associated IIGP1

#### III.B.4.1. Myristoylation is Important for Membrane Attachment.

IIGP1 has a putative N-terminal myristoylation site MGQLFSS which refers to the attachment of a fourteen-carbon saturated fatty acid (C14:0) to the glycine residue by an amide bond. The lipidated proteins are found to be associated with membranes post modification, implying access for potential interactions (Boutin, 1997). To analyse the influence of myristoylation, single point substitution of the glycine residue to alanine was done, which is known to prevent myristoyl modification. Cellular fractionation into the soluble and membrane bound forms indicate solubilisation of a significant proportion of the membrane bound IIGP1 in

comparison to the wild type. This is demonstrated in figure 4.5, where the distribution of the transfected myristoylation mutant IIGP1-Nm is shown in comparison to the transfected IIGP1-wt.

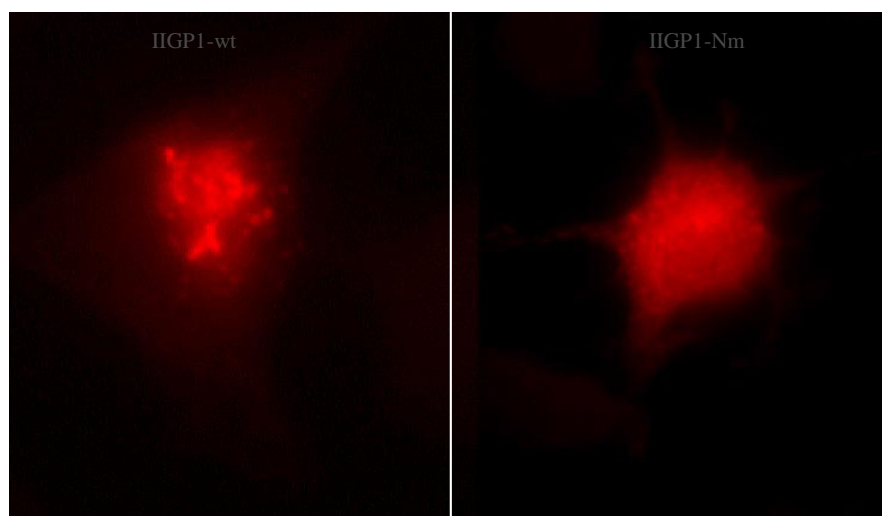


Figure 3.16. Myristoylation is important for membrane attachment.

L929 cells grown on cover slips, and were transfected with the respective mutants for 24 h with FuGENE™ 6 reagent. The cells 24 h post transfection were fixed with 3% paraformaldehyde, and permeabilised with 0.1% saponin and stained with  $\alpha$ 10D7 antibody, and used Alexa 546 coupled secondary antibody. The staining was analysed with an Axioplan II fluorescence microscope, a cooled CCD camera and the pictures are processed using the Metamorph software. Immunofluorescence studies with IIGP1-Nm mutant (G2A), prevents myristoylation and renders the protein more soluble as shown by the more soluble staining in the IIGP1-Nm mutant.

However, there is a small fraction of the protein still in the membrane fraction, independent of this fatty acid modification, showing that it possibly utilizes another mode of attachment to the membranes. Immunofluorescence studies on IIGP1 Nm in L929 cells, shows a more diffused pattern compared to the transfected IIGP1 wt cellular distribution as shown in figure 3.16. This suggests the significance of this post-translational modification on IIGP1 for its association with the membrane.

#### III.B.4.2. C-terminal Mutants

Several biochemical properties of the two C-terminal mutants (Table 1), IIGP1-m with the two different and 9 extra residues and IIGP1-His with the C-terminal his tag (6x) has been described. To recapitulate, the IIGP1-m has similar features as the wild type, but not IIGP1-his. *In vitro* studies demonstrated that IIGP1-m and IIGP1-wt and IIGP1-his maintained similar binding affinities for the nucleotides irrespective of their different c-terminal modifications. All the three

proteins hydrolyse GTP to GDP, but with different features. IIGP1-his failed to demonstrate cooperativity and GTP oligomerisation as opposed to the former two proteins. This articulates the influence of the 6x his residues, although the IIGP1-m likewise has nine extra residues and still behaves like the wild type, which is a contrariety. Probably, the nature of the two different C-terminal extension is the reason for such an observation.

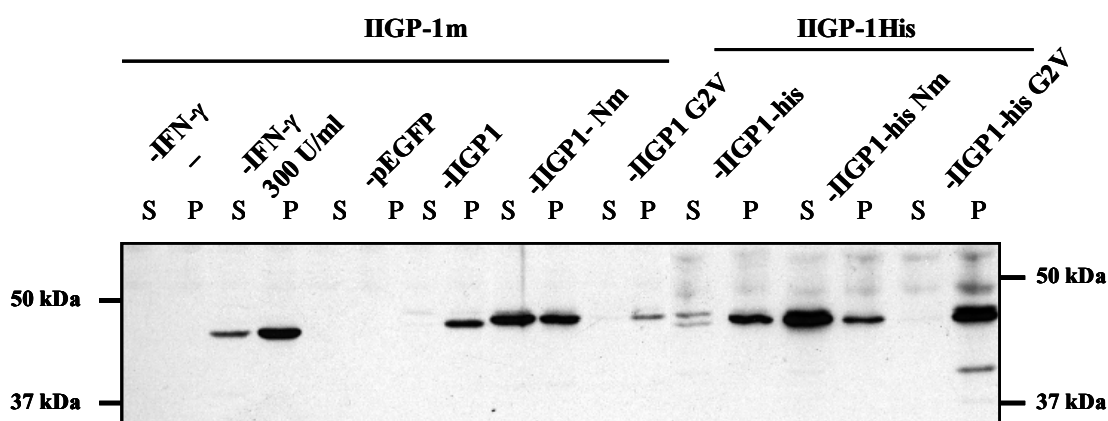


Figure.3.17. *In-vivo* characterisation of the C-terminal mutants

L929 cells were either induced or uninduced with 200 U/ml IFN- $\gamma$ , or transfected the respective constructs with FuGENE<sup>TM</sup> 6 reagent. 24 h post induction/ transfection, cells were lysed under hypotonic buffer conditions, and the post-nuclear supernatant and pellet were subjected to SDS-PAGE and western blotting.

*In vivo* studies on these mutants were therefore carried out to understand the importance of the C-terminal region of IIGP1. Immunofluorescence studies, as described above (figure 3.10) show the typical reticular stain of the ER in case of the latter two, but is not evident in the former, leading to certain accumulations in the perinuclear region. This confirms the nature of IIGP1-his to be again different from IIGP1m and IIGP1wt. When the cellular distribution of both the proteins were analysed, both IIGP1-m and IIGP1-his show the differential distribution between the soluble and the membrane bound forms showing accordance with the transfected IIGP1-wt and the endogenous (IFN- $\gamma$  induced) IIGP-1. The additional N-terminal myristoylation (Nm) mutant of IIGP1-m and IIGP1-his clearly shows a shift from the membrane to the soluble form as IIGP1-Nm described in figure 3.17.

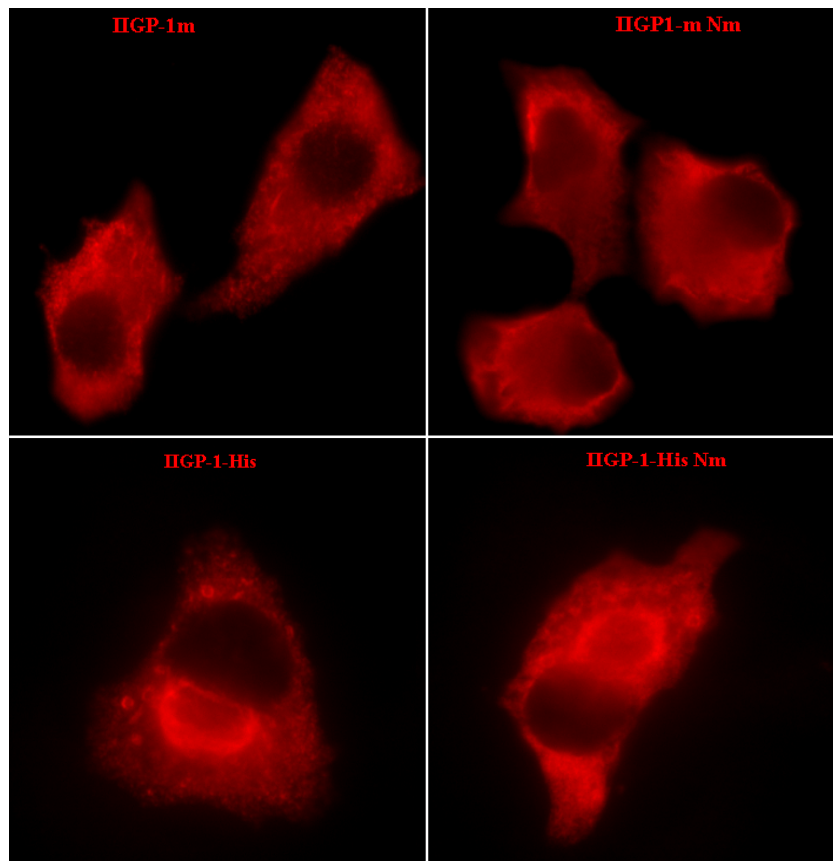


Figure.3.18. Localisation of the C-terminal mutants, IIGP1-m and IIGP1-his.

L929 cells grown on cover slips, and were transfected with the respective mutants for 24 h with FuGENE™ 6 reagent. The cells 24 h post transfection were fixed with 3% paraformaldehyde, and permeabilised with 0.1% saponin and stained with  $\alpha$  10D7 antibody, and used Alexa 546 coupled secondary antibody. The staining was analysed with an Axioplan II fluorescence microscope, a cooled CCD camera and the pictures are processed using the Metamorph software.

This confirms the influence of myristoylation on the membrane attachment of IIGP1. However, the additional G2V mutants of IIGP1-m and IIGP1-his are predominantly membrane bound indicating no influence of nucleotide binding. Additionally, localisation studies also comply with the fractionation studies, where the myristoylation mutants show a diffuse, cytosolic stain in comparison to the wildtype as shown in the upper panels (IIGP1-m and the additional myristoylation mutant) and the lower panels (IIGP1-his and the additional myristoylation mutant) in the figure 3.18. Rather, myristoyl modification seems to be modulating the IIGP1 localisation. Also, size exclusion chromatography of the unmyristoylated IIGP1 always runs as a monomer (data not shown).

### III.B.4.3. Myristoylation independent association to the membrane

A significant fraction of IIGP1 is membrane associated. Myristoylation has been shown to be important for the membrane association of IIGP1, although not solely (figure 4.5 and figure 3.16). Therefore the properties of membrane binding of demyristoylated IIGP1 was analysed. L929 cells were either induced with 200 U/ml IFN- $\gamma$ , or transfected with the respective constructs with FuGENE<sup>TM</sup> 6 reagent. 24 h post induction/ transfection, the cells were lysed in a hypotonic buffer. The distribution of endogenous IIGP1 is consistent being mostly membrane bound and partly soluble (upper panel, hypotonic supernatant, lane 2) as shown in figure 3.19. The membrane bound fraction of IIGP1 was solubilised with a high salt (lane 3), and then a high pH buffer (lane 4). Interestingly, a small fraction of the protein is solubilised under high salt (750 mM NaCl supernatant), and also in a high pH buffer (Na<sub>2</sub>CO<sub>3</sub>S supernatant) as shown. This suggests that the membrane association of IIGP1 is dependent on protein-protein interactions. Still, a considerable amount of the protein is intact, on the membrane (Na<sub>2</sub>CO<sub>3</sub>S pellet, lane 5).

The same experiment was repeated for the IIGP1-Nm mutant, which is mostly cytosolic (IIGP1-Nm panel, lane 2). Interestingly, there is a significant proportion of the protein still bound to the membrane. This suggests another means of membrane association of IIGP1, apart from myristoylation and ionic interactions. IIGP1-his on the other hand, has a significant portion of the protein that is membrane bound, and some of them are solubilised with a high salt wash, and a high pH wash, but a significant portion is intact on the membrane. This is possibly the myristoylated IIGP1-his, and another fraction whose mode of membrane attachment is not known; unless the cysteine residue at the C-terminal end -CLRN- is subjected to lipid modification. The LRG-47 is used as a control for this experiment where it shows very tight membrane binding, and is resistant to a high salt/ high pH wash. This proves that apart from myristoylation, there are other features that allow membrane binding of IIGP1, mediated by protein-protein interactions, or other protein-lipid interactions.

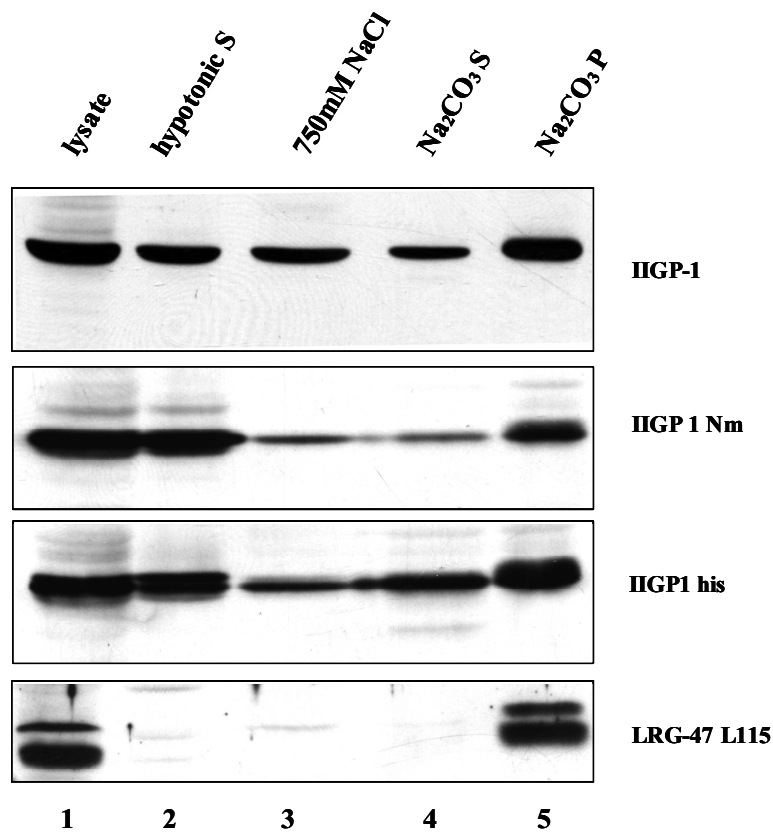


Figure 3.19. Membrane association of IIGP1.

L929 cells were either induced or uninduced with 200 U/ml IFN- $\gamma$ , or transfected with the respective constructs (IIGP1-Nm, IIGP1-his) with FuGENE<sup>TM</sup> 6 reagent. 24 h post induction/ transfection, cells were lysed under hypotonic buffer conditions, and the insoluble membrane pellet was first washed with 750 mM NaCl, and further washed with Na<sub>2</sub>CO<sub>3</sub>S-pH 11, and the pellets were subjected to SDS-PAGE and western blotting. Lane 1 contains the hypotonic lysate; hypotonic treated supernatant in lane 2; hypotonic pellet solubilised with high salt in lane 3, salt insoluble pellet treated with high pH (11) showing a small soluble fraction in lane 4, and the still membrane bound protein in lane 5. The first panel shows the distribution of IIGP1 in IFN- $\gamma$  induced cells, followed by transfected IIGP1-Nm and transfected IIGP1-his detected with  $\alpha$  10D7 antibody. LRG-47 (member of the GMS subfamily) in IFN- $\gamma$  induced cells is used as a control, and was detected with  $\alpha$  LRG47 antiserum.

## IV. RESULTS II

### IV. A. Structural Features and Mutational Analysis

#### IV.A.1. Crystal Structure of IIGP1

Full length IIGP1 crystals diffracted to 2.1 Å resolution. The structural determination of IIGP1 was done by Dr. Eva Wolf. The crystals belong to the orthorhombic space group P212121 and contain two molecules per asymmetric unit (figure 4.1). The IIGP1 molecule has two domains, the globular GTPase domain and a helical domain. The helical domain contains 10 helices, first three helices form the N-terminal region (dark grey), followed by the G-domain (fluorescent green), and last seven helices form the C-terminal region (orange). A linker helix connects the G domain to the C-terminal helical regions (cyan). The topology of the G domain is identical to Ras (Wittinghofer and Pai, 1991).

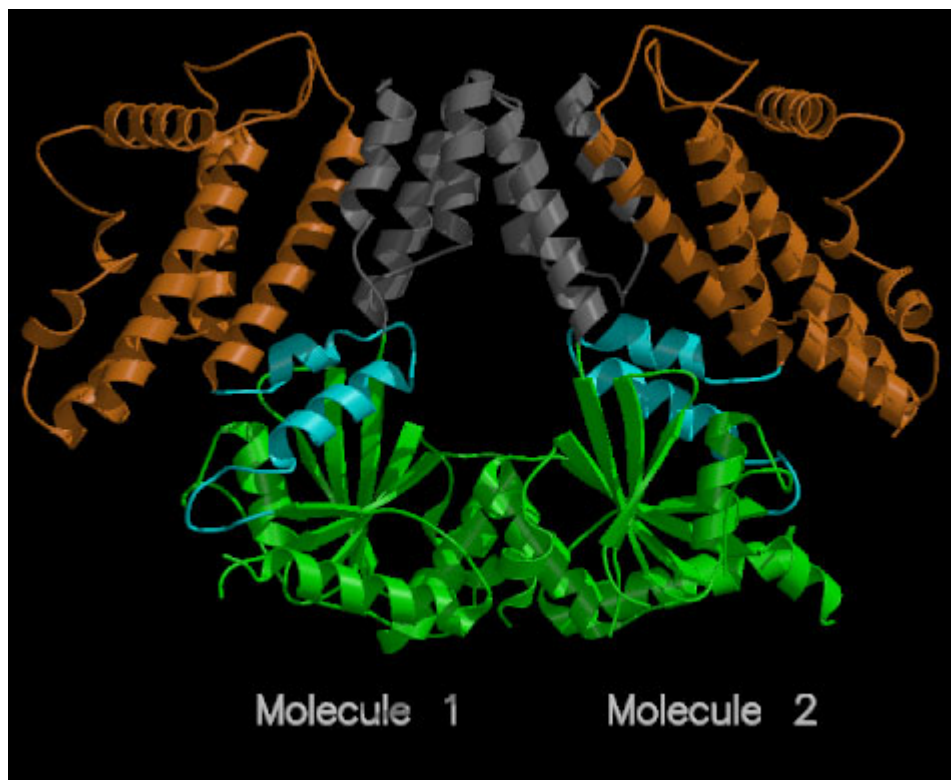


Figure 4.1. Nucleotide free structure of IIGP1 showing the N-terminal helical region (dark grey) followed by the G-domain (fluorescent green) continuing to form the c-terminal helical region (orange). The linker helix connecting the G-domain with the c-terminal helical domain is shown in cyan.

The G domain consists of a 6 stranded  $\beta$ -sheet of mixed topology with five parallel and one anti-parallel  $\beta$ -strand, which is surrounded by five alpha helices, a short  $3_{10}$  helix and several loop regions. In comparison to Ras, the IIGP1 molecule has a 13 amino acid insertion (residues 190-201) in the G domain.

The two IIGP1 molecules have two dimerisation interfaces. Interface I involves knobs into holes side chain interactions between two N-terminal helices, and Interface II is characterised by a remarkable surface complementarity resulting from reciprocal hydrophilic and hydrophobic interactions between the G domain. Dimerisation leads to the formation of a prominent roundish hole with a diameter of roughly 20 Å. The lower part of the hole is formed by the GTPase domain, whereas the upper part of the hole is formed by the N-terminal helices. The roundish shape of the hole suggests a clamp-like function of the dimer, e.g as shown for several DNA- binding proteins (Brino et al., 2000; Ghosh et al., 1995). However, the walls of the hole are not positively charged. The electrostatic surface potential of IIGP1 reveals a polar distribution of charges with a cluster of negatively charged residues polarised on either sides of the dimer. This could be a potential effector binding site. The best structural homologues of the GTPase domain of IIGP1 from the PDB databank are EF-Tu, Ras and Arf1.

#### IV.A.2. Features of the IIGP1-GDP and the IIGP1-GppNHp Complex Structure

The crystals of the GDP and GppNHp complex of IIGP1 diffracted to 2.0 and 2.7 Å respectively. The structures were solved by molecular replacement using the refined structure of nucleotide-free IIGP1 as a search model by Agnidipta Ghosh. These two complex nucleotide structures have similarities in their G domain to the nucleotide bound structures of Ras, Arf, Ef-Tu,  $\alpha$ -subunit of G protein and SRP. From the complex structures, the five GTP binding motifs were identified; G2 and G5 were revealed from the nucleotide bound structures; G1, G3, and G4 were already evident from the primary sequences (Bourne et al., 1991) as shown in figure 4.2A. The G2 motif in IIGP1 is within the switch I region, identified as Thr 108, corresponding to Thr 35 of Ras and the G5 motif <sup>231</sup>SNK<sup>233</sup> has been identified as an additional base binding motif corresponding to the SAK/L of small GTPases.



#### 4.2A

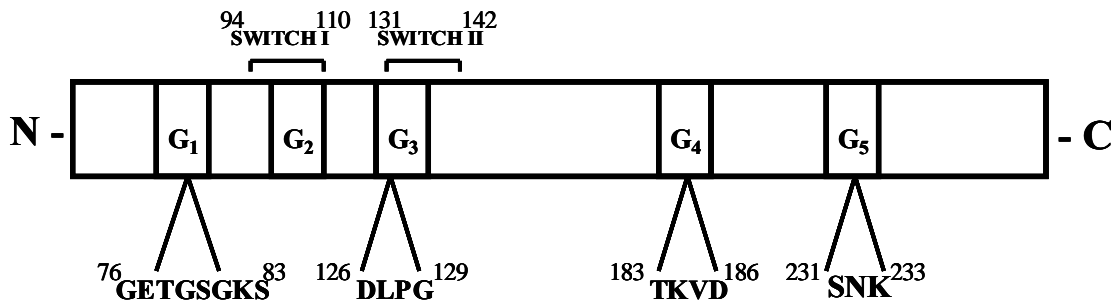


Figure.4.2A. GTP binding motifs of IIGP1

A. The nucleotide binding motifs are highly conserved among GTPases. Firstly, the phosphate binding loop, (P-loop) which has the characteristic GETGSGKS for IIGP1, and two regions switch I (G2) and switch II (G3) whose sequences vary between, and to a lesser extent within small GTP binding protein families. The specificity of the nucleotide is derived by N/TKXD motif, and the SNK motif, an additional base binding motif is described from the nucleotide bound structure.

#### 4.2B

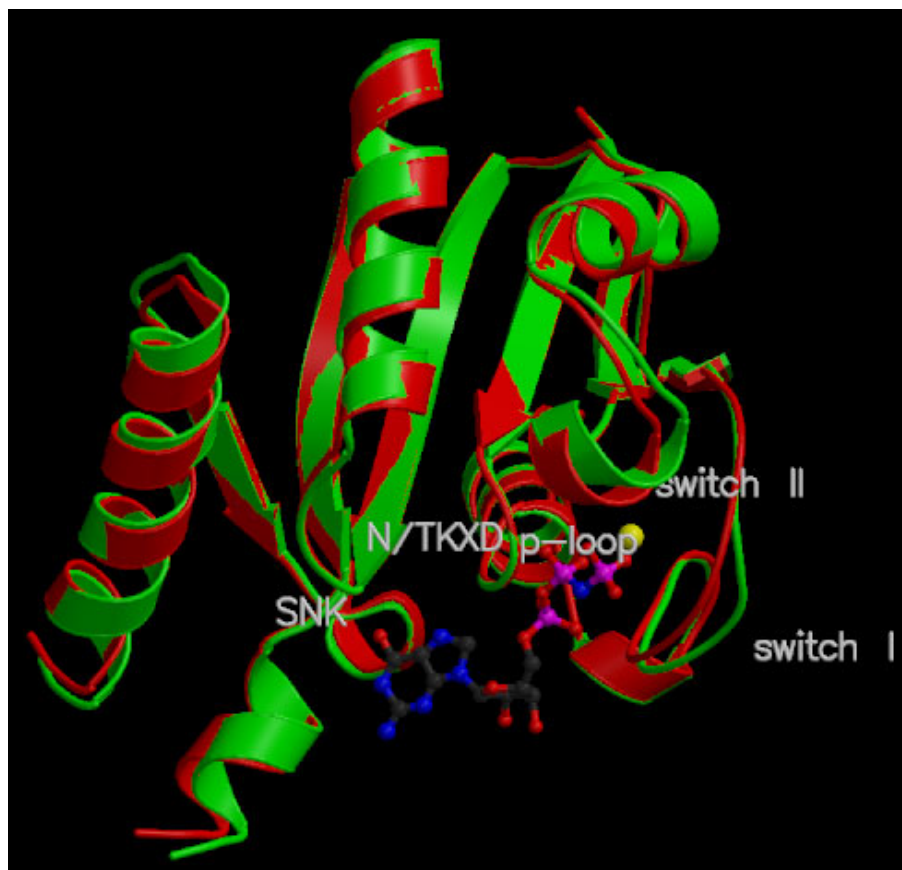


Figure.4.2B. IIGP1-GDP/GppNHp structure

The canonical GTP binding motifs (G1-G5) are described in the figure. The IIGP1-GDP structure is shown in red, superimposed with the IIGP1-GppNHp structure shown in green.

The nucleotide free IIGP1 structure and the IIGP1-GDP structures upon superposition do not show major differences and deviations in the overall structure. But the IIGP1-GDP and IIGP1-GppNHp structures do have some differences mainly in the G-domain as shown in figure 4.2B. All the GTP binding regions superimpose perfectly except for the conformation in the switch I region which moves away from the nucleotide binding site, as shown in the figure 4.2B.

#### IV.B. Mutational Analysis

Nucleotide binding parameters are very crucial, as they modulate the function of GTPases. In order to obtain nucleotide binding deficient and GTP hydrolysis deficient mutants, point mutations were introduced in the phosphate binding loop (P-loop) of the protein, which abolished binding or hydrolysis in other GTPases (Chung et al., 1993). The mutations were introduced in the G1 motif, <sup>76</sup>GETGSGKS<sup>83</sup> of IIGP1 and were called G2V (G76V / G81V), and K82A as depicted in the Table 3. G12V of Ras forms a constitutively active, oncogenic Ras (corresponding to G76 of IIGP1), and the K82A mutants show deficiency in nucleotide binding in other GTPases (Pai et al., 1990).

The crystal structure of IIGP1 shows two molecules related by a two fold non-crystallographic symmetry axis (figure 4.3 A,B,C,D showing the interface contacts). They share two dimer interfaces, interface I formed by the N-terminal domain and interface II formed by the two G-domains of the IIGP1 molecules. Based on the distance between the two molecules in both the interfaces, potential residues were mutated with a criterion to de-stabilise the dimer interfaces. Two G domain interface mutants were designed. The side chain oxygen of Ser172 is stabilised by intramolecular interaction with the backbone nitrogen of Met173, and also by intermolecular interaction with the side chain sulphur of Met173 from another molecule as shown in figure 4.3A. Met173 in turn is stabilised by the hydrophobic pocket created by the hydrophobic residues (Phe, Ile ) from the corresponding molecule as shown in figure 4.3B. The Ser172 residue was replaced by Arg, thereby a steric mutant. The Met173 was replaced by Ala which is likely to destabilise the dimer by creating two (reciprocal) cavities.

In the N-terminal interface, another steric mutation was introduced, Leu 44 to Arg. Leu44R interacts with itself forming hydrophobic interactions between the side chains. The carbonyl oxygen of Leu44 contacts the backbone nitrogen of Lys46 with a distance of 2.74 Å.

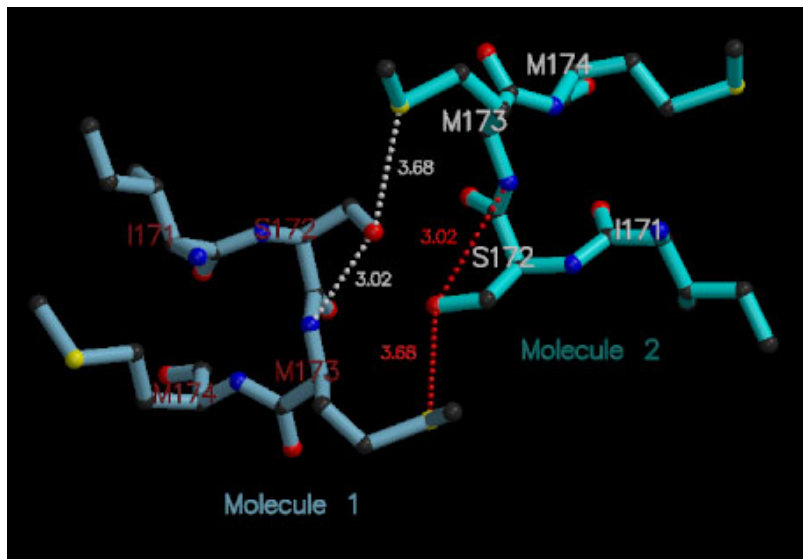


Figure.4.3A.

Ser172 and Met173 - The side chain oxygen (red) of Ser172 in molecule 2 is stabilised by intramolecular interaction with the backbone nitrogen (blue) of Met173, and also by intermolecular interaction with the side chain sulphur (yellow) of Met173 from molecule 1 as shown in figure 5a.

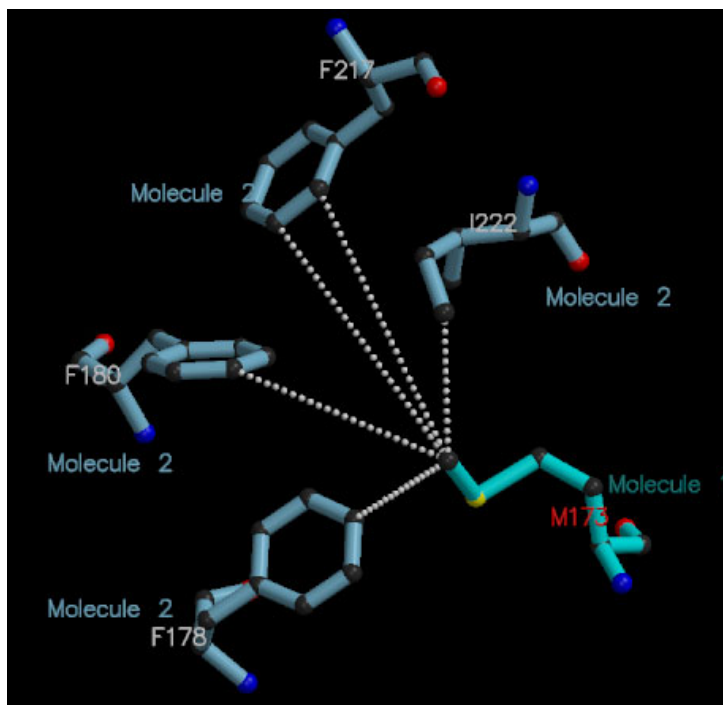


Figure.4.3B.

Met173 - The Met173 of molecule 1 in turn is stabilised by the hydrophobic pocket created by the surrounding hydrophobic residues (Phe, Ile ) of molecule 2 as shown by the white lines figure 5b.

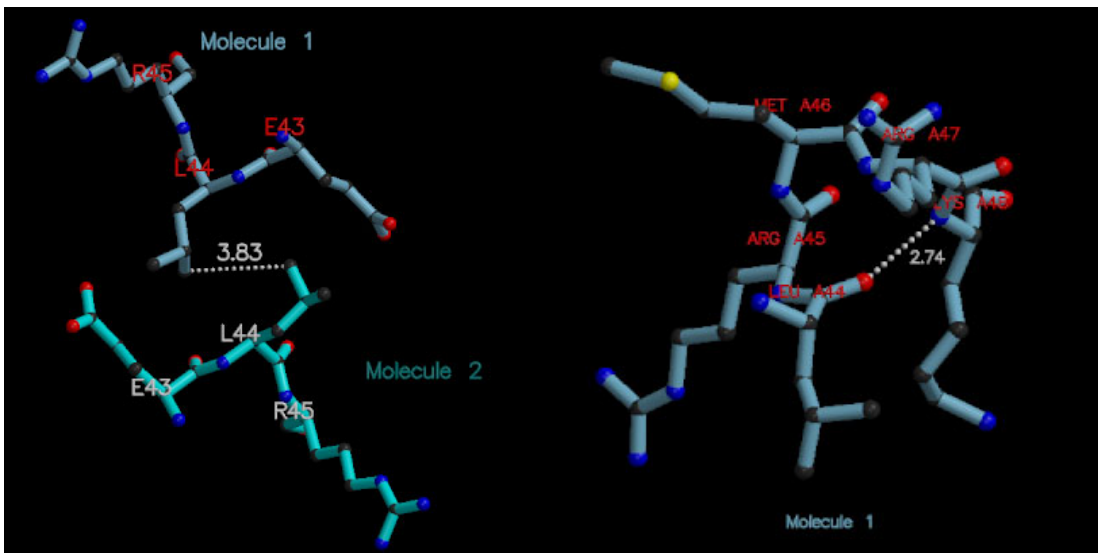


Figure.4.3C and D

Leu44, Lys48 - Leu44R interacts with itself forming hydrophobic interactions between the side chains. The carbonyl oxygen of Leu44 contacts the backbone nitrogen of Lys48 with a distance of 2.74 Å.

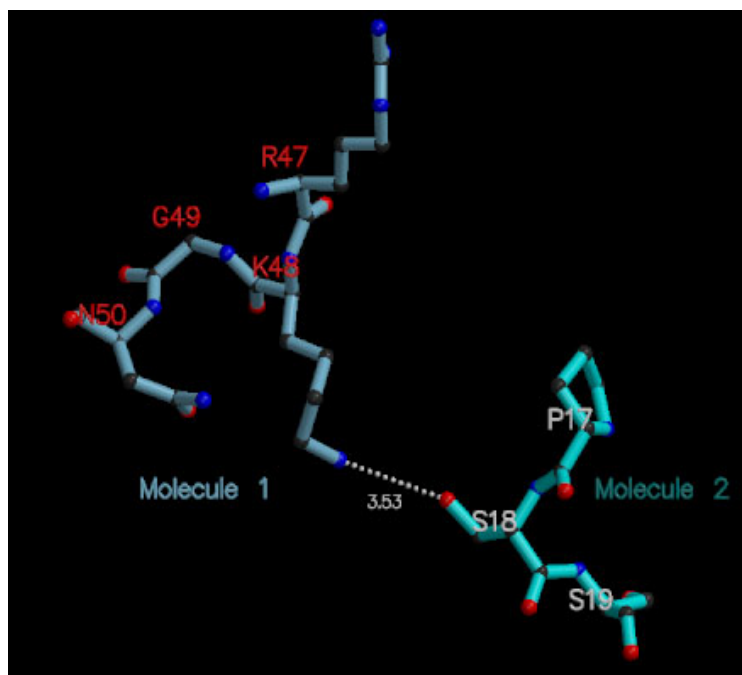


Figure.4.3E.

Lys48 - The side chain nitrogen (blue) of Lys48 of molecule1 interacts with side chain oxygen (red) of Ser from molecule 2. The distance of this salt bridge is found to be 3.53 Å

Lys 48 was replaced by either Ala or Glu. K48A probably eliminates a salt bridge in the helical dimer interface, thereby weakening dimerisation. K48E, seems suggestive of making alternative

salt bridges and seems like a mild destabilisation in the dimer interface. Also, a double steric mutant L44R/ S172R (L/S) was also designed which is believed to dissociate the dimers. The figures dealing with the IIGP1 structure were made by Agnidipta Ghosh.

#### IV.B.1. Biochemical Features

The mutants were expressed as GST fusion proteins. The proteins were purified as described in Materials & Methods. Recombinant purified proteins are nucleotide free and are stable in the absence of nucleotides.

##### IV.B.1.1. Analysis of the binding mutants

	mGTP	mGDP
GETGSGKS <b>G2V</b>	Not done	- No binding -
GKS <b>K82A</b>	- No binding -	0.69 $\mu$ M
TKVD <b>D186N</b>	- No binding -	15 $\mu$ M
	mXppNHp : 55 $\mu$ M	mXDP : (0.07 $\mu$ M)

Table 4.1. Nucleotide binding affinities of the mutants to mant labelled guanine and xanthine nucleotides.

The nucleotide binding properties of the p-loop mutants were analysed by stopped flow (Table 4.1). The G2V mutant did not show any mGDP binding. Since the G2V mutant did not bind mGDP, although IIGP1-wt has a 15-fold higher affinity to GDP than GTP, we supposed that this protein could not bind GTP either. Therefore the mGTP binding was not checked.

However, we analysed the GTPase activity of this mutant, and found its inability to bind GTP. In case of the K82A mutant, mGDP binding was similar to the wild type as shown in the table. Besides, it did not bind GTP. The Aspartic acid residue of the TKVD motif is responsible for guanine nucleotide specificity. Henceforth, we mutated the D186 to Asparagine (N). D186N which showed a 15-fold weak binding for mGDP in comparison to the wild type, as opposed to no binding for mGTP, and could not hydrolyse GTP. However, this mutation led to specificity for xanthine nucleotides (borrowed from Dr. J Reinstein), where it shows nanomolar affinity binding for mXDP, and low affinity binding to mXppNHp. The exchange of D for N has been shown to lower affinity for GTP and increase the affinity for XTP (Kang et al., 1994; Yu et al., 1997). The binding parameters for D186 residue of IIGP1 thus determines guanine nucleotide specificity, as described for the other GTPases

#### IV.B.1.2. Analysis of the Interface Mutants

##### IV.B.1.2.1. Analysis of the Nucleotide Binding Parameters of the Interface Mutants

The nucleotide binding affinities of the interface mutants are very similar to IIGP1-wt as shown in Table 4.2, thereby implying that interference with the dimer interface does not hamper nucleotide binding properties

##### IV.B.1.2.2. Studies on GTP Hydrolysis

To study the influence of these mutations on GTP hydrolysis and cooperativity, the GTPase activity of all the mutants were measured. The interface mutants hydrolyse GTP to GDP as the wildtype, however all of them fail to show co-operativity displaying disparity with the wildtype as shown in the figure 4.3. IIGP1-wt shows an eight fold increase in the specific activity with increase in protein concentration ( $0.1- 0.8 \text{ min}^{-1}$ ). Distinctly all the mutants fail to display cooperativity, and have a specific activity of  $0.04 - 0.1 \text{ min}^{-1}$  with the exception of K48E, showing a modest increase in activity with increase in concentration of the protein ( $0.3 \text{ min}^{-1}$ ). The G domain interface mutants S172R and M173A have the lowest activity of  $0.04 \text{ min}^{-1}$ .

Table 4.2. Comparative nucleotide binding affinities of IIGP1 and the mutants.

STOPPED FLOW				FLUORESCENCE TITRATION
Nucleotides	$k_{ov}$ ( $\mu\text{M}^{-1}\text{s}^{-1}$ )	$k_{off}$ ( $\text{s}^{-1}$ ) (displacement)	$K_d$ ( $\mu\text{M}$ )	$K_d$ ( $\mu\text{M}$ )
<b><u>mGTP</u></b>				
IIGP1- wt	0.98	21.6	22	
IIGP1- m	1.30	21	16.1	
IIGP1- his	1.11	14.28	12.9	
L44R	1.14	14.82	12.9	
K48A	2.2	16.6	7.6	
K48E	1.29	34.54	26.6	
S172R	1.85	11.73	6.3	
M173A	0.87	9.1	10.4	
L/S	0.73	16.46	22.4	
<b><u>mGDP</u></b>				
IIGP1- wt	1.55	0.99	0.64	
IIGP1- m	1.65	1.6	0.97	0.90
IIGP1- his	1.31	0.698	0.53	
L44R				0.46
K48A				0.64
K48E	2	1.17	0.58	
S172R	1.43	1.19	0.83	
M173A	1.57	1	0.64	
L/S	1.83	0.89	0.49	

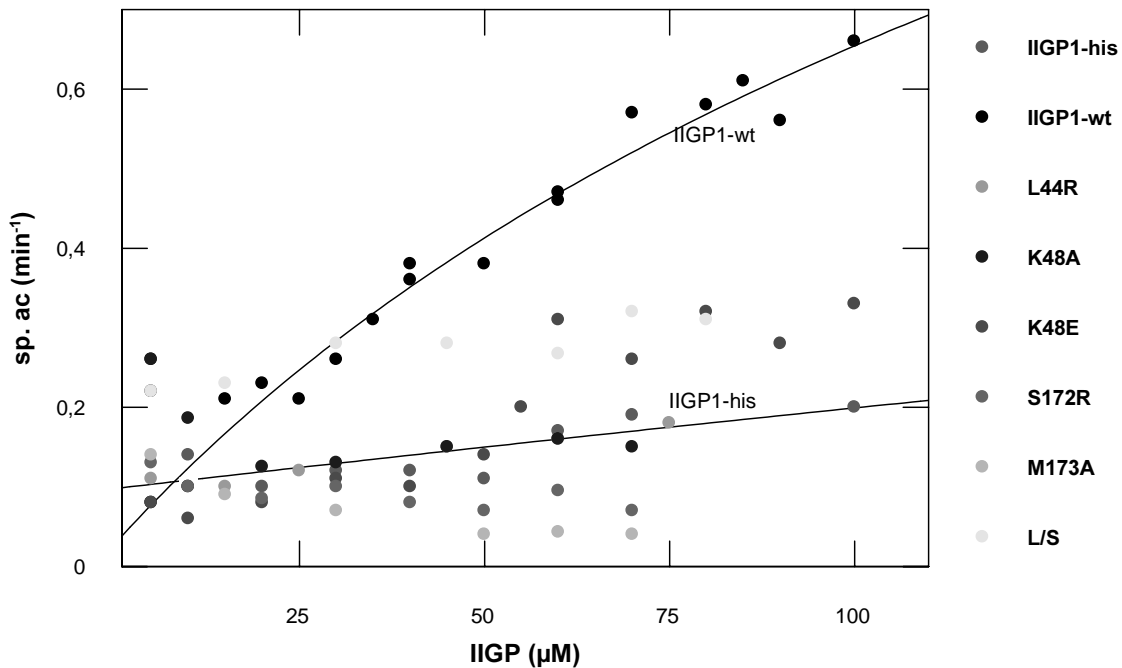


Figure 4.3. Interface mutants have depleted cooperativity.

GTPase activity was measured at 37°C, with 700  $\mu\text{M}$  GTP and varying concentrations of the protein (2  $\mu\text{M}$  – 100  $\mu\text{M}$ ) as shown above. The interface mutants do not show co-operative mechanism of GTP hydrolysis like the IIGP1 wt protein (black filled circles), but is in accordance with the IIGP1 his (dark green circles) as shown in the figure.

#### IV.B.1.3. *In vivo* Characterisation of the IIGP1 Mutants

As shown in figure 4.3 (above), interfering with the interface mutants resulted in abrogated co-operativity. Therefore to understand the cellular behaviour, all the interface mutants were subjected to cell biological characterisation. They were cloned into an eukaryotic expression vector pGW1H (Materials & Methods, and were characterised with respect to their localisation and distribution, upon transfecting these constructs to L929 fibroblasts.

##### IV.B.1.3.1. Cellular Localisation of the Binding and the Interface mutants

The interface mutants were transiently transfected into L929 cells by lipofection and 24 h post transfection, the cells were analysed by immunofluorescence studies with IIGP1 specific  $\alpha 10\text{D}7$  antibody. Some important features were evident from the localisation studies of these mutants as shown in figure 4.4. The features that seemed obviously distinct are the ring around the peri-nuclear region (like IIGP1-his), the dotted pattern as described for the transfected IIGP1 wt, and the regular reticular stain of the ER. L44R, S172R, M173A, and the L/S mutant had phenotypes



typically observed for the IIGP1-his, and none of them show cooperative GTPase activity. The K48A and the K48E mutant looked more like the transfected IIGP1-wt pattern (K48A showed no cooperativity as opposed to moderate cooperativity in the case of K48E). To conclude, all the mutants have distinct features in their cellular localisation. In comparison to the wild type. Co-localisation studies would be helpful in the identification and the characterisation of these features.

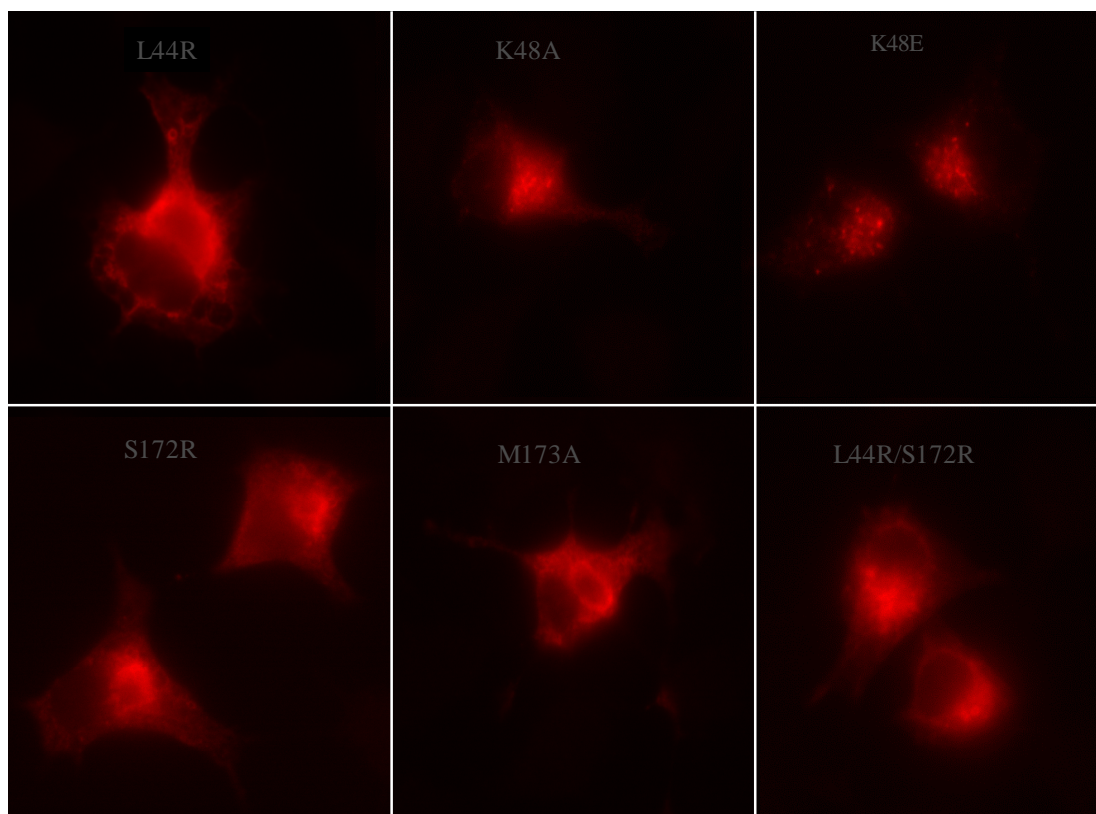


Figure.4.4. Localisation of the Interface mutants in L929 cells

L929 cells grown on cover slips, and were transfected with the respective mutants for 24h with FuGENE<sup>TM</sup> 6 reagent, a multiple component lipid based transfection reagent. The cells 24h post transfection/induction were fixed with 3% paraformaldehyde, and permeabilised with 0.1% saponin and stained with a 10D7 antibody, and used Alexa 546 coupled secondary antibody. The staining was analysed with an Axioplan II fluorescence microscope, a cooled CCD camera and the pictures are processed using metamorph software.

#### IV.B.1.3.2. Distribution of the Binding and the Interface mutants

IIGP1 has differential distribution in the cell, mostly membrane bound and partly in a soluble form as shown in figure 3.10. In order to analyse the influence of nucleotide binding, hydrolysis and the effects of the interface mutants on the differential distribution of IIGP1, cellular fractionation studies were carried out (figure 4.5). The binding mutants and the interface mutants

were transfected to L929 fibroblasts. 24h post-transfection, the cells were subjected to hypotonic lysis, the soluble and membrane forms were separated and subjected to SDS- PAGE and western blotting with the  $\alpha$ 10D7 serum as shown in the figure. The endogenous IIGP1 is consistently shown in the soluble and membrane bound form, the transfected IIGP1 wt and IIGP1-his also shows a similar distribution.

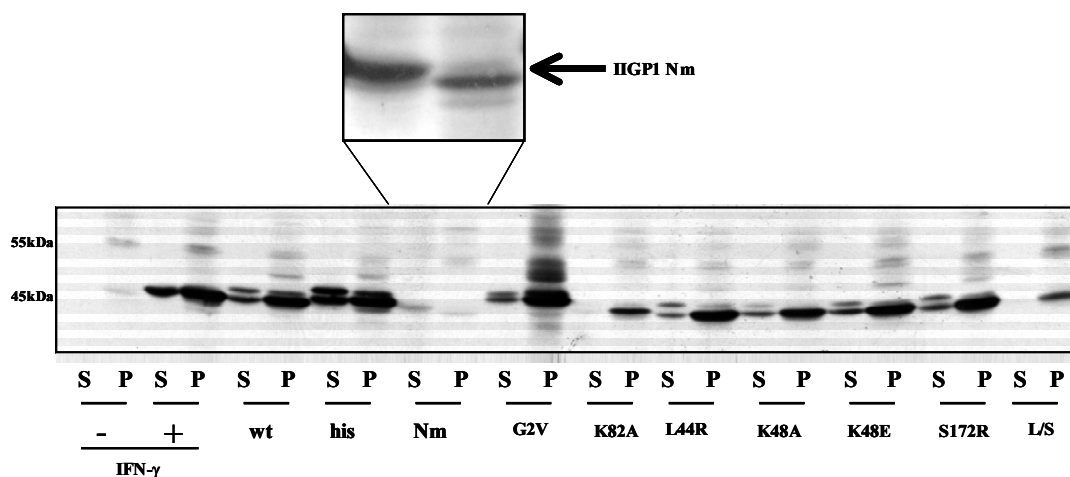


Figure. 4.5. Cellular distribution of the interface mutants

L929 cells were either induced or uninduced with 200 U/ml IFN- $\gamma$ , or transfected with FuGENE<sup>TM</sup> 6 reagent. 24 h post induction/ transfection, cells were lysed under hypotonic buffer conditions, and the post-nuclear supernatant and pellet were subjected to SDS-PAGE and western blotting. IIGP1-Nm mutants is the myristoylation mutant, the description for which is included in the section III.B.4.1.

The nucleotide binding mutants K82A and G2V, does not show any affect in their membrane attachment in comparison to the wild type, although they have defect in the nucleotide binding properties (the former deficient for GTP binding and the latter for GTP as well as GDP binding). Additionally, all the dimer interface mutants (L44R, K48A, K48E, S172R, M173A, L/S) without any exception, can still bind to the membranes as the wild type. This indicates that neither nucleotide binding nor interference with the dimer interface interferes with the membrane attachment of IIGP1.

## V. DISCUSSION

This study encompasses biochemical, structural and cellular studies on IIGP1. The biochemical characterisation focuses on understanding the properties of IIGP1 as a GTPase. GTPases modulate diverse functions by binding to a variety of effectors and regulators in the different nucleotide states (Bourne, 1991). In comparison to other GTPases, the properties of IIGP1 with respect to the nucleotide binding parameters, hydrolytic mechanism and structural features are analysed.

### V.1. Nucleotide Binding Parameters of IIGP1 in Comparison to Several GTPases

To position IIGP1 in the context of the other GTPases, a comparative analysis of their properties are tabulated (table 5.1). The family of small GTPases has a very high affinity for nucleotides, and are stable only in the presence of nucleotides. IIGP1, on the other hand has very low nucleotide affinities (micromolar  $K_d$  value) and is stable in the absence of nucleotides. Therefore IIGP1 is grouped with the large GTPases, the dynamins, hGBP1 and Mx GTPase which have very low nucleotide affinities and are also stable in the absence of nucleotides. However dynamin and Mx exist as oligomers in solution (Danino and Hinshaw, 2001; Haller and Kochs, 2002). Additionally, the nucleotide free IIGP1 structure and the IIGP1-GDP structures upon superposition do not show major differences and deviations in the overall structure. The regions which undergo alteration upon nucleotide binding are designated as switch regions (switch I and switch II) in the small GTPase family (Vetter and Wittinghofer, 2001). The stability of the switch regions in the nucleotide free IIGP1 structure and the IIGP1-GDP structures presumably explains the stability of the protein in solution.

IIGP1 has higher affinity for GDP than for GTP (15-fold) as listed in table 5.2 and therefore may be considered EF-Tu like in this respect. Ras and EF-Tu have very slow nucleotide dissociation rates (table 5.2). Both of them bind GDP very tightly (pM and nM  $K_d$  values) and therefore the GDP release is regulated by the guanylate exchange factors (GEFs), Sos and EF-Ts respectively (Gromadski et al., 2002; Boriack-Sjodin et al., 1998; Chardin et al., 1993). The guanylate exchange factors function by increasing the dissociation rates. The dissociation rates for IIGP1 are very high,  $21 \text{ s}^{-1}$  for GTP and  $3.6 \text{ s}^{-1}$  for GDP. This indicates a very short life span for the complexes as compared to Ras-like GTPases,  $G\alpha$  or EF-Tu. The GEF catalysed GDP dissociation rates of Ras and EF-Tu are comparable to the intrinsic dissociation rates of IIGP1 as shown in table 5.2. Therefore, guanylate exchange factors (GEF) do not seem to be necessary to promote activation of IIGP1 through replacement of GDP with GTP. This is also supported by structural observations

where the GDP-IIGP1 structure already mimics a GEF bound conformation. Therefore we presume that GEF is not necessary for IIGP1. Given the nucleotide binding properties of IIGP1 and the relative cellular concentrations of GTP (90 %) and GDP (10 %), the molar ratio of the GDP and GTP states should be close to one. Here, we can only speculate about a shift in the relative populations invoked by a potential interaction partner, which might change the relative affinities of GDP and GTP.

Table 5.1. Summary of the comparative nucleotide binding affinities in GTPases (upper panel) and the lower panel shows the GTP versus GDP affinities. (Similar means less than 5 fold difference and higher means more than 10 fold). (Binns et al., 1999; Binns et al., 2000; Eccleston, 1984; Eccleston et al., 2002; Gromadski et al., 2002; John et al., 1990; Klebe et al., 1995; Richter et al., 1995; Romero et al., 1985).

<b>Very high affinity</b> $10^{-12}$ - $10^{-11}$ M	<b>High affinity</b> $10^{-9}$ - $10^{-7}$ M	<b>Low affinity</b> $> 10^{-6}$ M
Ras, Ran	EF-Tu $G\alpha$	hGBP1, MxA, Dynamins, <b>IIGP1</b>

<b>Similar GTP/GDP affinity</b>	<b>Higher GTP affinity</b>	<b>Higher GDP affinity</b>
Ras, Ran, hGBP1, Mx,	Dynamins	EF-Tu, <b>IIGP1</b>

Table 5.2. Features of nucleotide binding and hydrolysis in GTPases.

GTPase	$K_d$ ( $M^{-1}$ )	$k_{off}$ ( $s^{-1}$ )	$k_{cat}$ ( $min^{-1}$ )	GAP $k_{cat}$ ( $s^{-1}$ )	References
<b>IIIGPI</b> mGDP mGTP	<b><math>0.98 \times 10^6</math></b> <b><math>15 \times 10^6</math></b>	<b>3.6</b> <b>21</b>	<b>2</b>		
<b>Mx</b> mGDP mGppNHp	<b><math>20 \times 10^6</math></b> <b><math>0.75 \times 10^6</math></b>	<b>8.5</b> <b>0.012</b>	<b>27</b>		Melen et al., 1994 Richter et al., 1995
<b>Dynamin</b> mGDP mGTP	<b>~ 40-fold weaker</b> <b><math>2.5 \times 10^6</math></b>	<b>93</b> <b>2.1</b>	<b>100</b>		Binns et al., 1999, Binns et al., 2000 Marks et al., 2001 Sever et al., 1999
<b>hGBP1</b> mGDP mGppNHp	<b><math>2.4 \times 10^6</math></b> <b><math>1.1 \times 10^6</math></b>	<b>8.2</b> <b>0.66</b>	<b>80</b>		Praefcke et al., 1999 Schwemmle et al., 1995
<b>Ras</b> mGDP mGTP	<b><math>7.9 \times 10^{11}</math></b> <b><math>1.8 \times 10^{11}</math></b>	<b><math>1.8 \times 10^{-5}</math></b> <b><math>1.7 \times 10^{-5}</math></b>	<b>0.028</b>	<b>19.1</b>	Schweins et al., 1997 (Moser et al., 1997)
<b>Ran</b> mGDP mGTP	<b><math>4.9 \times 10^{11}</math></b> <b><math>8 \times 10^{10}</math></b>	<b>5</b> <b>(RCC1)</b>	<b>0.0032</b>	<b>5 – 15</b> <b>(RanGAP)</b>	Klebe et al., 1995, Haberland and Gerke, 1999
<b>EF-Tu</b> GDP GTP	<b><math>2 \times 10^8</math></b> <b><math>9 \times 10^6</math></b>	<b>1270</b> <b>(EF-Ts)</b> <b><math>13 s^{-1}</math></b>	<b>0.008</b>	<b>500</b>	Romero et al., 1985, Chau et al., 1981, Rodnina and Wintermeyer, 2001
<b>EF-G (T.therm)</b> GDP GTP	<b><math>1.5 \times 10^6</math></b> <b><math>94 \times 10^6</math></b>		<b>0.04</b>	<b>0.63</b>	Martemyanov and Gudkov, 2000

## V.2. Significance of GTP Hydrolysis

The GTPase activity has been shown to be crucial for the regulation of almost all GTPases. The GTPase superfamily can be described as switch GTPases, the GTP bound form interacting with downstream effectors, which dissociate upon GTP hydrolysis. The time from the binding of GTP to the hydrolysis is critical for downstream cellular functions and is therefore targeted for precise modulation. For example, Ras has a low hydrolytic rate ( $0.02 \text{ min}^{-1}$ ). Here, functional efficiency is achieved by accelerating the turnover rate by a factor of  $10^5$  by an activating protein RasGAP (Scheffzek et al., 1997; Ahmadian et al., 1997). The GAPs negatively regulate cell signalling by increasing the slow intrinsic GTP to GDP hydrolytic rate. The lowest hydrolytic activity of IIGP1 was documented as  $\sim 0.1 \text{ min}^{-1}$ , the highest documented is  $2 \text{ min}^{-1}$  under saturating conditions. In comparison with the GTPase activity of several GTPases from the table, IIGP1 can be placed somewhere between the small and the large family of GTPases. The activity looks more similar to  $G\alpha$  (Tesmer et al., 1997) than other GTPases. Therefore the query is, if IIGP1 needs a GAP, and whether a internal or an external GAP.

The GAP stimulated GTPase mechanism is conserved among the Ras family of GTPases; Rho/ Ras/ Rabs/ Ypts/ Ran/ Arfs (Vetter and Wittinghofer, 2001; Takai et al., 2001). GTP is hydrolysed by an attack on the  $\gamma$  phosphate by a nucleophilic water molecule. GAP interacts with the GTPase and reduces the flexibility of the switch regions. For e.g GAP-334 of Ras has an arginine residue pointing into the nucleotide binding site and neutralising the negative charges of the  $\beta$  and  $\gamma$  phosphates. Over and above, it anchors Gln 61 of the switch II region which stabilises the water molecule. This is called the arginine finger and a secondary positively charged residue stabilises this finger loop. Therefore, Gln61 at the amino-terminus of switch II is the residue that abstracts the proton from the attacking water molecule (Scheffzek et al., 1997; Scheffzek et al., 1998; Mittal et al., 1996; Ahmadian et al., 1997). Besides, the regulators of G protein signalling, the RGS proteins accelerate  $G\alpha$  catalysed GTP hydrolysis to nearly a 100-fold with a similar principle, with the exception of the intrinsic catalytic arginine residue (De Vries and Gist, 1999). This residue is provided by the helical insertion of the G protein itself as shown in figure 5.1, and the RGS proteins are apparently needed only to stabilise the switch regions in conformations that are complementary to the transition state (Coleman et al., 1994; Sondek et al., 1994). In short, Ras has an external GAP and  $G\alpha$  has an internal GAP.

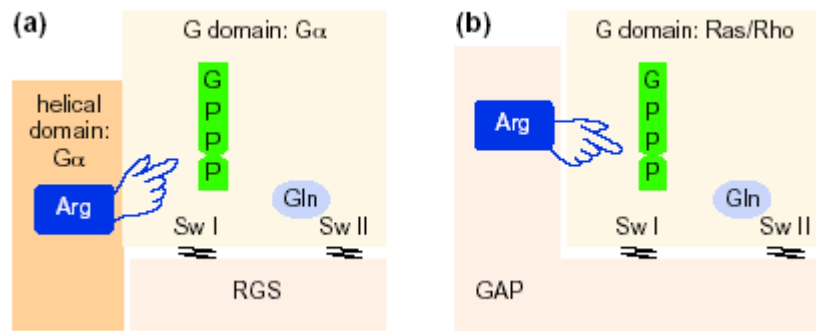


Figure 5.1. The stabilising arginine finger is supplied in -trans in the case of Ras/Rho superfamily, and -cis in the case of G  $\alpha$  proteins (Scheffzek et al., 1998).

Sequence analysis shows that IIGP1 has a Ile in the place of Gln61, suggesting some variation in the catalytic mechanism in comparison to the Ras family of GTPases. All the members of the large family of GTPases, the dynamins, Mx and hGBP1 also have a hydrophobic residue as in IIGP1 (Prakash et al., 2000), implicating a different catalytic mechanism from the small GTPases. Interestingly, we could not detect any AIF<sub>x</sub> binding to IIGP1-GDP like Ras (Mittal et al., 1996), again suggesting the need for an activating protein, since binding of AIF<sub>x</sub> to the small GTPases in the GDP-bound state has been shown only in the presence of a GAP. AIF<sub>x</sub> essentially plays the role of the leaving  $\gamma$  phosphate and mimics the transition state of GTP hydrolysis. The lack of binding of AIF<sub>x</sub> to IIGP1-GDP may be due to the relatively strong binding of GDP itself, in comparison to the GTP bound state or the transition state, thereby not needing AIF<sub>x</sub> to stabilise the interaction. Yet, another explanation may be the unavailability of a GAP crucial for stabilizing the transition state analogous complex IIGP1-GDP-AIF<sub>x</sub>. Recently, AIF<sub>x</sub> binding to hGBP1-GDP (hGBP1 is a 67kDa interferon induced GTPase) in the absence of an external GAP has been documented (Praefcke et al., 1999). In the interests of consistency, this result can be explained by the proposition that hGBP1 might have an internal GAP domain like the G $\alpha$ . This suggests that IIGP1 would need a GAP to accelerate the GTP hydrolysis, and unlike hGBP1 might be an external GAP, and probably a different mechanism than the small GTPases. In contrast, the argument towards an internal GAP is also plausible as IIGP1 shows increase in activity with increase in the concentration of the protein, conforming to the family of large GTPases.

However, an exception among the small GTPases is the Rho family. Certain members of the Rho family GTPases e.g Rho A, Rac2 and Cdc 42Hs form reversible homodimers under physiological buffer conditions *in vivo* and *in vitro*. Intriguingly the presence of a C-terminal polybasic motif located N-terminal to the isoprenylation CAAX isoprenylation sequence correlates with the homotypic interaction of Rho family members. Besides a built-in arginine finger has been shown to

confer a self-stimulatory GAP activity through homotypic interactions (Zhang et al., 2001; Zhang and Zheng, 1998; Zhang et al., 1999). There are polybasic residues in the c-terminal end of hGBP1, but is not apparent in Mx, Dynamin and IIGP1.

### V.3. Relationship of IIGP1 to the Family of Dynamin like large GTPases

To note the similarities and differences in the properties of IIGP1 to the members of the dynamin family, the characteristic features of three representative GTPases are compared. Dynamins are large GTPases (~100kDa), essential for vesicle formation in receptor mediated endocytosis, synaptic vesicle recycling, caveolae internalisation and vesicle trafficking (Danino and Hinshaw, 2001). Mx (~ 80kDa) and hGBP1 (67kDa) are dynamin family members, and are most abundantly expressed in response to interferons (Haller and Kochs, 2002; Praefcke et al., 1999; Schwemmler and Staeheli, 1994). hGBP1 is shown to block the replication of several viruses (Anderson et al., 1999), and the Mx proteins exhibit strong antiviral activity.

IIGP1 differs from this family of GTPases (Dynamin/Mx/hGBP1) having high GDP affinity (15-fold) and low GTPase activity ( $2 \text{ min}^{-1}$  under saturating protein conditions, see table 5.2). There is no sequence homology between IIGP1 and Dynamin /Mx/ hGBP1 proteins outside the G domain. (Mx and dynamins share a low sequence homology). Although there are many variations in the structural features, Mx and dynamins possess a N-terminal GTPase domain of ~ 300 residues, a middle or assembly domain (150-200 residues) and a GED domain (100 residues) (Urrutia et al., 1997). These domains correspond to the LG domain, helical bundle, and  $\alpha$ 12/13 domains of hGBP1 respectively (Prakash et al., 2000). IIGP1 also has a N-terminal G domain, as well as the C-terminal helical regions (figure 5.2).

There exist many analogous features in the dynamin family like the low nucleotide binding affinities and higher nucleotide dissociation rates (table 5.2). The distinctive feature of this family is that none of the four members has a glutamine residue in the switch II region. IIGP1 shares the property of cooperative GTPase activity (figure 3.7) with the members of this family. This indicates a different functioning from the small GTPases, but a common mechanism for this family of GTPases. An internal GAP for all the three GTPases has been suggested, since self assembly leads to increased GTPase activity. It was concluded that the GED domain in dynamin supplies a catalytic arginine residue acting as an assembly dependent internal GAP when the isolated GED domains were added in *trans* to the G domain of dynamin (Sever et al., 1999), as the C-terminal 60 residues are required for the GTPase reaction of Mx (Schwemmler et al., 1995). In hGBP1, an arginine from the p-loop suggested to have a catalytic role (Prof. Christian Herrmann, personal



communication). This suggests that the self assembly is an important feature in this family of GTPases. In addition, another layer of regulation is mediated by the nucleotide dependence of the self assembly process which is observed in all the members of this family.

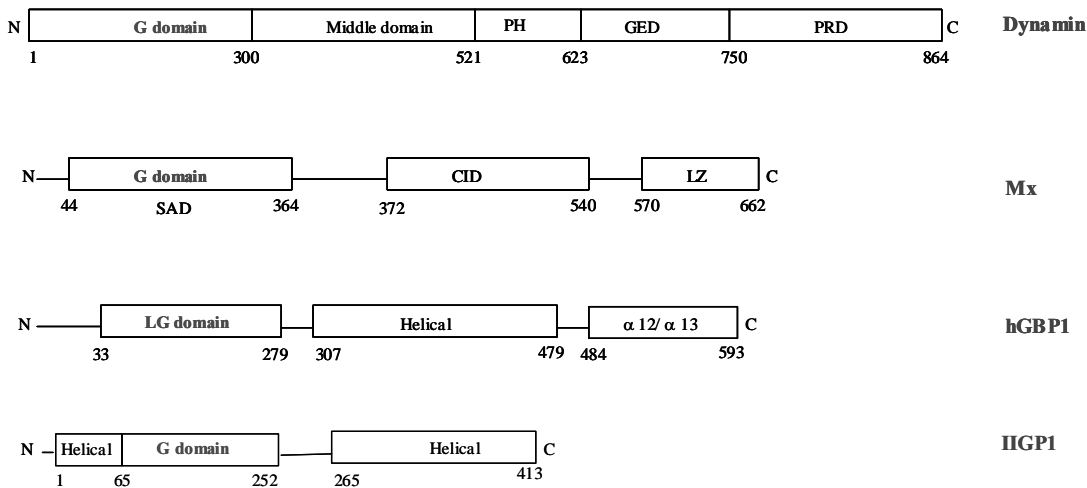


Figure 5.2. Secondary structure analysis of the large family of GTPases

The dynamin family possess specific domains that perform distinct functions. A highly conserved tripartite GTP binding domain at the N-terminus followed by a membrane binding pleckstrin homology domain (PH), the GTPase effector domain (GED) to activate dynamin GTPase activity and the proline rich domain demonstrated to interact with numerous other proteins. Mx proteins have the N-terminal globular G domain containing the tripartite GTP-binding motifs and the self assembly domain (SAD). The C-terminal effector region comprises the central interactive region (CID) and the leucine zipper region (LZ). hGBP1 has the N-terminal globular domain followed by the helical bundle, and the two c-terminal helices make a coiled-coil structure ( $\alpha 12$ - $\alpha 13$ ). IIGP1 also contains an N-terminal G domain followed by a helical domain though there is neither sequence nor structural similarity to any of the other GTPase families

#### V.4. Nucleotide Dependent Self Assembly

The characteristic feature of the family of large GTPases is their ability to self-assemble into defined structures. This has been well documented in dynamin and Mx. For example, dynamins *in vitro* form rings or stacks (Carr and Hinshaw, 1997; Hinshaw and Schmid, 1995), and into helices and spirals around the necks of clathrin coated pits *in vivo* (Takei et al., 1998). These rings and helices have the same dimensions as the electron dense collars formed by the temperature sensitive

dynamamin mutant *shibirein Drosophila melanogaster*. Assembly of dynamamin is favoured by low ionic strength, GTP analogues, GDP in combination with  $\gamma$  phosphate analogues and acidic lipid membranes (Carr and Hinshaw, 1997; Hinshaw and Schmid, 1995; Stowell et al., 1999; Klockow et al., 2002). Assembled dynamamin on a lipid tube underwent fission upon GTP hydrolysis, thus behaving like a molecular motor (Sweitzer and Hinshaw, 1998). Additionally, dynamamin mediates tubular-vesicular complexes in cells or in cell-free assays (Hinshaw, 1999; Hinshaw, 2000; Thompson and McNiven, 2001). The membranes from hypotonically lysed rat brain synaptosomes incubated with rat brain cytosol and GTP $\gamma$ S could support the formation of tubular invaginations decorated with dense staining rings of dynamamin (Takei et al., 1998; Takei et al., 1999). Therefore mechanochemical models for the action of dynamamins are based either on constriction as discussed above or stretching of the helix (Kozlov,1999). This function of dynamamin has been challenged by the suggestion that GTP-bound dynamamin activated downstream effectors (Sever et al., 1999, 2000). However recent studies show that GTP hydrolysis and an associated conformational change is required for endocytosis, supporting a mechanochemical function for dynamamin (Marks et al., 2001). A critical and unresolved issue is whether the interferon inducible GTPases behave as conventional GTPases or as mechanochemical enzymes.

Mx proteins like the dynamamins interact with lipid membranes which become deformed by the formation of structured oligomers. They assemble into regular rod and ring like structures, and can bind and tubulate lipids *in vitro* (Accola et al., 2002; Melen et al., 1992; Di Paolo et al., 1999), and the structures are also nucleotide dependent (Accola et al., 2002; Nakayama et al., 1993; Kochs et al., 2002). Mx associates with smooth ER and is shown to alter the organelle morphology (Accola et al., 2002). Only in the GTP bound form, MxA associates with the nucleocapsids of thogotovirus by binding to the nucleoprotein component. This suggests that unlike dynamamin Mx does not need GTP hydrolysis for its function (Haller and Kochs, 1999). An oligomerisation deficient mutant in Mx, did not show detectable GTPase activity but provided antiviral resistance against thogotovirus. It is therefore suggested that an intracellular pool of MxA is maintained in the oligomeric form. Upon GTP hydrolysis, monomers are released from such oligomeric structures from which antivirally active monomers could be recruited over prolonged periods of time (Janzen et al., 2000). But there is no direct evidence for the dispersal of the monomers upon GTP hydrolysis. In contrast Warnock., et al show the destabilisation of assembled dynamamin 1 structures with the addition of GTP $\gamma$ S, GTP and GDP in the decreasing degrees of potency respectively. Only *in vitro* studies have been done for the p67 GTPase hGBP1. The special feature of hGBP1 is that it binds GTP, GDP and GMP with similar affinity. hGBP1 is a monomer in the nucleotide free form and in the presence of

GDP. It forms dimer with GppNHp, and a still bigger size molecular form with GDP.AIFx (Prakash et al., 2000). On the other hand, the *in vivo* significance of self assembly in hGBP1 has not been investigated.

Dynamic light scattering studies show that IIGP1 oligomerises only in the presence of GTP, and a time dependent increase in the size of particles is observed (Figure 3.8). Increased assembly is also seen in the case of Mx in the GTP bound form, but the significance of this property is unknown (Accola, 2002). Since oligomerisation in IIGP1 was possible only in the presence of GTP or GppNHp, and not in the presence of GDP, the reversibility of these oligomers was tested with respect to GTP hydrolysis. The self assembly process of IIGP1 was found to be a reversible process, upon GTP hydrolysis (figure 3.9). This suggests that GDP formation inhibits oligomerisation. The GDP is bound more tightly than GTP, and therefore a shift in the GDP-bound to the GTP-bound population mostly occurs, the former inhibiting and the latter favoring self assembly. IIGP1 is present as a monomer in solution, like hGBP1, whereas dynamin and Mx are always present as monomers, and could oligomerise without nucleotides. However, IIGP1 crystallised as a dimer, without nucleotides or with GDP, although a monomer in solution. Therefore it may not be a very stable dimer (figure 4.1). Nonetheless, the two dimer interfaces are obvious from the structure. Interface I is formed between the N-terminal helices and interface II is formed between the G-domains. To check the importance of the dimer, several mutations were designed to investigate the influence of the dimer on the properties of IIGP1 (figure 4.3). Firstly, mutations presumably interfering with dimerisation had no effect on nucleotide binding as shown in table 4.2. Secondly, putative interference with the dimer interface led to abolished cooperativity in L44R, K48A, S172R, M173A, L44R/S172R mutations and reduced cooperative GTPase activity in K48E (figure 4.3). The cooperativity of K48E could be explained by the ability to form alternate interactions gaining stability. The nucleotide dependent oligomerisation has not been investigated for these mutants. The correlation between oligomerisation (if persistent) and abrogated cooperativity would give a better understanding of the different interface mutants.

The cooperative activity and GTP dependent oligomerisation of IIGP1 are likely to be essential for regulating its function *in vivo*. There is some evidence that IIGP1 can form stable oligomers under *in vivo* conditions. Size exclusion chromatographic analysis of induced IIGP1 cell lysates show that the soluble IIGP1 always fractionates as a monomer with a size of 47 kDa, and the membrane bound IIGP1 elutes as a 150 kDa complex (probably a detergent artefact). The components of this membrane bound complex could be either homomeric or heteromeric (figure 3.12). Since *in vitro* nucleotide dependent oligomerisation is evident, it is tempting to say that this complex is probably homomeric. Additionally myristoylation has been shown to push the protein towards aggregation.

The only clue for this speculation comes from the dissociation of the complex upon pre-treating it with 1% SDS solution. In these experiments, the interaction of the protein with detergents cannot be ruled out, as the Tx-100 series detergent, thesitol, used for the size exclusion column runs has been documented to have a molecular weight of ~90 kDa at the critical micelle concentration. The molecular mass of the complex observed, fits to the size of the predicted components (micelle and IIGP1). On the other hand, if the ~150 kDa IIGP1 complex is heteromeric, then it would be interesting to identify the molecular partners of IIGP1. In this regard, co-precipitation studies for IIGP1 by metabolic labelling of IFN- $\gamma$  induced L929 fibroblasts with  $\alpha$  165 showed three potential interacting molecules (~ 100 kDa, ~ 25 kDa and a ~ 40 kDa). The added size of these molecules fits to the size of the complex (figure 3.14A). On the other hand, the three co-precipitating molecules were not observed in the Tx-114 detergent phase, although they were coprecipitated in the aqueous phase. This could be explained by the temperature shift in this experiment which could possibly destroy the complex. The short cut way to understanding the IIGP1 complex would be to identify the coprecipitated molecules. Furthermore, the monoclonal antibodies can also immunoprecipitate IIGP1, and the specific co-precipitation of IIGP1 partners is to be investigated.

However IIGP1 is massively induced by IFN- $\gamma$  to at least  $2 \times 10^6$  molecules per cell (Jia Zeng, unpublished results). Such an abundant protein (and IIGP-1 is only one of many p47 GTPases for which this argument will have to be made) may be retained in an inactive state with slow GTP hydrolysis, preventing its futile hydrolysis of GTP. On this argument IIGP1 may needs a regulatory signal, which could either be derived from pathogens upon infection, or from the host immune system itself for activation. IIGP1 has very high dissociation rate for GTP, and slow GTPase activity. Therefore it is likely to be present in the GDP form *in vivo*. Thus activation of IIGP1 probably means holding the IIGP1 in the GTP bound form, to be able to bind to pathogen components thereby arresting their propagation prior to their hide out in the intracellular membranes. The significance of the *in vivo* GTP dependent homooligomerisation of IIGP1 in context to a pathogen has to be understood. It is clear from dynamins that self assembly is essential for their biological function, where the dynamin assembled around clathrin coated pits, clip off the vesicles, and dissociate the oligomers upon GTP hydrolysis. The significance of the self assembly of Mx on the antiviral activity is not understood. There is only one report showing the formation of protein complexes upon binding of MxA to the viral nucleocapsid protein of La Crosse virus (LACV) suggesting that the oligomerisation of MxA is due to viral target recognition (Kochs et al., 2002). On the other hand, no quantitative nucleotide binding parameters or cellular characterisation with respect to their nucleotide states is available for the p47 GTPases to make comparisons with

IIGP1. *ex vivo* purified IGTP was detectable only in the GTP bound form (Taylor et al., 1996), suggesting very low GTPase activity. With these studies, we cannot conclude whether IIGP1 would behave as a conventional GTPase or a mechanochemical enzyme like the dynamins. This is not clear for Mx or GBPs.

#### V.5. Association of IIGP1 with Membranes

The cellular IIGP1 is predominantly membrane-bound and partly cytosolic. The free cytosolic pool may be in equilibrium with the membrane bound material, although other scenarios are also possible. If the two pools are in equilibrium with each other, the equilibrium could be maintained by nucleotide binding and hydrolysis however the experiments reported here (figure 4.5, table 4.1) argue against this idea. Thus, the nucleotide binding/hydrolysis deficient mutants (G2V, K82A) do not influence the equilibrium between the membrane and the soluble fractions of IIGP1. This also seems to be evident with the dimer interface mutants (L44R / K48A / K48E / S172R / M173A / L44R/S172R), which equally do not show any distinctive change in the distribution relative to IIGP1.

When the glycine residue in the putative N-terminal myristoylation motif (MGQLFSS) was mutated to Ala (the mutant designated as IIGP1-Nm), a considerable shift of the membrane bound IIGP1 to the soluble form occurs (figure 4.5). Analysis of the IIGP1-Nm mutant by immunofluorescence showed cytosolic staining unlike wild type IIGP1 (figure 3.16). Similar results were obtained when the same experiments was done with the myristoylation mutants of IIGP1-m and IIGP1-his (table 3.1) as shown in figure 3.17 and 3.18). This strongly supports a role of myristoylation in the membrane attachment of IIGP1, although perhaps not alone. The shift from the membrane to the soluble form is not complete, suggesting that demyristoylated IIGP1 can still interact with membranes. This would bring IIGP1 in line with IGTP or LRG47 which also interact with membranes even though they do not have a myristoylation signal. A small fraction of membrane-bound demyristoylated IIGP1 could be washed off with a high salt and a high pH wash, suggesting the need of ionic interactions in the membrane binding of IIGP1. Besides, a small portion of the protein is still bound to the membrane irrespective of the above proposed interactions. This could be explained (see comment above) by the possibility of another additional lipid modification at the C-terminal. This has not been checked, although the extreme C terminal sequence IIGP1 has a CaaX like sequence (CLRN) Therefore we conclude that myristoylation and other ionic interactions are important for the attachment of IIGP1 on membranes.

## V.6. Cellular Localisation

Endogenous, interferon-induced IIGP1 shows a reticular ER distribution. However, transfected IIGP1 shows a somewhat variable appearance, often including apparent accumulations of IIGP1, in addition to a more or less normal looking reticular stain (figure 3.10) and the typical reticular peri-nuclear ER stain. The identity of these accumulations is not known. The different features of the induced and transfected IIGP1 could mean that there is an influence of the IFN- $\alpha$  response on the localisation of IIGP1. IIGP1-his, however, (table 1, results part I) shows a different phenotype in comparison to the wild type. *In vitro* studies of this C-terminal mutant show that it lacks cooperativity as a GTPase as well as nucleotide dependent oligomerisation, as shown in figure 3.7 and figure 3.8 respectively. Nonetheless, comparison of the nucleotide binding parameters of IIGP1-wt and IIGP1-his show no difference (Table 2b). This indicates that IIGP1-his has a role in interfering with oligomerisation rather than shielding or delaying the GTP binding/hydrolysis, and also suggests the importance of the C-terminal. In contrast the properties of IIGP1-m with a different C-terminal modification (table 3.1) conforms to the wild type.

The localisation data for the interface mutants (figure 4.4) showed phenotypes like the typical peri-nuclear staining of the induced IIGP1 (L44R, S172R), a pattern of dots in addition to the reticular ER stain of the transfected IIGP1-wt (K48E, K48A) or the re-organisation of the ER as in transfected IIGP1-his (L44R, S172R, M173A). Recently a similar observation was seen for a mutant of MxA (K83A, the P-loop lysine) which showed only slightly different distribution from the wild type by immunofluorescence, but a dramatic expansion of a membranous compartment apparently corresponding to the smooth ER was seen by electron microscopy (Accola et al., 2002). The phenotypes observed for IIGP1 and its mutants could give more insights into the function, and more information could be extracted by electron microscopy.

Conclusively, studies on the membrane attachment of IIGP1 and the identification of the interaction molecules seem to be crucial to understand the function of IIGP1. Similar to the ER membrane distortions in IIGP1-his, re-organisation of the respective membranes has been shown for Mx and dynamins, as described above. Since these GTPases are associated with different intracellular membranes, and they are known to modulate membrane compartments, and share a strong relationship with respect to their biochemical features, it is possible that they all have a common mode of regulation.

## V.7. Functional Cues for IIGP1

The primary sequence of IIGP1 shows several clues for the derivation of the function. IIGP1 has a F/YxxxxF/Y sequence (residue numbers) which is considered a strong endocytosis and putative AP2 binding motif. In addition to this sequence, a second motif which is a double phenylalanine motif (FF) residue when present together has been shown to bind sec 23 which is a part of the COP II coat (Dominguez et al., 1998). In addition, IIGP1 also has the di-acidic motif (DXE) which has been shown to bind to the sec23p-sec24p COPII sub complex, facilitating ER export (Votsmeier and Gallwitz, 2001). COP II is involved in ER to golgi transport by forming transport vesicles and segregating biosynthetic cargo from ER-resident proteins (Barlowe, 2002). Interestingly, only ER staining of IIGP1 was observed by immunofluorescence (Sascha Martens unpublished results) as opposed to both golgi and ER staining (Zerrahn et al., 2002) under the same conditions, and cell lines used. Further analysis is necessary to count for this discrepancy.

## V.8. IIGP1 in the p47 Family

IIGP1 is not constitutively expressed but is stimulated by IFN- $\gamma$  which is an immune or inflammatory stimulus, therefore may probably prove to be a resistance factor against intracellular pathogens by analogy with its p47 relatives IGTP, TGTP, LRG-47 and IRG-47. A significant observation in three members of this family (LRG47, IGTP and GTPI), in addition to other shared sequence features, is a radical substitution in the P-loop from lysine (GKS) to methionine (GMS) which is unique only to this subfamily of GTPases (Sorace et al., 1995; Taylor et al., 1997b; Boehm et al., 1998). The lysine to methionine substitution is compatible with GTPase activity at least in the context of the p47 structure since the GMS p47 GTPases, IGTP and LRG-47 bind GTP and IGTP has been shown to hydrolyse GTP to GDP. Interestingly, *ex vivo* purified IGTP was detectable only in the GTP bound form (Taylor et al., 1996), suggesting slow GTPase activity. Unfortunately, no quantitative nucleotide binding parameters are available to make comparisons with IIGP1.

The crystal structure of IIGP1 is a representative structure for the p47 family of GTPases. This conclusion arises firstly, from secondary structure analysis of other members of the family which are very similar to IIGP-1 and conform to the expectation derived from the crystal structure, and secondly from the conservation of several pairs of distant residues in other p47 family members which interact to stabilise the IIGP-1 structure. This conservation could not be explained unless the structures of the other p47 GTPases are very similar to IIGP-1. Structural analysis of IIGP1 with respect to the sequence comparison with the members show several conserved regions, forming the core regions. However large deviations in the primary structure between the members, especially at

the N and C termini suggests their non-redundancy as indicated by their distinct subcellular locations, and resistance to specific pathogens (Collazo et al., 2001; Halonen et al., 2001; Taylor et al., 1997; Taylor et al., 2000).

#### V.9. Proposed Function

Pathogens have developed several mechanisms to block and subvert normal cellular processes, thereby contributing to pathogenesis. They use and alter several cellular targets like the cytoskeletal network, signal transduction pathways and vesicle transport machinery for their propagation (Knodler et al., 2001). Many pathogens use the cellular membrane systems for creating a protected intracellular niche, securing themselves from the host immune system (Ploegh, 1998; Meresse et al., 1999). Since the p47 GTPases, including IIGP1 are associated with several intracellular membranes in the cell, it is a hypothesis that IIGP1 might be protecting the cell by interfering with the life cycle of specific pathogens. By doing so, it probably prevents the exploitation of the ER/Golgi membrane by the pathogens. Nothing is yet known about how the p47 GTPases exercise their adaptive function.

The studies presented here have given an insight into understanding IIGP1 as a GTPase, and show analogous properties to the dynamin family of GTPases. However, the structural features do not show any homology. It seems crucial to get a detailed view of the oligomerisation property of IIGP1 *in vitro* and *in vivo* in order to understand its regulatory mechanism. Still, the nucleotide bound structures of IIGP1 (GDP and the GppNHp) do not give clues to the GTPase mechanism of IIGP1. A key task is now to identify the protein neighbours or regulators of IIGP1 in its native environment in the IFN- $\gamma$  induced cell, in the present context especially to identify possible GAPs or other regulatory proteins. This could help us to couple the oligomeric behaviour of IIGP1 to its biological function. With respect to the biological significance of IIGP1, it is worthwhile to examine whether these regulatory molecules could be derived from the pathogens themselves or might be stimulated by the entry of the pathogen into the cell, mainly due to their expression only upon IFN- $\gamma$  induction.

The data described here formulates a platform for further analysis on IIGP1 function and provides essential parameters to understand the molecular mechanism by which IIGP1 participates in this complex resistance programme. The characterisation of IIGP1 has given an understanding to the behaviour and properties of the protein *in vitro* and *in vivo*.



## VI. REFERENCES

- Aaronson,D.S. and Horvath,C.M. (2002). A road map for those who know JAK-STAT. *Science* 296, 1653-1655.
- Abbas,A.K. and Janeway,C.A., Jr. (2000). Immunology: improving on nature in the twenty-first century. *Cell* 100, 129-138.
- Accola,M.A., Huang,B., Al Masri,A., and McNiven,M.A. (2002). The antiviral dynamin family member, MxA, tubulates lipids and localizes to the smooth endoplasmic reticulum. *J. Biol. Chem.* 277, 21829-21835.
- Ahmadian,M.R., Stege,P., Scheffzek,K., and Wittinghofer,A. (1997). Confirmation of the arginine-finger hypothesis for the GAP-stimulated GTP-hydrolysis reaction of Ras. *Nat. Struct. Biol.* 4, 686-689.
- Anderson,S.L., Carton,J.M., Lou,J., Xing,L., and Rubin,B.Y. (1999). Interferon-induced guanylate binding protein-1 (GBP-1) mediates an antiviral effect against vesicular stomatitis virus and encephalomyocarditis virus. *Virology* 256, 8-14.
- Asundi,V.K., Stahl,R.C., Showalter,L., Conner,K.J., and Carey,D.J. (1994). Molecular cloning and characterization of an isoprenylated 67 kDa protein. *Biochim. Biophys. Acta* 1217, 257-265.
- Barlowe,C. (2002). COPII-dependent transport from the endoplasmic reticulum. *Curr. Opin. Cell Biol.* 14, 417-422.
- Bercovich,J.A., Grinstein,S., and Zorzopulos,J. (1992). Effect of DNA concentration on recombinant plasmid recovery after blunt-end ligation. *Biotechniques* 12, 190, 192-190, 193.
- Binns,D.D., Barylko,B., Grichine,N., Atkinson,M.A., Helms,M.K., Jameson,D.M., Eccleston,J.F., and Albanesi,J.P. (1999). Correlation between self-association modes and GTPase activation of dynamin. *J. Protein Chem.* 18, 277-290.
- Binns,D.D., Helms,M.K., Barylko,B., Davis,C.T., Jameson,D.M., Albanesi,J.P., and Eccleston,J.F. (2000). The mechanism of GTP hydrolysis by dynamin II: a transient kinetic study. *Biochemistry* 39, 7188-7196.
- Birnboim,H.C. and Doly,J. (1979). A rapid alkaline extraction procedure for screening recombinant plasmid DNA. *Nucleic Acids Res.* 7, 1513-1523.
- Boehm,U., Guethlein,L., Klamp,T., Ozbek,K., Schaub,A., Futterer,A., Pfeffer,K., and Howard,J.C. (1998). Two families of GTPases dominate the complex cellular response to IFN-gamma. *J. Immunol.* 161, 6715-6723.
- Boehm,U., Klamp,T., Groot,M., and Howard,J.C. (1997). Cellular responses to interferon-gamma. *Annu. Rev. Immunol.* 15, 749-795.

- Bogdan,C. (2001). Nitric oxide and the immune response. *Nat. Immunol.* 2, 907-916.
- Bollag,D.M. (1994). Gel-filtration chromatography. *Methods Mol. Biol.* 36, 1-9.
- Boriack-Sjodin,P.A., Margarit,S.M., Bar-Sagi,D., and Kuriyan,J. (1998). The structural basis of the activation of Ras by Sos. *Nature* 394, 337-343.
- Bourne,H.R., Sanders,D.A., and McCormick,F. (1990). The GTPase superfamily: a conserved switch for diverse cell functions. *Nature* 348, 125-132.
- Bourne,H.R., Sanders,D.A., and McCormick,F. (1991). The GTPase superfamily: conserved structure and molecular mechanism. *Nature* 349, 117-127.
- Boutin,J.A. (1997). Myristoylation. *Cell Signal.* 9, 15-35.
- Braciale TJ, Morrison LA, Sweetser MT, Sambrook J, Gething MJ, Braciale VL. (1987)Aug;Antigen presentation pathways to class I and class II MHC-restricted T lymphocytes.*Immunol Rev.* 98:95-114. Review.
- Briken,V., Ruffner,H., Schultz,U., Schwarz,A., Reis,L.F., Strehlow,I., Decker,T., and Staeheli,P. (1995). Interferon regulatory factor 1 is required for mouse Gbp gene activation by gamma interferon. *Mol. Cell Biol.* 15, 975-982.
- Brinkmann,T., Daumke,O., Herbrand,U., Kuhlmann,D., Stege,P., Ahmadian,M.R., and Wittinghofer,A. (2002). Rap-specific GTPase activating protein follows an alternative mechanism. *J. Biol. Chem.* 277, 12525-12531.
- Brino,L., Urzhumtsev,A., Mousli,M., Bronner,C., Mitschler,A., Oudet,P., and Moras,D. (2000). Dimerization of Escherichia coli DNA-gyrase B provides a structural mechanism for activating the ATPase catalytic center. *J. Biol. Chem.* 275, 9468-9475.
- Brownlee,G.G. and Sanger,F. (1969). Chromatography of 32P-labelled oligonucleotides on thin layers of DEAE-cellulose. *Eur. J. Biochem.* 11, 395-399.
- Burnette,W.N. (1981). Western blotting : electrophoretic transfer of proteins from sodium dodecyl sulfate--polyacrylamide gels to unmodified nitrocellulose and radiographic detection with antibody and radioiodinated protein A. *Anal. Biochem.* 112, 195-203.
- Carlow,D.A., Teh,S.J., and Teh,H.S. (1998) . Specific antiviral activity demonstrated by TGTP, a member of a new family of interferon-induced GTPases. *J. Immunol.* 161, 2348-2355.
- Carr,J.F. and Hinshaw,J.E. (1997). Dynamin assembles into spirals under physiological salt conditions upon the addition of GDP and gamma-phosphate analogues. *J. Biol. Chem.* 272, 28030-28035.
- Carter,M.J. and Milton,I.D. (1993). An inexpensive and simple method for DNA purifications on silica particles. *Nucleic Acids Res.* 21, 1044.

- Casadevall,A. and Pirofski,L. (2001). Host-pathogen interactions: the attributes of virulence. *J. Infect. Dis.* 184, 337-344.
- Chardin,P., Camonis,J.H., Gale,N.W., van Aelst,L., Schlessinger,J., Wigler,M.H., and Bar-Sagi,D. (1993). Human Sos1: a guanine nucleotide exchange factor for Ras that binds to GRB2. *Science* 260, 1338-1343.
- Cheng,Y.S., Patterson,C.E., and Staeheli,P. (1991) . Interferon-induced guanylate-binding proteins lack an N(T)KXD consensus motif and bind GMP in addition to GDP and GTP. *Mol. Cell Biol.* 11, 4717-4725.
- Cherfils,J. and Chardin,P. (1999). GEFs: structural basis for their activation of small GTP-binding proteins. *Trends Biochem. Sci.* 24, 306-311.
- Chesler,D.A. and Reiss,C.S. (2002). The role of IFN-gamma in immune responses to viral infections of the central nervous system. *Cytokine Growth Factor Rev.* 13, 441-454.
- Chung,C.T. and Miller,R.H. (1988). A rapid and convenient method for the preparation and storage of competent bacterial cells. *Nucleic Acids Res.* 16, 3580.
- Chung,H.H., Benson,D.R., and Schultz,P.G. (1993). Probing the structure and mechanism of Ras protein with an expanded genetic code. *Science* 259, 806-809.
- Cohen,S.N., Chang,A.C., and Hsu,L. (1972). Nonchromosomal antibiotic resistance in bacteria: genetic transformation of *Escherichia coli* by R-factor DNA. *Proc. Natl. Acad. Sci. U. S. A* 69, 2110-2114.
- Coleman,D.E., Berghuis,A.M., Lee,E., Linder,M.E., Gilman,A.G., and Sprang,S.R. (1994). Structures of active conformations of Gi alpha 1 and the mechanism of GTP hydrolysis. *Science* 265, 1405-1412.
- Collazo,C.M., Yap,G.S., Sempowski,G.D., Lusby,K.C., Tessarollo,L., Woude,G.F., Sher,A., and Taylor,G.A. (2001). Inactivation of LRG-47 and IRG-47 reveals a family of interferon gamma-inducible genes with essential, pathogen-specific roles in resistance to infection. *J. Exp. Med.* 194, 181-188.
- Cutler,P. (1996). Size-exclusion chromatography. *Methods Mol. Biol.* 59, 255-267.
- D'Acquisto,F. and Ghosh,S. (2001). PACT and PKR: turning on NF-kappa B in the absence of virus. *Sci. STKE.* 2001, RE1.
- Danino,D. and Hinshaw,J.E. (2001). Dynamin family of mechanoenzymes. *Curr. Opin. Cell Biol.* 13, 454-460.
- De Vries,L. and Gist,F.M. (1999). RGS proteins: more than just GAPs for heterotrimeric G proteins. *Trends Cell Biol.* 9, 138-144.

- Decker,T., Stockinger,S., Karaghiosoff,M., Muller,M., and Kovarik,P. (2002) . IFNs and
- Dever,T.E., Glynias,M.J., and Merrick,W.C. (1987). GTP-binding domain: three consensus sequence elements with distinct spacing. *Proc. Natl. Acad. Sci. U. S. A* 84, 1814-1818.
- Di Paolo,C., Hefti,H.P., Meli,M., Landis,H., and Pavlovic,J. (1999). Intramolecular backfolding of the carboxyl-terminal end of MxA protein is a prerequisite for its oligomerization. *J. Biol. Chem.* 274, 32071-32078.
- Dominguez,M., Dejgaard,K., Fullekrug,J., Dahan,S., Fazel,A., Paccaud,J.P., Thomas,D.Y., Bergeron,J.J., and Nilsson,T. (1998). gp25L/emp24/p24 protein family members of the cis-Golgi network bind both COP I and II coatomer. *J. Cell Biol.* 140, 751-765.
- Eccleston,J.F. (1984). A kinetic analysis of the interaction of elongation factor Tu with guanosine nucleotides and elongation factor Ts. *J. Biol. Chem.* 259, 12997-13003.
- Eccleston,J.F., Binns,D.D., Davis,C.T., Albanesi,J.P., and Jameson,D.M. (2002). Oligomerization and kinetic mechanism of the dynamin GTPase. *Eur. Biophys. J.* 31, 275-282.
- Enninga J, Levy DE, Blobel G, Fontoura BM.Role of nucleoporin induction in releasing an mRNA nuclear export block. (2002) *Science.* 295(5559):1523-5.
- Ganusov,V.V., Bergstrom,C.T., and Antia,R. (2002). Within-host population dynamics and the evolution of microparasites in a heterogeneous host population. *Evolution Int. J. Org. Evolution* 56, 213-223.
- Ghosh,G., van Duyn,G., Ghosh,S., and Sigler,P.B. (1995). Structure of NF-kappa B p50 homodimer bound to a kappa B site. *Nature* 373, 303-310.
- Gill,S.C. and von Hippel,P.H. (1989). Calculation of protein extinction coefficients from amino acid sequence data. *Anal. Biochem.* 182, 319-326.
- Gilles,R., Bittner,C., Cramer, M., Mierau, R. and Jaenicke, L. Radioimmunoassay for the sex inducer of *Volvox cartieri* F, *Nagariensis*. *FEBS letters* .116 (1), 102-106.
- Gilly,M. and Wall,R. (1992). The IRG-47 gene is IFN-gamma induced in B cells and encodes a protein with GTP-binding motifs. *J. Immunol.* 148, 3275-3281.
- Glasel,J.A. (1995). Validity of nucleic acid purities monitored by 260nm/280nm absorbance ratios. *Biotechniques* 18, 62-63.
- Gorbacheva VY, Lindner D, Sen GC, Vestal DJ.(2002) The interferon (IFN)-induced GTPase, mGBP-2. Role in IFN-gamma-induced murine fibroblast proliferation. *J Biol Chem.* 277(8):6080-7.
- Gromadski,K.B., Wieden,H.J., and Rodnina,M.V. (2002). Kinetic mechanism of elongation factor Ts-catalyzed nucleotide exchange in elongation factor Tu. *Biochemistry* 41, 162-169.

Guan,K.L. and Dixon,J.E. (1991). Eukaryotic proteins expressed in *Escherichia coli*: an improved thrombin cleavage and purification procedure of fusion proteins with glutathione S-transferase. *Anal. Biochem.* 192, 262-267.

Guenzi,E., Topolt,K., Cornali,E., Lubeseder-Martellato,C., Jorg,A., Matzen,K., Zietz,C., Kremmer,E., Nappi,F., Schwemmle,M., Hohenadl,C., Barillari,G., Tschachler,E., Monini,P., Ensoli,B., and Sturzl,M. (2001). The helical domain of GBP-1 mediates the inhibition of endothelial cell proliferation by inflammatory cytokines. *EMBO J.* 20, 5568-5577.

Guidotti LG, Chisari FV Noncytolytic control of viral infections by the innate and adaptive immune response (2001). *Annu Rev Immunol.*19:65-91. Review.

Haller,O. and Kochs,G. (2002). Interferon-induced mx proteins: dynamin-like GTPases with antiviral activity. *Traffic.* 3, 710-717.

Haller,O., Acklin,M., and Staeheli,P. (1986). Genetic resistance to influenza virus in wild mice. *Curr. Top. Microbiol. Immunol.* 127, 331-337.

Halonen,S.K., Taylor,G.A., and Weiss,L.M. (2001). Gamma interferon-induced inhibition of *Toxoplasma gondii* in astrocytes is mediated by IGTP. *Infect. Immun.* 69, 5573-5576.

Han,B.H., Park,D.J., Lim,R.W., Im,J.H., and Kim,H.D. (1998) . Cloning, expression, and characterization of a novel guanylate-binding protein, GBP3 in murine erythroid progenitor cells. *Biochim. Biophys. Acta* 1384, 373-386.

Henson PM, Bratton DL, Fadok VA. (2001) Apoptotic cell removal. *Curr Biol.*;11(19):R795-805. Review.

Herrmann,C. and Nassar,N. (1996). Ras and its effectors. *Prog. Biophys. Mol. Biol.* 66, 1-41.

Hinshaw,J.E. (1999). Dynamin spirals. *Curr. Opin. Struct. Biol.* 9, 260-267.

Hinshaw,J.E. (2000). Dynamin and its role in membrane fission. *Annu. Rev. Cell Dev. Biol.* 16, 483-519.

Hinshaw,J.E. and Schmid,S.L. (1995). Dynamin self-assembles into rings suggesting a mechanism for coated vesicle budding. *Nature* 374, 190-192.

Hirano,T. (2002) . Cytokines in autoimmune disease and chronic inflammatory proliferative disease. *Cytokine Growth Factor Rev.* 13, 297.

Ihle,J.N. (1995). Cytokine receptor signalling. *Nature* 377, 591-594.

Ikeda,H., Old,L.J., and Schreiber,R.D. (2002). The roles of IFN gamma in protection against tumor development and cancer immunoediting. *Cytokine Growth Factor Rev.* 13, 95-109.

- Janeway,C.A., Jr. and Medzhitov,R. (2002). Innate immune recognition. *Annu. Rev. Immunol.* 20, 197-216.
- Janzen,C., Kochs,G., and Haller,O. (2000). A monomeric GTPase-negative MxA mutant with antiviral activity. *J. Virol.* 74, 8202-8206.
- John,J., Sohmen,R., Feuerstein,J., Linke,R., Wittinghofer,A., and Goody,R.S. (1990). Kinetics of interaction of nucleotides with nucleotide-free H-ras p21. *Biochemistry* 29, 6058-6065.
- Kalies,K.U. and Hartmann,E. (1998). Protein translocation into the endoplasmic reticulum (ER)--two similar routes with different modes. *Eur. J. Biochem.* 254, 1-5.
- Kang,C., Sun,N., Honzatko,R.B., and Fromm,H.J. (1994). Replacement of Asp333 with Asn by site-directed mutagenesis changes the substrate specificity of Escherichia coli adenylosuccinate synthetase from guanosine 5'-triphosphate to xanthosine 5'-triphosphate. *J. Biol. Chem.* 269, 24046-24049.
- Klebe,C., Prinz,H., Wittinghofer,A., and Goody,R.S. (1995). The kinetic mechanism of Ran-nucleotide exchange catalyzed by RCC1. *Biochemistry* 34, 12543-12552.
- Klockow,B., Tichelaar,W., Madden,D.R., Niemann,H.H., Akiba,T., Hirose,K., and Manstein,D.J. (2002). The dynamin A ring complex: molecular organization and nucleotide-dependent conformational changes. *EMBO J.* 21, 240-250.
- Knodler,L.A., Celli,J., and Finlay,B.B. (2001). Pathogenic trickery: deception of host cell processes. *Nat. Rev. Mol. Cell Biol.* 2, 578-588.
- Kochs G, Haller O (1999) Interferon-induced human MxA GTPase blocks nuclear import of Thogoto virus nucleocapsids. *Proc Natl Acad Sci U S A.* 96(5):2082-6.
- Kochs,G., Haener,M., Aebi,U., and Haller,O. (2002). Self-assembly of human MxA GTPase into highly ordered dynamin-like oligomers. *J. Biol. Chem.* 277, 14172-14176.
- Kuersten,S., Ohno,M., and Mattaj,I.W. (2001). Nucleocytoplasmic transport: Ran, beta and beyond. *Trends Cell Biol.* 11, 497-503.
- Kumar,S., Tamura,K., Jakobsen,I.B., and Nei,M. (2001). MEGA2: molecular evolutionary genetics analysis software. *Bioinformatics.* 17, 1244-1245.
- Lafuse,W.P., Brown,D., Castle,L., and Zwilling,B.S. (1995) . Cloning and characterization of a novel cDNA that is IFN-gamma-induced in mouse peritoneal macrophages and encodes a putative GTP-binding protein. *J. Leukoc. Biol.* 57, 477-483.
- Lee,L.G., Connell,C.R., Woo,S.L., Cheng,R.D., McArdle,B.F., Fuller,C.W., Halloran,N.D., and Wilson,R.K. (1992). DNA sequencing with dye-labeled terminators and T7 DNA polymerase: effect of dyes and dNTPs on incorporation of dye-terminators and probability analysis of termination fragments. *Nucleic Acids Res.* 20, 2471-2483.

- Levy,D.E. (2002). Whence interferon? Variety in the production of interferon in response to viral infection. *J. Exp. Med.* 195, F15-F18.
- Liew,F.Y. (2002). T(H)1 and T(H)2 cells: a historical perspective. *Nat. Rev. Immunol.* 2, 55-60.
- Luria,S.E. (1970). The recognition of DNA in bacteria. *Sci. Am.* 222, 88-92.
- Melen,K., Ronni,T., Broni,B., Krug,R.M., von Bonsdorff,C.H., and Julkunen,I. (1992). Interferon-induced Mx proteins form oligomers and contain a putative leucine zipper. *J. Biol. Chem.* 267, 25898-25907.
- Meresse,S., Steele-Mortimer,O., Moreno,E., Desjardins,M., Finlay,B., and Gorvel,J.P. (1999). Controlling the maturation of pathogen-containing vacuoles: a matter of life and death. *Nat. Cell Biol.* 1, E183-E188.
- Michelsen,B.K. (1995). Transformation of *Escherichia coli* increases 260-fold upon inactivation of T4 DNA ligase. *Anal. Biochem.* 225, 172-174.
- Mittal,R., Ahmadian,M.R., Goody,R.S., and Wittinghofer,A. (1996). Formation of a transition-state analog of the Ras GTPase reaction by Ras-GDP, tetrafluoroaluminate, and GTPase-activating proteins. *Science* 273, 115-117.
- Moser,C., Mol,O., Goody,R.S., and Sinning,I. (1997). The signal recognition particle receptor of *Escherichia coli* (FtsY) has a nucleotide exchange factor built into the GTPase domain. *Proc. Natl. Acad. Sci. U. S. A* 94, 11339-11344.
- Mullis,K.B. and Faloona,F.A. (1987). Specific synthesis of DNA in vitro via a polymerase-catalyzed chain reaction. *Methods Enzymol.* 155, 335-350.
- Nakamura,K., Tanaka,T., Kuwahara,A., and Takeo,K. (1985). Microassay for proteins on nitrocellulose filter using protein dye-staining procedure. *Anal. Biochem.* 148, 311-319.
- Nakayama,M., Yazaki,K., Kusano,A., Nagata,K., Hanai,N., and Ishihama,A. (1993). Structure of mouse Mx1 protein. Molecular assembly and GTP-dependent conformational change. *J. Biol. Chem.* 268, 15033-15038.
- Nantais,D.E., Schwemmle,M., Stickney,J.T., Vestal,D.J., and Buss,J.E. (1996). Prenylation of an interferon-gamma-induced GTP-binding protein: the human guanylate binding protein, huGBP1. *J. Leukoc. Biol.* 60, 423-431.
- Nassar,N., Horn,G., Herrmann,C., Scherer,A., McCormick,F., and Wittinghofer,A. (1995). The 2.2 Å crystal structure of the Ras-binding domain of the serine/threonine kinase c-Raf1 in complex with Rap1A and a GTP analogue. *Nature* 375, 554-560.
- Neugebauer,J.M. (1990). Detergents: an overview. *Methods Enzymol.* 182, 239-253.

- Neun,R., Richter,M.F., Staeheli,P., and Schwemmler,M. (1996). GTPase properties of the interferon-induced human guanylate-binding protein 2. *FEBS Lett.* 390, 69-72.
- Nguyen,T.T., Hu,Y., Widney,D.P., Mar,R.A., and Smith,J.B. (2002). Murine GBP-5, a New Member of the Murine Guanylate-Binding Protein Family, Is Coordinately Regulated with Other GBPs In Vivo and In Vitro. *J. Interferon Cytokine Res.* 22, 899-909.
- Nilsson,T. and Warren,G. (1994). Retention and retrieval in the endoplasmic reticulum and the Golgi apparatus. *Curr. Opin. Cell Biol.* 6, 517-521.
- O'Shea,J.J., Ma,A., and Lipsky,P. (2002) . Cytokines and autoimmunity. *Nat. Rev. Immunol.* 2, 37-45.
- Pai,E.F., Krengel,U., Petsko,G.A., Goody,R.S., Kabsch,W., and Wittinghofer,A. (1990). Refined crystal structure of the triphosphate conformation of H-ras p21 at 1.35 Å resolution: implications for the mechanism of GTP hydrolysis. *EMBO J.* 9, 2351-2359.
- Pavlovic J, Schroder A, Blank A, Pitossi F, Staeheli P. Mx proteins: GTPases involved in the interferon-induced antiviral state. (1993) *Ciba Found Symp.*176:233-43; Review.
- Ploegh,H.L. (1998). Viral strategies of immune evasion. *Science* 280, 248-253.
- Praefcke,G.J., Geyer,M., Schwemmler,M., Robert,K.H., and Herrmann,C. (1999). Nucleotide-binding characteristics of human guanylate-binding protein 1 (hGBP1) and identification of the third GTP-binding motif. *J. Mol. Biol.* 292, 321-332.
- Prakash,B., Praefcke,G.J., Renault,L., Wittinghofer,A., and Herrmann,C. (2000). Structure of human guanylate-binding protein 1 representing a unique class of GTP-binding proteins. *Nature* 403, 567-571.
- Prakash,B., Renault,L., Praefcke,G.J., Herrmann,C. and Wittinghofer,A., (2000). Triphosphate structure of guanylate-binding protein 1 and implications for nucleotide binding and GTPase mechanism. *The EMBO Journal.* 19(17),4555-4564
- Prochazka,M., Staeheli,P., Holmes,R.S., and Haller,O. (1985). Interferon-induced guanylate-binding proteins: mapping of the murine Gbp-1 locus to chromosome 3. *Virology* 145, 273-279.
- Richter,M.F., Schwemmler,M., Herrmann,C., Wittinghofer,A., and Staeheli,P. (1995). Interferon-induced MxA protein. GTP binding and GTP hydrolysis properties. *J. Biol. Chem.* 270, 13512-13517.
- Riemer,C., Queck,I., Simon,D., Kurth,R., and Baier,M. (2000). Identification of upregulated genes in scrapie-infected brain tissue. *J. Virol.* 74, 10245-10248.



- Rittinger,K., Walker,P.A., Eccleston,J.F., Smerdon,S.J., and Gamblin,S.J. (1997). Structure at 1.65 Å of RhoA and its GTPase-activating protein in complex with a transition-state analogue. *Nature* 389, 758-762.
- Romero,G., Chau,V., and Biltonen,R.L. (1985). Kinetics and thermodynamics of the interaction of elongation factor Tu with elongation factor Ts, guanine nucleotides, and aminoacyl-tRNA. *J. Biol. Chem.* 260, 6167-6174.
- Roy,B.A. and Kirchner,J.W. (2000). Evolutionary dynamics of pathogen resistance and tolerance. *Evolution Int. J. Org. Evolution* 54, 51-63.
- Samuel,C.E. (2001) . Antiviral actions of interferons. *Clin. Microbiol. Rev.* 14, 778-809, table.
- Sato,M., Taniguchi,T., and Tanaka,N. (2001) . The interferon system and interferon regulatory factor transcription factors -- studies from gene knockout mice. *Cytokine Growth Factor Rev.* 12, 133-142.
- Scheffzek,K., Ahmadian,M.R., and Wittinghofer,A. (1998). GTPase-activating proteins: helping hands to complement an active site. *Trends Biochem. Sci.* 23, 257-262.
- Scheffzek,K., Ahmadian,M.R., Kabsch,W., Wiesmuller,L., Lautwein,A., Schmitz,F., and Wittinghofer,A. (1997). The Ras-RasGAP complex: structural basis for GTPase activation and its loss in oncogenic Ras mutants. *Science* 277, 333-338.
- Schwemmle,M. and Staeheli,P. (1994). The interferon-induced 67-kDa guanylate-binding protein (hGBP1) is a GTPase that converts GTP to GMP. *J. Biol. Chem.* 269, 11299-11305.
- Schwemmle,M., Kaspers,B., Irion,A., Staeheli,P., and Schultz,U. (1996) . Chicken guanylate-binding protein. Conservation of GTPase activity and induction by cytokines. *J. Biol. Chem.* 271, 10304-10308.
- Sedmak,J.J. and Grossberg,S.E. (1977). A rapid, sensitive, and versatile assay for protein using Coomassie brilliant blue G250. *Anal. Biochem.* 79, 544-552.
- Seewald,M.J., Korner,C., Wittinghofer,A., and Vetter,I.R. (2002). RanGAP mediates GTP hydrolysis without an arginine finger. *Nature* 415, 662-666.
- Seliger,B., Hammers,S., Hohne,A., Zeidler,R., Knuth,A., Gerharz,C.D., and Huber,C. (1997). IFN-gamma-mediated coordinated transcriptional regulation of the human TAP-1 and LMP-2 genes in human renal cell carcinoma. *Clin. Cancer Res.* 3, 573-578.
- Sever,S., Muhlberg,A.B., and Schmid,S.L. (1999). Impairment of dynamin's GAP domain stimulates receptor-mediated endocytosis. *Nature* 398, 481-486.
- Shapiro,A.L. and Maizel,J.V., Jr. (1969). Molecular weight estimation of polypeptides by SDS-polyacrylamide gel electrophoresis: further data concerning resolving power and general considerations. *Anal. Biochem.* 29, 505-514.

- Sondek,J., Lambright,D.G., Noel,J.P., Hamm,H.E., and Sigler,P.B. (1994). GTPase mechanism of Gproteins from the 1.7-A crystal structure of transducin alpha-GDP-AIF-4. *Nature* 372, 276-279.
- Sorace,J.M., Johnson,R.J., Howard,D.L., and Drysdale,B.E. (1995). Identification of an endotoxin and IFN-inducible cDNA: possible identification of a novel protein family. *J. Leukoc. Biol.* 58, 477-484.
- Spriggs,M.K. (1996). One step ahead of the game: viral immunomodulatory molecules. *Annu. Rev. Immunol.* 14, 101-130.
- Spriggs,M.K. (1999). Virus-encoded modulators of cytokines and growth factors. *Cytokine Growth Factor Rev.* 10, 1-4.
- Staehele,P., Prochazka,M., Steigmeier,P.A., and Haller,O. (1984). Genetic control of interferon action: mouse strain distribution and inheritance of an induced protein with guanylate-binding property. *Virology* 137, 135-142.
- Stowell,M.H., Marks,B., Wigge,P., and McMahon,H.T. (1999). Nucleotide-dependent conformational changes in dynamin: evidence for a mechanochemical molecular spring. *Nat. Cell Biol.* 1, 27-32.
- Strehlow,I., Lohmann-Matthes,M.L., and Decker,T. (1994). The interferon-inducible GBP1 gene: structure and mapping to human chromosome 1. *Gene* 144, 295-299.
- Studier,F.W. (1973). Analysis of bacteriophage T7 early RNAs and proteins on slab gels. *J. Mol. Biol.* 79, 237-248.
- Studier,F.W., Rosenberg,A.H., Dunn,J.J., and Dubendorff,J.W. (1990). Use of T7 RNA polymerase to direct expression of cloned genes. *Methods Enzymol.* 185, 60-89.
- Sun,H., Jackson,M.J., Kundu,N., and Fulton,A.M. (1999). Interleukin-10 gene transfer activates interferon-gamma and the interferon-gamma-inducible genes Gbp-1/Mag-1 and Mig-1 in mammary tumors. *Int. J. Cancer* 80, 624-629.
- Sweitzer,S.M. and Hinshaw,J.E. (1998). Dynamin undergoes a GTP-dependent conformational change causing vesiculation. *Cell* 93, 1021-1029.
- Takai,Y., Sasaki,T., and Matozaki,T. (2001). Small GTP-binding proteins. *Physiol Rev.* 81, 153-208.
- Takei,K., Haucke,V., Slepnev,V., Farsad,K., Salazar,M., Chen,H., and De Camilli,P. (1998). Generation of coated intermediates of clathrin-mediated endocytosis on protein-free liposomes. *Cell* 94, 131-141.
- Takei,K., Slepnev,V.I., Haucke,V., and De Camilli,P. (1999). Functional partnership between amphiphysin and dynamin in clathrin-mediated endocytosis. *Nat. Cell Biol.* 1, 33-39.

Taylor,G.A., Collazo,C.M., Yap,G.S., Nguyen,K., Gregorio,T.A., Taylor,L.S., Eagleson,B., Secrest,L., Southon,E.A., Reid,S.W., Tessarollo,L., Bray,M., McVicar,D.W., Komschlies,K.L., Young,H.A., Biron,C.A., Sher,A., and Vande Woude,G.F. (2000). Pathogen-specific loss of host resistance in mice lacking the IFN-gamma-inducible gene IGTP. *Proc. Natl. Acad. Sci. U. S. A* 97, 751-755.

Taylor,G.A., Jeffers,M., Largaespada,D.A., Jenkins,N.A., Copeland,N.G., and Woude,G.F. (1996). Identification of a novel GTPase, the inducibly expressed GTPase, that accumulates in response to interferon gamma. *J. Biol. Chem.* 271, 20399-20405.

Taylor,G.A., Stauber,R., Rulong,S., Hudson,E., Pei,V., Pavlakis,G.N., Resau,J.H., and Vande Woude,G.F. (1997) . The inducibly expressed GTPase localizes to the endoplasmic reticulum, independently of GTP binding. *J. Biol. Chem.* 272, 10639-10645.

Tesmer,J.J., Sunahara,R.K., Gilman,A.G., and Sprang,S.R. (1997). Crystal structure of the catalytic domains of adenylyl cyclase in a complex with G $\alpha$ .GTP $\gamma$ S. *Science* 278, 1907-1916.

Thompson,H.M. and McNiven,M.A. (2001). Dynamin: switch or pinchase? *Curr. Biol.* 11, R850.

Urrutia,R., Henley,J.R., Cook,T., and McNiven,M.A. (1997). The dynamins: redundant or distinct functions for an expanding family of related GTPases? *Proc. Natl. Acad. Sci. U. S. A* 94, 377-384.

van Baalen,M. (1998). Coevolution of recovery ability and virulence. *Proc. R. Soc. Lond B Biol. Sci.* 265, 317-325.

Vestal,D.J., Buss,J.E., McKercher,S.R., Jenkins,N.A., Copeland,N.G., Kelner,G.S., Asundi,V.K., and Maki,R.A. (1998). Murine GBP-2: a new IFN-gamma-induced member of the GBP family of GTPases isolated from macrophages. *J. Interferon Cytokine Res.* 18, 977-985.

Vetter,I.R. and Wittinghofer,A. (1999). Nucleoside triphosphate-binding proteins: different scaffolds to achieve phosphoryl transfer. *Q. Rev. Biophys.* 32, 1-56.

Votsmeier,C. and Gallwitz,D. (2001). An acidic sequence of a putative yeast Golgi membrane protein binds COPII and facilitates ER export. *EMBO J.* 20, 6742-6750.

Wakui,M., Yamaguchi,A., Sakurai,D., Ogasawara,K., Yokochi,T., Tsuchiya,N., Ikeda,Y., and Tokunaga,K. (2001). Genes highly expressed in the early phase of murine graft-versus-host reaction. *Biochem. Biophys. Res. Commun.* 282, 200-206.

Wilkinson,A.J., Fersht,A.R., Blow,D.M., and Winter,G. (1983). Site-directed mutagenesis as a probe of enzyme structure and catalysis: tyrosyl-tRNA synthetase cysteine-35 to glycine-35 mutation. *Biochemistry* 22, 3581-3586.

Williams,B.R. (2001). Signal integration via PKR. *Sci. STKE*. 2001, RE2.

Winter,G., Fersht,A.R., Wilkinson,A.J., Zoller,M., and Smith,M. (1982). Redesigning enzyme structure by site-directed mutagenesis: tyrosyl tRNA synthetase and ATP binding. *Nature* 299, 756-758.

Wiseman,T., Williston,S., Brandts,J.F., and Lin,L.N. (1989). Rapid measurement of binding constants and heats of binding using a new titration calorimeter. *Anal. Biochem.* 179, 131-137.

Wittinghofer,A. and Pai,E.F. (1991). The structure of Ras protein: a model for a universal molecular switch. *Trends Biochem. Sci.* 16, 382-387.

Wu,S.K., Zeng,K., Wilson,I.A., and Balch,W.E. (1996). Structural insights into the function of the Rab GDI superfamily. *Trends Biochem. Sci.* 21, 472-476.

Wynn,T.A., Nicolet,C.M., and Paulnock,D.M. (1991) . Identification and characterization of a new gene family induced during macrophage activation. *J. Immunol.* 147, 4384-4392.

Yu,B., Slepak,V.Z., and Simon,M.I. (1997). Characterization of a G $\alpha$  mutant that binds xanthine nucleotides. *J. Biol. Chem.* 272, 18015-18019.

Zerrahn,J., Schaible,U.E., Brinkmann,V., Guhlich,U., and Kaufmann,S.H. (2002). The IFN-inducible Golgi- and endoplasmic reticulum- associated 47-kDa GTPase IIGP is transiently expressed during listeriosis. *J. Immunol.* 168, 3428-3436.

Zerrahn,J., Schaible,U.E., Brinkmann,V., Guhlich,U., and Kaufmann,S.H. (2002). The IFN-inducible Golgi- and endoplasmic reticulum- associated 47-kDa GTPase IIGP is transiently expressed during listeriosis. *J. Immunol.* 168, 3428-3436.

Zhang,B. and Zheng,Y. (1998). Negative regulation of Rho family GTPases Cdc42 and Rac2 by homodimer formation. *J. Biol. Chem.* 273, 25728-25733.

Zhang,B., Gao,Y., Moon,S.Y., Zhang,Y., and Zheng,Y. (2001). Oligomerization of Rac1 gtpase mediated by the carboxyl-terminal polybasic domain. *J. Biol. Chem.* 276, 8958-8967.

Zhang,B., Zhang,Y., Collins,C.C., Johnson,D.I., and Zheng,Y. (1999). A built-in arginine finger triggers the self-stimulatory GTPase-activating activity of rho family GTPases. *J. Biol. Chem.* 274, 2609-2612.

Zhou,A., Paranjape,J.M., Der,S.D., Williams,B.R., and Silverman,R.H. (1999). Interferon action in triply deficient mice reveals the existence of alternative antiviral pathways. *Virology* 258, 435-440.

## VII. SUMMARY

My thesis work focuses on the biochemical, structural and cellular characterisation of IIGP1, a member of the p47 family of GTPases.

The p47 family of GTPases are induced transcriptionally from very low resting levels in mouse cells by interferons and are implicated in cell autonomous resistance to intracellular pathogens. A vast subset of genes are regulated by IFNs and the mechanistic details of only a few have been described. Therefore, to understand the function and features of this family of GTPases, an in depth study on IIGP1, a member of this family is investigated. Recombinant IIGP1 was expressed in *E.coli* and purified to homogeneity, and a detailed biochemical characterisation of IIGP1 was carried out. IIGP1 is a GTPase with low affinity for nucleotides (micromolar range) and a low GTPase activity. The GTPase activity is concentration dependent and functional interaction between IIGP1 molecules occur in a nucleotide dependent manner. IIGP1 shares micromolar nucleotide affinities, and oligomerisation-dependent hydrolytic activity with the 67 kDa GTPase hGBP1 (induced by type I and type II interferons), with the antiviral Mx proteins (type I interferon induced) and with the paradigm of the self-activating large GTPases, the dynamins. Besides, IIGP1 differs by having a high affinity for GDP and low GTPase activity.

The crystal structure of IIGP1 has a N- terminal helical domain followed by a typical G- domain fold and C- terminal helical regions. IIGP1 structure is a representative structure for the p47 family of GTPases. This conclusion arises firstly, from secondary structure analysis of other members of the family which are very similar to IIGP-1 and conform to the expectation derived from the crystal structure. Secondly, from the conservation of several pairs of distant residues in other p47 family members which interact to stabilise the IIGP-1 structure. This conservation could not be explained unless the structures of the other p47 GTPases are very similar to IIGP-1. Structural analysis of IIGP1 with respect to the sequence comparison with the members show several conserved regions, forming the core regions. However large deviations in the primary structure between the members, especially at the N- and C- termini explains their non-redundancy as indicated by their distinct subcellular locations, and resistance to specific pathogens.

Cellular characterisation of IIGP1 was investigated in order to understand the features of IIGP1 in the cell. Previous studies on IIGP1 has shown the association of IIGP1 with the endoplasmic

reticulum. Since the primary sequence does not indicate signal sequences, or ER retention or retrieval signals, IIGP1 is rather peripherally associated with the ER. Cellular fractionation studies reveal differential distribution of the protein, present mostly in the membrane bound form and partly in the soluble form. Membrane attachment is dependent on myristoyl modification, although not solely. There is evidence for ionic interactions which could allow the association of IIGP1 to the membranes, and another pool of the protein is independent of the above two modifications for membrane attachment. This could be accomplished by the C-terminal CaaX like motif for IIGP1 (CLRN) which has not been tested so far. IIGP1 could be immunoprecipitated with  $\alpha$  165 serum, as well as with monoclonal antibodies. Co-precipitation of three putative proteins was achieved, but the identity of these molecules remains to be unknown.

IIGP1 is a monomer in the nucleotide-free state in solution, and also in the presence of GDP, but crystallised as a dimer with or without GDP. In the presence of nucleotide triphosphates, IIGP1 forms higher oligomers. The importance of the dimer on the properties of IIGP1 was investigated by interfering with the dimer interfaces. The interface mutants have no defects in nucleotide binding but have abrogated cooperativity unlike the wild type, suggesting the functional importance of the dimer. However, the oligomerisation properties of the interface mutants has not been analysed.

The data described here formulates a platform for further analysis on IIGP1 function and provides essential parameters to understand the molecular mechanism by which IIGP1 participates in this complex resistance programme. The characterisation of IIGP1 gives an understanding to the behaviour and properties of the protein *in vitro* and *in vivo*.

## VIII. ZUSAMMENFASSUNG

Die hier vorgelegte Arbeit befaßt sich mit der biochemischen, strukturellen und zellulären Charakterisierung der 47 kDa GTPase IIGP1.

Die Familie der 47 kDa GTPasen wird durch Interferon auf Transkriptionsebene stark induziert und mit der zellautonomen Resistenz gegen intrazelluläre Pathogene in Verbindung gebracht. Eine große Anzahl von Genen wird durch Interferone induziert aber nur für wenige dieser Gene sind mechanistische Details bekannt. Deshalb schien es notwendig die Funktion der 47 kDa GTPasen näher zu untersuchen. IIGP1 ist als Mitglied dieser Familie das Objekt dieser Studie. IIGP1 wurde in *E. coli* exprimiert, hoch aufgereinigt und biochemisch untersucht. IIGP1 ist eine GTPase mit niedriger Affinität für Nukleotide und niedriger GTPase Aktivität. Darüber hinaus ist die GTPase Aktivität konzentrationsabhängig und es findet eine nukleotidabhängige, funktionelle Interaktion zwischen IIGP1 Molekülen statt. Wie die 67 kDa GTPase hGBP-1 (durch Typ I und Typ II Interferon induziert), die antiviralen Mx Proteine (durch Typ I Interferon induziert) und die großen, selbstaktivierenden Dynamine weist IIGP1 eine mikromolare Affinität zu Nukleotiden und eine oligomerisationsabhängige Hydrolyseaktivität auf. IIGP1 unterscheidet sich jedoch von den aufgeführten Proteinen durch den Befund, daß seine Affinität zu GDP höher ist als zu GTP.

Die Kristallstruktur zeigt, daß IIGP1 aus 3 strukturellen Domänen besteht. Auf die N-terminale helikale Domäne, folgt eine GTP-Bindungsdomäne, die strukturell auch bei anderen GTP-bindenden Proteinen zu finden ist. Die C-terminale Domäne weist wie der N-Terminus des Proteins eine helikale Struktur auf. Primär- und Sekundärstrukturanalysen lassen den Schluss zu, daß die Kristallstruktur von IIGP1 repräsentativ für alle 47 kDa GTPasen ist. Die geringe Sequenzhomologie an N- und C-Terminus könnte jedoch die nicht-redundante Funktion und unterschiedliche subzelluläre Lokalisierung der 47 kDa GTPasen erklären.

Zelluläre Studien von IIGP1 wurden durchgeführt um die Eigenschaften und Funktion des Proteins näher zu untersuchen. Vorhergehende Untersuchungen ergaben, daß IIGP1 mit dem Endoplasmatischen Retikulum assoziiert ist. Da die Sequenzanalyse keine Hinweise auf Signalsequenzen, ER-Retention- oder ER-Zurückgewinnungs-Signale ergab, scheint IIGP1 peripher an die ER Membran gebunden zu sein. Der größte Teil des Proteins ist membrangebunden und nur ein kleinerer Teil ist löslich. Die Membranbindung ist teilweise von der Myristoylierung von IIGP1 abhängig. Es gibt zudem Hinweise auf ionische Wechselwirkungen, welche die Assoziation des Proteins mit der Membran vermitteln könnten. Eine weitere Population bindet unabhängig von der

Myristoylierung und ionischen Wechselwirkungen an die Membran. Dies könnte durch das C-terminale CaaX-ähnliche Motiv vermittelt werden. Um Interaktionspartner von IIGP1 zu indentifizieren wurden Immunpräzipitationen mit dem anti-IIGP spezifischen  $\alpha$ 165 Antiserum durchgeführt. Diese Untersuchungen ergaben drei coisolierte Proteine. Die genaue Identifizierung dieser möglichen Interaktionspartner steht jedoch noch aus.

IIGP1 liegt in Lösung im nukleotidfreien und im GDP gebundenen Zustand als Monomer vor, kristallisierte jedoch unter beiden Bedingungen als Dimer. In Anwesenheit von GTP befindet sich IIGP1 in hocholigomerer Form. Die Eigenschaften der Dimerisierung von IIGP1 wurden durch Einsatz von gezielten Mutationen analysiert. Diese Mutanten zeigen keine Änderung der Nukleotidbindung, besitzen jedoch im Gegensatz zum Wildtyp einen Defekt in der funktionalen Kooperativität. Dies weist stark auf eine funktionelle Bedeutung des Dimers hin.

Die hier vorgestellten Untersuchungen vermitteln einen Einblick in die molekularen Eigenschaften von IIGP1 und bilden die Grundlage für weitere Analysen zur Funktion von IIGP1, an deren Ende letztendlich die Aufklärung des funktionellen Beitrags von IIGP1 bei der zellautonomen Abwehr von Pathogenen stehen könnte.



## IX. ACKNOWLEDGEMENT

My thanks to Jonathan, who showed me the “varieties in science” , lessons about “scientific discipline” and recited experiences about the “big wide world”, amidst pushing me with “eager expectation”.

I owe my gratitude to Christian, who has been a advisor as well as a good friend. For the “right words at the right time” without which I would have been lame.

To Eva, who has been supportive, helpful and enterprising in all my endeavours, and for putting up with me with immense patience.

Balaji, if we hadn’t chosen the same destinations that day, we wouldn’t have met! Thanks for initiating the fruitful collaboration with Dortmund and for the thoughts shared.

Fred, for immediately starting the collaboration, and encouragement throughout my stay in Dortmund.

Mathias, who helped me through all the bureaucracy involved, and for the kindness and concern.

Michael, who saved me through many situations and encouraged me during the rough times.

Gerrit, who put up with all my stupid questions, one with an undying enthusiasm for experiments, with whom I atleast tried to be a good listener.

To Sascha, who has been so supportive and considerate, especially at adverse circumstances, and for making me believe that “short breaks amidst busy days are immensely relaxing”.

To Jann and Ana who took me through “initial intense moments” and helped me grow with several intense discussions about every discipline.

Karin and Hamid, for their continuous reassurance, and for being there, during the “initial phases” pleasant or unpleasant.

Toby and Penns for their friendship , with who I got to know Cologne.

Silke, for many many pleasant memorable moments, and for all the profound discussions which helped me deal with many deep and silly situations.

Rita, who always had a way out for me for every situation, sorrow or event. Libby, for alluring me with the colourful and variety of things she did, and had.

To Kirsten, Rainer, Jesper, Helle and Monty who served as my adapted family.

Steffi and Christine who cared and helped me every now and then, since the day I met them.

Hicham, who showed me the “moundful of earth” to hold onto, when there was none.

Judith, for being a good friend, a good listener, who analysed every situation with a skill, more than enough to regain my balance immediately.

Arzu and Stefan (chimney boy) who made me laugh at every single conversation.

To Shreens, Sajith, Smita for good discussions, delicious food, silly recovering jokes.

To, Bharath, Taru, Sirsho, Nandini and Raina who managed to get me out of the lab, more often than I could.

Christine, Sabine, Utz, Daniel and Simone who put up with all my “doings” in the lab in Dortmund.

Anna and Barun-da, thanks for being “the bodyguards”. Partha for the coffee breaks.

To Uli, Thorsten, Gaby, Philip, Doris, Nina, Daniella, Eva, Iana, Claudia, Julia, Christoph, Sarah and Ralph for changing patterns of moods and motivation in the lab during their respective times.

To all my friends Ashi, Sri, Lavs, Vinu, Jo, Vivek, Niharika, Vikas, Appu, Vindu, Uma, Ln, Sridhar, Renuka, Suma, Preeta, Rajju, Anu, Shal, Kheer, Vee, Ashi, Sin, Naveen and Jagath who always cheered me by sending jokes, and regular updates on world events, helpful discussions (Jagath especially) and kept me informed and in balance.

To Jia and Chemali who imparted the last bulk of energy essential for my writing and decision making, for very many pleasant moments, realisations, discussions, for being my victims, and for loads of fun.

Holger and Oli, for the helpful discussions and for your precious time spent for helping me put this piece of work together.

Agni, thanks for the immense support, views and thoughts shared, and helpful discussions.

Niru, for introducing me to Germany, for so many things I learnt from you.

Viji, as you appear and disappear -  
Sundae, without you, I would be insane.

To my big family,  
To Pa, Ma, Prath and Praveen, who got me through until here.

## X. ERKLÄRUNG

Ich versichere, dass ich die von mir vorgelegte Dissertation selbständig angefertigt, die benutzen Quellen und Hilfsmittel vollständig angegeben und die Stellen der Arbeit - einschließlich Tabellen, Karten und Abbildungen -, die anderen Werken im Wortlauf oder dem Sinn nach entnommen sind, in jedem Einzelfall als Entlehnung kenntlich gemacht habe; dass diese Dissertation noch keiner anderen Fakultät oder Universität zur Prüfung vorgelegen hat; dass sie - abgesehen von unten angegebenen Teilpublikationen - noch nicht veröffentlicht worden ist sowie, dass ich eine solche Veröffentlichung vor Abschluss des Promotionsverfahrens nicht vornehmen werde.

Die Bestimmungen dieser Promotionsordnung sind mir bekannt. Die von mir vorgelegte Dissertation ist von Jonathan C. Howard betreut worden.

Köln, Dec 2002.

## XI. PUBLICATIONS

1. **Revathy C.Uthaiiah**, Gerrit G. J. K. Praefcke, Jonathan C. Howard, Christian Herrmann. IIGP1, an interferon- $\gamma$  inducible 47 kDa GTPase of the Mouse, showing cooperative enzymatic activity and GTP-dependent multimerisation (submitted to JBC).
2. Agnidipta Ghosh, **Revathy C.Uthaiiah (equal contribution)**, Jonathan C.Howard, Christian Herrmann and Eva Wolf. Crystal structure of IIGP1, a paradigm for the p47 family of resistant GTPases in the mouse (*Manuscript in preparation*).

## XII. LEBENSLAUF

**Name: Revathy Uthaiiah Chottekalapanda**

Geburtsdatum: 11.04.1975

Geburtsort: Karnataka (Indien)

Staatsangehörigkeit: Indisch

Familienstand: Ledig

Wohnort: Dürener Strasse 178,

Lindenthal, 50931 Köln

Instituts-Adresse: Institut für Genetik

Zülpicher Str. 47/ 50674 Köln

1979-1990

**Schuliche Ausbildung:**

St. Joseph's Convent (Indien)

St. Thomas Convent (Indien)

Kodagu-District-School (Indien)

1990-1991

**Vorstudium MLA College**

Bangalore University (Indien)

1992-1995

**Grundstudium, BMS College**

Bangalore University (Indien)

Juni 1995

Bachelors' Degree in Mikrobiologie,

Chemie und Zoologie

1995-1997

**Hauptstudium (Masters' Programme)**

University of Mysore (Indien)

Juli 1997

**Masters' in Mikrobiologie**

1997-1998

**Junior Research Programme,**

National Centre for Biological Sciences,

Bangalore (Indien)

**Forschungsprojekt:** Molekularbiologische Studien  
zum 5HT-1F-Gen und seiner Funktion bei der  
Neurotransmission

1998-2002

**Dissertation bei Prof. J. C. Howard** am Institut für Genetik der  
Universität zu Köln.

**Thema der Promotionsarbeit:** Biochemische, strukturelle und  
zelluläre Studien zur Interferon  $\gamma$ -induzierbaren p47 GTPase IIGP1.